NDM-3: A Study of the Expression, Purification, and Characterisation of a B1-type metallo β-lactamase.

A Thesis submitted to Maynooth University in fulfilment of the requirements for the degree of

MASTER OF SCIENCE

By

Emer Phelan BSc.

Department of Chemistry,

Maynooth University, Maynooth,

Co. Kildare,

April 2023

Research Supervisors: Dr. Nataša Mitić and Professor Gary Schenk

Head of Department: Prof. Denise Rooney

Dedication Page

I would like to dedicate this to Kathleen Phelan, my grandmother, who sadly passed away after I started this research project. She was a force of nature and she taught me to have and state an opinion when it was needed. She was an exceptional lady.

Certificate of Originality

I, Emer Phelan, hereby certify that the work carried out in this thesis is my original work and that it was not been submitted to Maynooth University or any other institution at any other time. I also confirm that it is the original writings of this author, that anything published is noted and that nothing has been copied from a published book, photograph, magazine, or work carried out by another person.

Signed: _____

Emer Phelan

Date: April 2023

Acknowledgements

Nobody can be successful without the people around them. This is especially true for undertaking something as challenging and rewarding as postgraduate research. A lot has happened in the time since undertaking this research project on, and I would like to thank everyone who has been there during that time.

Firstly, to my family; thank you all so much for your support and help over the years. To my Mam and Dad – Clare and Dermott Phelan, I want to sincerely thank you for always being so encouraging to me and my siblings regarding studying and furthering our education. Without this interest and understanding from you both, we would not be able to do what we wanted to. To Aoife, my sister, best friend, and one of the best people I know – I hope you will learn from my challenges and enjoy your own biomedical research adventure. Thanks for the listening ear and all the support over this time. To Cormac, Trish, Noah, and Liam – Thanks for being a breath of fresh air to see and spend time with! To my extended family – you are just mighty altogether!

To my Grandad, who is one of my favourite people in the world, I hope to be as inspired and inspiring as you are when I am 93! I think you are a fantastic, warm, and wonderful person to be around and to learn from. You are still learning despite being wise, and that willingness to learn has definitely been passed on!

To Michael Fay, words will never fully express how much you have helped me in the last few years, through some of the toughest times in relation to this research and not. Your support, positivity, sushi kindness, regular kindness, and love will always be a happy memory around an otherwise stressful time.

To my friends outside of academia, thanks for the memories, and the songs and laughter. Music is what gets you through, or at least does for me! To Mandy – thanks for your help with the end of the lab. Denise – for always knowing exactly what I was going through. To Laura for being my cheerleader, and anyone else who has been as encouraging and helpful. So many others but cannot mention everyone, you all know who you are and how wonderfully you helped.

To my supervisors over the years – Dr Natasa Mitic, Professor Gary Schenk, Professor John Lowry, and even Dr Malachy McCann for a while there in the beginning, thank you all for your knowledge, teachings, and for the support. Particularly to John thanks for your kind help in the later years.

To Manfredi, Marcelo, Jacob, Chris, and everyone I worked alongside in the lab, I wish you all prosperous and rewarding careers. I hope you all get exactly what you are looking for.

To my friends in the Department – Karen especially – thank you for the social nights, for the coffee room chats, the cinema dates, and the sanity doses. I hope we can keep going to the worst Christmas movies ever – Justine, Michelle, Caroline, Jessica. And Ula who was always there to have the chats and fight injustice! Also, to Andrew who started with me. Such a wonderful group of intelligent women and men, it was a pleasure to be around you all.

Again, Karen – thanks for everything. It is worth another mention!

Abbreviations List

AHL	N-acyl homoserine lactone
AIM	Australian Imipenemase MBL from *Pseudomonas aeruginosa*
BcII	MBL from *Bacillus cereus* type II
BJP	MBL from *Bradyrhizobium japonicum*
BLAST	Basic Local Alignment Search Tool
CAR	MBL from *Erwinia carotovora*
CphA	MBL from Carbapenem hydrolysing and A from *Aeromonas hydrophila*
CSA	MBL from *Cronobacter Sakazakii*
DFT	Density Functional Theoretical
EBR	MBL from *Empedobacter brevis*
EDTA	Ethylenediaminetetraacetic acid
FEZ	MBL from *Fluoribacter gormanii*
FDA	U.S. Food and Drug Administration
FF	Fast Flow
FIM	MBL from *Pseudomonas aeruginosa*
FPLC	Fast protein liquid chromatography
GIM	MBL from *Pseudomonas aeruginosa*
GOB	MBL from *Elizabethkingia meningoseptica*
HEPES	N-2-hydroxyethylpiperazine-N'-2-ethanesulfonic acid
IMAC	Immobilized Metal Affinity Chromatography
IMP	Imipenemase MBL from *Pseudomonas aeruginosa and Klebsiella Pneumoniae*
IND	MBL from *Chryseobacterium indologenes*
IPTG	Isopropyl β-D-1-thiogalactopyranoside
ITC	Isothermal titration calorimetry
L1	Labile enzyme *Stenotrophomonas maltophilia*
LB	Lysogeny broth
MBL	Metallo beta lactamase
MF	Mag-Fura-2
MIM	MBL from *Novosphingobium pentaromativorans and Simiduia Agarivorans*
ML	Metal and Ligand
NaCl	Sodium Chloride
ND	No data

NDM	New Delhi MBL
NDM-3(NC)	NDM-3 (New construct)
NDM-3+Ub	NDM-3+ubiquitin Tag
PAR	4-(2-pyridylazo) resorcinol
PDB	Protein Data Bank
QLD	Queensland
QM/MM	Quantum mechanics/Molecular mechanics
RSD	Relative Standard Deviation
SBL	Serine beta lactamase
SDS-PAGE	Sodium dodecyl sulphate - polyacrylamide gel electrophoresis
SFB	MBL from *Shewanella frigidimarina*
SIM	MBL from *Acinetobacter baumannii*
SLB	MBL from *Shewanella livingstonensis*
SMB	MBL from *Serratia marcescens*
SPM	MBL from *Pseudomonas aeruginosa*
SPR	MBL from *Serratia Proteamaculans*
TGX	Tris-glycine buffer SDS-PAGE gels
THIN-B	MBL from *Janthinobacterium lividium*
USP2cc	Deubiquitylating enzyme
UV	Ultra violet
UV/Vis	Ultra violet visible spectroscopy
VIM	MBL from *Pseudomonas aeruginosa*
WHO	World Health Organisation

Table of Contents

Table of Contents

Abstract

Antibiotic resistance is a prevalent and global problem. It is one of the biggest, if not the biggest, health care challenge we face this century. Metallo-beta-lactamases (MBLs) are a group of enzymes that play a pivotal role in the spread of resistance. There are many contributing factors for the success of MBLs at overcoming current antibiotics, and why they evade and evolve to overcome potential new antibiotics before said antibiotics would make it to market. One of these reasons is the sheer number of MBLs and more specifically, the number of mutants of these MBLs. There are as many as four subgroups in the MBL family, labelled B1 to B4. B1 is the best-studied subgroup, and the one that is most prevalent in pathogenic microorganisms. Members of this subgroup employ two metal ions (generally Zn^{2+}) in their active sites for hydrolysis of antibiotics. NDM (**N**ew **D**elhi **M**BL) is a prominent example that has spread quickly and poses a real threat to society's use of antibiotics. Known as a "superbug," NDM-1 has made use of various tools to spread rapidly (horizontal gene transfer), evade inhibition, and evolve catalytic efficiency. The introduction of specific mutations has led to the emergence of at least 15 known variants of this enzyme that vary in their substrate preference and catalytic properties.

NDM-3 is one such variant and is the topic of this research project, which aims to determine and characterise its catalytic properties and compare those to corresponding parameters reported for the original NDM variant discovered, NDM-1.

What was discovered during this thesis was the optimised process to isolate, express, and purify NDM-3. This was completed with two constructs of NDM-3: NDM-3+Ub, and NDM-3(NC) – NDM-3(NC) did not have the ubiquitin tag attached.
Purification of both of these constructs were completed using hexahistidine IMAC chromatography. NDM-3+Ub then underwent cleavage using USP2cc protease, however no activity was ever witnessed on this cleaved enzyme.

Activity assays were performed on both the uncleaved NDM-3+Ub, and NDM-3(NC). These results were compared with the NDM-3(NC) showing stronger activity than the construct with the ubiquitin tag.

Overall, NDM-3(NC) has lower activity than NDM-1. From these works it is shown that like NDM-1, NDM-3(NC) was shown to have activity across a wide range of substrates but NDM-1 has superior hydrolytic activity against most β-lactam antibiotics tested. As an example, the k_{cat} values of NDM-1 for the hydrolysis of ampicillin and penicillin are 182 s^{-1} and 142 s^{-1}, respectively. The corresponding parameters for NDM-3(NC) are only 47 s^{-1} and 38 s^{-1}, respectively, effectively showing only ~40% of NDM-1 activity.

Similarly, NDM-3(NC) underwent pH profile assays to determine the pH range it has activity against various beta lactam antibiotic substrates, and to determine the pH point that activity is the strongest. As would be expected for a virulent and pathogen that infects humans, NDM-3(NC) like NDM-1, has strongest activity at physiological pH points (i.e. around pH 7.5) and showing the strongest activity overall against ampicillin and meropenem across the pH ranges.

Chapter 1 – Introduction and Research Background to β-lactamases and Antibiotic Resistance

Antibiotic resistance is one of the most worrying threats facing our world today (1). Finding new ways to fight off pathogenic bacteria which have become resistant to most of the commonly prescribed antibiotics is a global challenge. This bacterial resistance emerged as a result of many factors. These include the over-prescription of antibiotics to humans, over-use of antibiotics in livestock, increased accessibility due to better transport worldwide, unfinished antibiotic courses, sub-optimal hygiene standards, and fewer new antibiotics being discovered in recent times. The first step in overcoming this challenge is to fully characterise and comprehend how these bacteria become resistant and how they have and continue to evolve to build resistance (2).

Antibiotics have been around since the 1920s (3). Originally discovered in the form of penicillin by Sir Alexander Fleming (2), soon after derivatives of penicillin and then cephalosporins, carbapenams, monobactams and cephamycins became available. These β-lactam type antibiotics are so named due to their four-membered β lactam ring. β-lactamases are a family of enzymes produced by bacteria that exhibit resistance to β-lactam antibiotics (4). These enzymes inactivate the antibiotics by hydrolysing and opening the β-lactam ring. β- lactamases consist of four subgroups – groups A, B, C, and D. Groups A, C, and D are serine β-lactamases (SBLs), and group B are metallo β-lactamases (MBLs). While SBLs employ a serine residue in their active site to initiate the hydrolysis of the antibiotic, MBLs use a metal-bound hydroxide for the same purpose. MBLs require either one or two Zn(II) ions to be catalytically active, and depending on their metal ion requirement and mechanism they are further divided into four subgroups – B1, B2, B3, and B4. All four subgroups have characteristic traits which will be discussed further into this chapter within research background.

To date, extensive research has been carried out on the many non-pathogenic and pathogenic MBLs. Naturally, of highest importance are the most virulent and dangerous MBLs (e.g., NDM-1) which can be transferred between different pathogens by horizontal gene transfer; NDM-1 is able to confer resistance to almost all known antibiotics, including carbapenems, and has been detected in over 70 countries worldwide. For this reason, it is imperative that more research is done in this area until a solution can be found and that as a matter of urgency, we should look for solutions as quickly as possible. Years ago, I recall being informed that there was approximately 20 years or so before it affected us significantly. Since then, those projections seem to have decreased time-wise and we should expect the impact sooner rather than later.

In response to this worrying increase in antibiotic resistance the World Health Organisation (1) has outlined some of the practices advised to combat the threat. Apart from new antibiotics and inhibitors being developed, there are some steps everyone can take, including changing the way we view and use antibiotics, following advice from healthcare professionals when antibiotics are not needed, generally improving good health,

hygiene, and common sense regarding avoiding people who are unwell, and educating ourselves on the limits of antibiotics. The WHO warns that without caution and invigorated research we will again face a time when common infections and injuries will become fatal.
Another problem facing us in our search for new antibiotics is the speed of evolution these pathogenic bacteria can become resistant to the newer generations of antibiotics. Ideally, a universal inhibitor would be developed that could inhibit all β-lactamases through a mechanism that cannot easily be circumvented by mutations. Whether this is a possibility remains to be seen, but it is imperative that further research and investigation be done into both characterisation of these enzymes, and into potential inhibitors.

The aim and scope of this project was to further the scientific community's knowledge by selecting a novel enzyme, NDM-3 – a variant of well-known pathogenic "superenzyme" NDM-1, and includes the purification, isolation, and analysis of NDM-3. At the time of the research project and subsequent thesis write-up, NDM-3 was a novel enzyme. Since this time, NDM-3 has been further characterised by other research groups (5; 6). The comparison between NDM-3 and NDM-1 was intended to provide insight into factors that are essential for the catalytic efficiency of this enzyme. NDM-3 differs from NDM-1 by a single amino acid on the surface of the enzyme rather than in the active site. The analysis of NDM-3 included a pH study in the presence of four β-lactam antibiotics, with one from each family of antibiotics selected. The comparison of NDM-3 to NDM-1, along with other NDM variants was conducted, to ascertain any further understanding of the mechanism of action of these specific enzymes.

Throughout chapters one to four of this thesis, the research background of this area in MBLs is outlined, including relevant kinetic equations and principles associated with this research topic. These calculations based on said equations are the basis for results chapters – chapter 3 and 4. Included later in this research background (chapter 1) is a review article written by the author of this thesis which includes a comparison of the available information about binding studies for MBLs in 2014 - the year the review was published. Following research background, chapter two lists and explains the materials and methods used during this research project. The chemicals, solutions, buffers used, and the methodologies employed for expression, purification, and characterisation of NDM-3 is outlined. In the final two chapters, the results of NDM-3 expression, purification, and characterization are reported. These results include the conditions and their determinations, SDS-PAGE gel images, column elution graphs, and cleavage results for the ubiquitin tag in chapter four. Due to research difficulties, two constructs of NDM-3 were used; namely NDM-3+Ub and NDM-3(NC). NDM-3+Ub is a construct which contains a ubiquitin tag that must be cleaved off using a protease. This is described in chapter 2, 3, and 4. NDM-3(NC) does not contain a ubiquitin tag and therefore does not require a cleavage step.
In chapter four the enzymatic characterisation of NDM-3's resistance to β-lactam antibiotics is reported. Here, comparisons are carried out with NDM-1 and other NDM mutants. A pH study is included in this report, and the lactonase initial assay results.

Finally, in the conclusion chapter, the main results from this research works are highlighted, and an outline provided on what can and must be achieved before the inevitable outcomes listed by WHO become a reality.

Review Article

The following review article (7) was published in 2014, with the author of this thesis as the first author, and was an up-to-date summary of the research occurring in the area of MBL research at that time. It is inserted below in its entirety for the sake of continuity with only reference figures changed. A small amount of new information is added, denoted by [...].
****

American Journal of Molecular Biology, 2014, 4, 89-104 Published Online July 2014 in SciRes. http://www.scirp.org/journal/ajmb http://dx.doi.org/10.4236/ajmb.2014.43011

Metallo-beta-lactamases: a major threat to human health

Emer K. Phelan; [1, 2] Manfredi Miraula; [1, 2] Gerhard Schenk; [2] Nataša Mitić[1]

[1]Department of Chemistry, National University of Ireland – Maynooth, Maynooth, Co. Kildare, Ireland

[2]School of Chemistry and Molecular Biosciences, The University of Queensland, Brisbane, QLD, Australia

Abstract

Antibiotic resistance is one of the most significant challenges facing global health in recent times. Antibiotics have been used to fight infections since the 1940's, initially with penicillin and various derivatives. Over the decades the arsenal of antibiotics (Figure 1a) has been expanded to include cephalosporins, cephamycins, carbapenams, and monobactams.

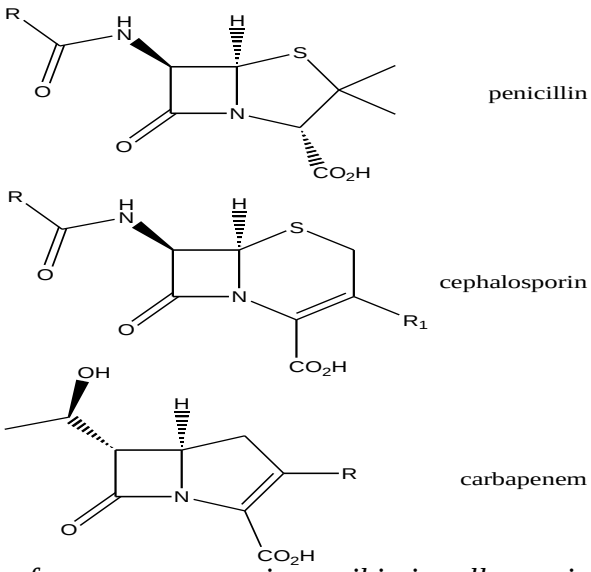

Figure 1a. Structures of some representative antibiotics all containing the signature β - lactam ring (Chem Draw)

All of these antibiotics have a common core structure, the four-membered β-lactam ring. In recent years a growing number of bacteria have acquired resistance to these antibiotics; strategies for resistance include the use of efflux pumps (8; 9), chemical modifications (10) and inactivation of the antibiotic. The latter strategy employs a family of enzymes, the β-lactamases, which hydrolyse and thus open the β-lactam ring of the antibiotic. Two main groups belong to this family, the serine β-lactamases (SBLs) and the metallo-β-lactamases (MBLs). While clinically useful inhibitors for SBLs are available (11) MBLs are a major threat to human health as no such inhibitor for these enzymes has yet been developed and they are highly proficient in inactivating nearly all commonly used β-lactam-based antibiotics. MBLs are thus the main focus of this mini review.

1.1 Introduction

β- lactamases are subdivided into four groups based on sequence similarity, *i.e.*, groups A, B, C, and D (11; 12; 13; 14; 15). Members of groups A, C and D are SBLs; they employ a serine residue in their active site to initiate hydrolysis of β-lactam substrates (11; 12; 13; 14; 15). SBLs have been extensively studied and their threat to human health is, at least currently, under some control as clinically applicable SBL inhibitors such as clavulanic acid can be co-administered with antibiotics to maintain the antibacterial effect of the latter (16; 17; 18; 19; 20). Class B β-lactamases are MBLs; they require at least one, but more often two zinc(II) ions in their active sites for catalytic activity (15). Based on sequence homology MBLs are divided into three subgroups, B1, B2 and B3. Common to all three subgroups is a characteristic αββα-fold (see below). Apart from some sequence variations the main difference between various MBLs is their requirement for metal ions. B3 and most of B1 MBLs require two Zn(II) in their active sites (13; 15; 21; 22; 23; 24); although the B1 MBL from *Bacillus cereus*, BcII, has been shown to be catalytically active in the presence of only one Zn(II) (21). In contrast, MBLs from the B2 subgroup have been shown to require only one Zn(II); binding of a second metal ion in the active site leads to inhibition of enzymatic activity (25). B2 MBLs are more selective in terms of antibiotics they are able to degrade (26), but they have a particular preference for monobactams, the broadest spectrum antibiotics (15; 26), but their activity against penicillin and cephalosporins is poor (26; 27).

While zinc is the naturally occurring metal ion employed by all MBLs, in *in vitro* studies it could be shown that catalytic activity can be reconstituted with a range of metal ions, including Co(II), Mn(II) and Cu(II) (28; 29; 30). While not biologically relevant, the derivatives of MBLs with these metal ions have provided detailed insight into mechanistic aspects of these enzymes (*vide infra*).

MBLs are encoded by genes that are either part of the chromosomal framework of the bacterial species (*e.g. Pseudomonas aeruginosa* (31)) or are encoded by mobile genetic elements that can easily be shared among species by horizontal gene transfer (*e.g. Acinetobacter baumannii, Pseudomonas aeruginosa, Klebsiella Pneumoniae*) (31; 32).

Especially the latter is a major concern for health care as it facilitates the rapid transfer and hence spread of MBLs amongst pathogenic bacteria (33; 34; 35; 36; 37; 38; 39; 40).

A series of excellent reviews on the structure, function, and clinical relevance of MBLs have been published over the past decade (13; 15; 31; 41; 42). In this mini review we will briefly summarise the main structural and mechanistic aspects of these diverse enzymes, but focus in particular on the interactions between metal ions and MBLs and their role(s) in catalysis. Universal inhibitors for MBLs are currently still unavailable but since metal ions are essential for MBL function a strategy that interferes with enzyme-metal ion interactions may prove beneficial for the future development of such inhibitors.

B1

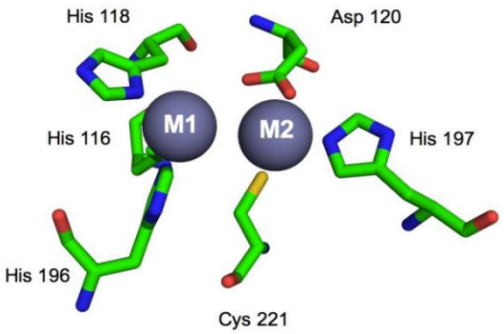

B2

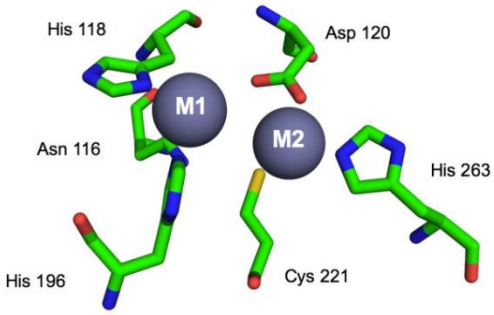

B3

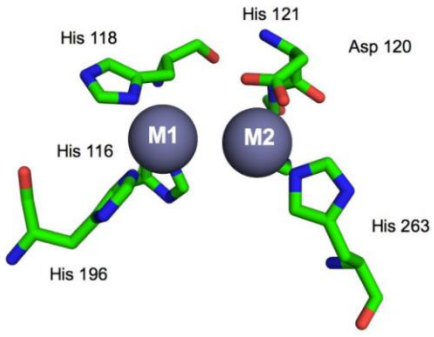

Figure 1b. The general structure of the active sites for each of the three subclasses.

1.2 Overall and active site structures of MBLs

MBLs, although divided into three subclasses, share certain structural similarities. They all have a αββα fold, with eight β strands connected by α helices (Figure 1c).

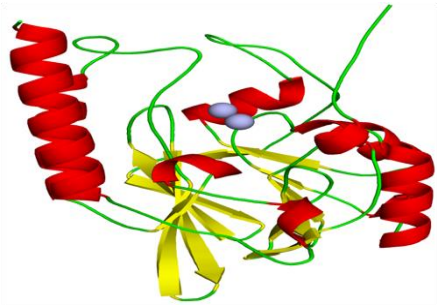

Figure 1c. The overall structure of an MBL.

The B1 subgroup is the most common and structurally most extensively studied group (11; 13; 15; 21; 22; 24; 43; 44). For instance, IMP-1 is the first of the MBL's that was considered a threat as it can be transferred on the mobile genetic element (22; 28; 29; 45; 46). More recently, NDM-1 made headlines because it is the most pathogenic and dangerous of the MBL's as it is multidrug resistant and can very easily spread by horizontal gene transfer. It has disseminated very rapidly and due to its pathogenic nature it is a great concern worldwide (44; 47; 48; 49; 50; 51; 52; 53).

Figure 1d. This map represents the global dissemination of the most prevalent antibiotic resistant infections. IMP, NDM, and VIM are most widespread (54).

Currently, crystal structures are available for eight B1 enzymes. These include BcII from *Bacillus cereus* (21), New Delhi MBL-1 from *Klebsiella Pneumoniae* (better known as NDM-1 (48)), IMP-1 from *Pseudomonas aeruginosa* and *Klebsiella Pneumoniae* (22), VIM-2 from *Pseudomonas aeruginosa* , SPM-1 from *Pseudomonas aeruginosa* (55), CcrA from *Bacteroides fragilis* (56; 57; 58; 59), BlaB from *Chryseobacterium meningosepticum* (60), IND-7 from *Chryseobacterium indologenes* (61), and GIM-1 from *Pseudomonas aeruginosa* (62). Other B1-type MBLs that have been studied in some detail but whose crystal structures have not yet been determined include SLB-1 from *Shewanella*

livingstonensis (63), SFB-1 from *Shewanella frigidimarina* (63), EBR-1 from *Empedobacter brevis* (64), VIM-1 from *Pseudomonas aeruginosa* (65; 66; 67; 68),VIM-4 from *Pseudomonas aeruginosa*, *Klebsiella Pneumoniae* and Enterobacter cloacae (69; 70; 71; 72), IMP-2 from *Pseudomonas aeruginosa* and *Klebsiella Pneumoniae* (73), IMP-4 from *Klebsiella Pneumoniae* (74), SIM-1 from *Acinetobacter baumannii* (75), and FIM-1 from *Pseudomonas aeruginosa* (76). B1-type MBLs have two loops, L3 and L8 (Figure 1e), in the vicinity of the metal ion-containing active site. These loops are believed to be crucial for determining the substrate specificity of these enzymes (15).

In contrast, MBLs from the B2 subgroup lack the extended L3 loop (Figure 1f). Instead, these enzymes have a kinked α helix positioned directly above the active site cleft (15). This feature facilitates the formation of a narrow, well defined active site; consequently, these enzymes have a distinct selectivity for carbapenem substrates (15). The three known representatives from this subgroup are CphA from *Aeromonas hydrophila* (77), Sfh-I from Serratia fonticola (78), and Imi-S from Aeromonas veronii (79). CphA is the most (25; 77; 80; 81; 82; 83) extensively studied of the three; common to all is the requirement of only one bound Zn(II) for catalytic activity. Binding of a second metal ion renders the enzymes inactive (25).

MBLs from the B3 subgroup, like those from the B2 subgroup, also lack the extended L3 (Figure 1g). However, they have a mobile loop, positioned between α3 and β7, which is located above the active site, thus influencing the substrate specificity of these enzymes. A preference for cephalosporins has been noted (15). Current members of the B3 subgroup include L1 from *Stenotrophomonas maltophilia* (84), FEZ-1 from *Fluoribacter gormanii* (85), BJP-1 from *Bradyrhizobium japonicum* (86), AIM-1 from *Pseudomonas aeruginosa* (87), and SMB-1 from *Serratia marcescens* (88), the crystal structures of which have been reported. Other members in this subclass include GOB-1 from *Chryseobacterium meningosepticum* [and *Elizabethkingia meningoseptica*] (89; 90), CAR-1 from *Erwinia carotovora* (91), THIN-B from *Janthinobacterium lividium* (92) and, most recently, SPR-1 from Serratia proteamaculans (93). Furthermore, a bioinformatics study has also identified likely B3-type MBLs in *Novosphingobium pentaromativorans* and *Simiduia Agarivorans* (MIM-1 and MIM-2) (94).

Figure 1e. Overall structure and active site of IMP-1, a representative of the B1 subclass (29).

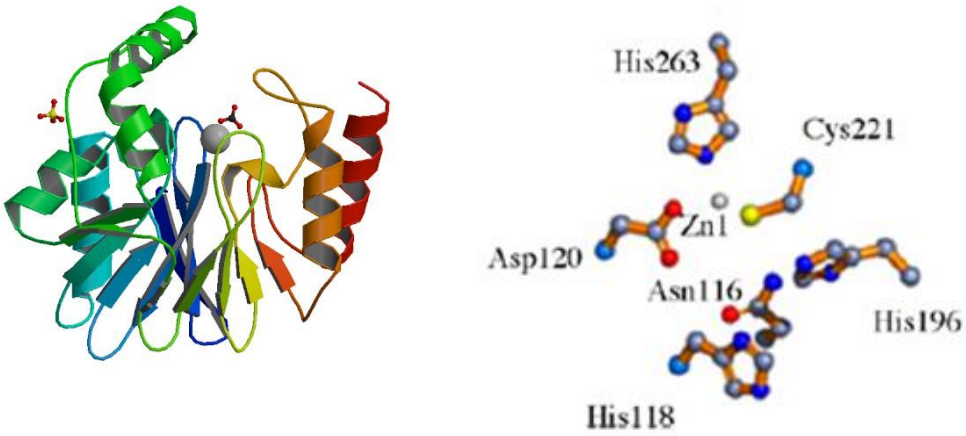

Figure 1f. Overall structure and active site of CphA, a representative of the B2 subclass (77)

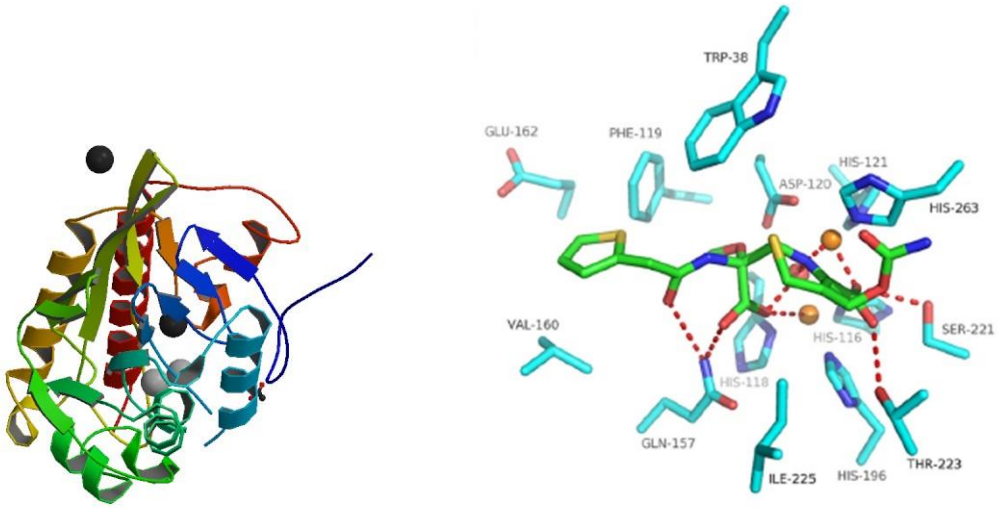

Figure 1g. Overall structure and active site of AIM-1, a representative of the B3 subclass (87)

The active sites of MBLs accommodate space for two metal ions (generally Zn(II), *i.e.,* Zn1 and Zn2) to bind. In both B1 and B3 enzymes the Zn1 ion is coordinated in a tetrahedral geometry by three histidine residues (His116, His118 and His196) and a water molecule (W1) that forms a bridge to Zn2. The Zn2 site displays a trigonal bipyramidal coordination sphere. In B1 MBLs in addition to W1 an aspartic acid (D120), a cysteine (C221) and a histidine (H263) interact with Zn2 (Figure 1e – 1g). In B3 MBLs D120, H121 and H263, as well as a second water molecule (M2) complement the coordination sphere. At least in some B1 MBLs only one metal ion is absolutely essential for catalysis; BcII could be shown to be catalytically active in mononuclear form (*i.e.* only Zn2 is bound) (41; 95). Furthermore, in available crystal structures it appears that the Zn1 site has a higher occupancy than the Zn2 site, suggesting a tighter binding for the former.

While B2 MBLs can also accommodate two metal ions in their active site, catalysis is only observed when the enzymes are in mononuclear form (*i.e.*, only the Zn2 site is occupied); occupation of the Zn1 site leads to inhibition (96). In contrast to B1 and B3 MBLs the Zn2 site in B2 MBLs adopt a tetrahedral geometry with D120, C221, H263 and a water molecule (W1) are the ligands. When a second zinc ion is in the Zn1 site this acts as an inhibitor. This site is empty usually. The variation in metal ion requirement between B2 and B1/B3 MBLs indicates mechanistic variations between these two groups (for detailed description of proposed reaction schemes see the reviews of Crowder *et al.* (31) and Page and Badarau (41)) but it is currently not known what the underlying structural causes for these differences are; *i.e.* the evolutionary advantage of using a binuclear metal site but requiring only one metal ion for catalysis in B2 MBLs is not yet understood.

Recently in the case of SPR-1 (a B3 metallo-β-lactamase), arginine 118 (Zn1) has been found instead of a histidine, which although rare is not unheard of. Also present in the structure of SPR-1 is a lysine residue at 263, which is highly unusual. Histidine 121 is replaced by glutamine 121 in SPR-1 too. In this case, two of the Zn2 amino acids that interact with the metal in the active site are different to others of the same subclass. This shows that although we can group the enzymes of the classes together, there will always be some that do not lie inside these general rules.

1.3 Metal Ion Binding Studies: Elucidation of the metal ion binding affinities

Since their initial discovery, various techniques have been employed to acquire information about the metal ion binding parameters of the MBLs (95; 97; 98; 99; 21). According to the structural analysis of MBLs, the differences in amino acids between the three sub classes may suggest different roles for the metal ions. The differences in behaviour and substrate specificity of the B1-, B2- and B3-type MBLs could potentially arise from distinct metal binding affinities. While class B1 and B3 MBLs are fully active as di-metallo enzymes and exhibit a broad-spectrum substrate profile, the B2-type MBLs exhibit a narrow substrate specificity and the binding of the second metal ion seems to inhibit the activity (100). The first and the most extensively studied B1 type enzyme is *B. cereus* BcII, in which the metal ions play an important role in the binding of the β-lactam ring (101). Of particular relevance to the study of MBLs is that the few reported binding affinities of metal ions to MBLs vary greatly, by several orders of magnitude. For example, reported values of binding constants for two zinc ions of BcII range from the low nM to 120 μM for the Zn1 site and 1.5 μM to 24 mM for the Zn2 site (97). Consequently, and not surprisingly, various aspects of the mechanistic strategy used by these enzymes, including the precise role(s) metal ions play, remain unknown. More recent structural and spectroscopic studies of *Bacillus cereus* 569/H/9 BcII indicated a positive cooperative binding of the two zinc ions (11). Thus, it was proposed that the di-zinc form is the one biologically active (19; 102). This positive cooperativity has also been observed within the

B1 sub class of MBLs, by the enzymes CcrA (103), and IMP-1 (104). In contrast, the B1 class enzyme, Bla2 from *B. anthracis*, which is speculated to be active in the mono-zinc form, shows a sequential binding of the two zinc ions (105). B2 type MBLs are believed to be catalytically active in mono-zinc form, while the second zinc ion seems to have an inhibitory effect (17; 18). The most extensively studied B2 class enzyme is CphA for which it has been confirmed that there is only one zinc ion present which is located in the Zn2 site (77). Another B2 type MBL, Sfh-I enzyme from the aquatic bacterium *Serratia fonticola* UTAD54, also shares these characteristics in its active site (27). Here, we will review the methodologies and principles employed to this date to study the metal binding of the metal ions to the sites of the MBLs, with focus on the kinetic parameters published for various MBLs.

Determination of the dissociation constants using competition assays

There are typically two assays which are commonly used to determine up to nanomolar concentrations of the first-row transition metal ions. The first assay uses the colorimetric compound 4-(2-pyridylazo) resorcinol (PAR) to quantitatively measure nanomolar range of Co(II), Ni(II), Cu(II) and Zn(II) ions (106; 107; 108; 109); the second assay employs the fluorimetric compound 5-Oxazolecarboxylic acid, 2-[6-[bis(carboxymethyl)amino]-5-(carboxymethoxy)-2-benzofuranyl] (Mag-Fura-2, MF) which can detect nano moles of Mn(II), Co(II), Ni(II), Cu(II), Zn(II) and Cd(II) ions (97; 98; 108). The colorimetric assay with PAR, follows the changes in the UV/Vis absorption spectrum of the M(II)-PAR complex (characterized by a maximum decrease at 410 nm and a maximum increase at 500 nm for Ni(II) and Zn(II) and 514 nm for Co(II) and Cu(II), respectively (106; 108). The changes in the absorption peaks are dependent on the metal ion concentrations (106; 108). Similarly, the fluorimetric assay with MF follows the change in the fluorescence spectrum of the M(II)-MF complex (107; 108). The fluorescence spectrum has distinct features, an excitation peak at 350 nm with a shoulder at 390 nm and an emission peak at 495 nm with a shoulder at 510-525 nm (98; 107; 108). The transition metal ions directly affect the spectrum in a concentration dependent manner. In particular, Mn(II), Co(II), Ni(II), Cu(II) quench the fluorescence of MF, whereas Zn(II) and Cd(II) enhance its fluorescence (108). The metal ion concentrations are correlated to the changes in the intensity of the spectra. Therefore, both of these assays can be used to evaluate a range of metal ion concentrations from 1 to 10 μM, in an efficient and straightforward manner with high sensitivity (108). Typically, dissociation constants for metal ions are obtained from the competition experiments with the chromophoric chelators (PAR or MF) where the chelator is normally titrated with the metal ion in the absence and presence of ligand (Apo-enzyme in this case) (97; 98; 108). Changes in the absorption or fluorescence spectra are monitored and are further correlated to binding constants using an appropriate set of equations [Eq. 1-2], (110).

$$\text{Eq. 1} \quad M + L \rightleftharpoons ML; \quad M + L = \frac{[ML]}{([M][L])} \qquad \text{Eq. 2} \quad M + L \rightleftharpoons ML, \quad M + A \rightleftharpoons MA; \; [M'] = [M] + [MA]$$

$$^{\alpha}K_{ML} = \frac{[ML]}{([M'][L])} \rightarrow {}^{c}K_{ML} = {}^{\alpha}K_{ML}\,(1 + {}^{c}K_{ML}[A])$$

Equation 1 represents the simplest model, the binding process, and the conditional binding constant ($^{c}K_{ML}$) associated with this process. The basic problem in this type of experiments is obtaining accurate concentrations of the species in solution (the metal M, the ligand L, and the complex ML) (110).

$$\text{Eq. 3} \quad Me + MF \quad Me + MF \xleftarrow{K(Me-MF)} K\,(Me - MF) = \frac{[Me][MF]}{[Me - MF]}$$

$$\text{Eq. 4} \quad Me + BcII \xleftarrow{K(mononuclear)} Me + Apo - BcII$$

$$\text{Eq. 5} \quad Me_2 + BcII \xleftarrow{K(binuclear)} Me + Me - BcII$$

It has been proposed that the upper limit for $^{c}K_{ML}$ is 20 times the reverse concentration of the observed molecule in the spectroscopic studies (111). The idea of introducing a competitor (A) in this type of experiment was developed in order to lower the equilibrium concentration of the free metal ion (M') so that the apparent stability constant $^{a}K_{ML}$ of the observed ligand decreases sufficiently to permit its determination (110). Using this approach, data can be fitted using a model proposed in Eq. 2. Overall, a competitor must not interfere with the binding process and control experiments must be carried out to exclude the possibility of any ternary complex formation (MLA) (110). In 2000 Valladares et al. studied the binding of the metal ions Zn(II), Cd(II) and Cu(II) to the B2 type MBL, CphA using two chromophoric chelators, quin-2 (to chelate the Zn(II) and Cd(II)) and phen-green (to chelate the Cu(II)), titrating the apo-enzyme at different protein/indicator ratios (1:1, 1:2. 1:3 respectively) (112). The change in absorbance was monitored at 266 nm for quin-2 and 493 nm for phen-green to determine the dissociation constants for the first metal ion bound to the apo-enzyme ($Kd'_{Zn(II)}$ 7±2 pM; $Kd'_{Cd(II)}$ 60±10 pM; $Kd'_{Co(II)}$ 220±25 nM; $Kd'_{Cu(II)}$ 620±55 nM, at pH 6.5. $Kd'_{Zn(II)}$ 6±2 pM; $Kd'_{Cd(II)}$ 80±7 pM; $Kd'_{Co(II)}$ 330±40 nM; $Kd'_{Cu(II)}$ 550±58 nM at pH 7.5). They have also determined the dissociation constant for the second metal ion bound to the apo-enzyme using equilibrium dialysis ($Kd''_{Zn(II)}$ 40±6 μM; $Kd''_{Cd(II)}$ 82±8 μM; $Kd''_{Co(II)}$ > 5 mM; $Kd''_{Cu(II)}$ <10 μM M, at pH 6.5. $Kd''_{Zn(II)}$ 10±3 μM M; $Kd''_{Cd(II)}$ 4±2 μM; $Kd''_{Co(II)}$ 500±48 μM; $Kd''_{Cu(II)}$ <20 μM at pH 7.5)[Table 1a] (112). The first attempt to obtain the metal ion binding constants of the B1 type enzyme BcII was conducted by de Seny et al. in 2001 (97). They used a competition type of assay between the enzyme and the chelator MF to obtain the binding constants of the two metal ion sites Zn1 and Zn2 for the B1 enzyme BcII and the following mutants H86S, H88S, and H149S (with a point mutation in the Zn1 site) and D90N, C168S, and H210S with a point mutation in the Zn2 site) (97). Following the changes in the emission band (at 340-360 nm) of the M(II)-MF complex with and without the enzyme at different metal ions concentrations, the metal ion binding constants are obtained using the following equations Eq. 3-5 (97) [Table 1a]. In conclusion, this study is consistent with the presence of two metal ion binding sites with different affinities, with the first metal ion binding with

an affinity that is at least two orders of magnitude greater than the affinity of the second site $Kd'_{Cd(II)}$ 8.3±0.5 nM, $Kd''_{Cd(II)}$ 5.9±1.0 μM for the wild type, $Kd'_{Cd(II)}$ 3.8±0.3 nM, $Kd''_{Cd(II)}$ 1.4±0.1 μM for the H88S mutant. In the study of Wommer, the fluorimetric chelator Mag-Fura-2 was used to determine the metal ion binding of the most representative MBLs from three different classes: the B1 enzymes BcII and BlaB, the B2 enzyme CphA and the B3 enzyme L1 (98). Upon measuring the dissociation constant of the complex MF-Zn(II) and the extinction coefficient of MF at the wavelength used in the titration experiment ($Kd'_{Zn(II)}$ 0.62±0.08 nM, $Kd''_{Zn(II)}$ 1.50±0.71 μM for the wild type, $Kd'_{Zn(II)}$ 5.30±2.34 nM, $Kd''_{Zn(II)}$ 0.32±0.11 μM for the H86S mutant, $Kd'_{Zn(II)}$ 0.38±0.15 nM, $Kd''_{Zn(II)}$ 1.13±0.19 μM for the H88S mutant, $Kd'_{Zn(II)}$ 3.11±0.05 nM, $Kd''_{Zn(II)}$ 0.19±0.02 μM for the H149S mutant, $Kd'_{Zn(II)}$ 2.00±0.39 nM, $Kd''_{Zn(II)}$ 5.02±2.39 μM for the D90N mutant; $Kd'_{Zn(II)}$ 0.61±0.19 nM, $Kd''_{Zn(II)}$ 2.34±0.59 μM for the C168S mutant; $Kd'_{Zn(II)}$ 0.43±0.11 nM, $Kd''_{Zn(II)}$ 2.53±0.50 μM for the H210S mutant), the competition experiments were conducted with MF/enzyme ratios of 1:1 and 1:3 (97). In order to obtain the binding constants upon metal binding in the presence of the substrate, a competitive type of assay using EDTA was carried out to define the concentration of the free metal ions in solution $[Zn(II)]_{free}$ (98). Essentially, substrate hydrolysis was monitored at different $[Zn(II)]_{total}/[EDTA]_{total}$ ratios, treating the system effectively as a titration (98). Subsequent numerical analysis was carried out using Eq. 6, where $\kappa_{app,ZnE}[ZnE]$ and $\kappa_{app,Zn2E}[Zn2E]$ were the apparent specific activities for the mono- and the di-zinc enzyme respectively, and ν_{obs} is the activity observed at specific ratios $[Zn(II)]_{total}/[EDTA]_{total}$ (98). For more details regarding the mathematical analysis see the reference (98) (Eq. 5-12).

Eq. 6 $$\nu_{obs} = k_{app,\,ZnE}[ZnE] + k_{app,\,Zn2E}[Zn2E]$$

A similar approach was used by Rasia and Vila in their work in 2002 in order to determine the metal ion binding constants of the BcII MBL and its R121C mutant while monitoring substrate hydrolysis (benzyl penicillin) upon adding increasing concentrations of Zn(II) (113). The assumption made here is that the activity of the enzyme increases proportionally with the metal concentration considering the apo-enzyme completely inactive, the mono-zinc enzyme partially active and the di-zinc enzyme completely active (113). Experimental data were fit using Eq. 7, where *a* and *b* represent the hydrolysis rates for the mono- and bi-nuclear enzyme and K_{D1} and K_{D2} are the binding constants (apparent dissociation constants) for the two zinc equivalents in presence of substrate (113).

Eq. 7 $$\text{rate} = \frac{a}{\frac{[Zn]}{KD2}+1+\frac{KD1}{[Zn]}} + \frac{b}{1+\frac{KD2}{[Zn]}+\frac{KD1 \cdot KD2}{[Zn]}}$$

In 2009, Jacquin et al. measured the metal ion binding constant of the BcII MBL using a competition assay and the competitor MF (114). While their experimental conditions were very similar to those used by de Seny et al, they have obtained a completely different value for the second metal binding event, estimating a binding constant to be > 80 nM (see Table

1a) (97; 114). These findings were in agreement and supported by the study of Badarau and Page, who used the Isothermal Titration Calorimetry (ITC) to study the metal ion binding of the BcII enzyme (115). Another chelator often used in metal ion binding studies is PAR as it weakly binds zinc ions and therefore, can be used to quantify the chelated zinc ions. Similarly to MF, this compound can be used to determine the binding constant of the enzyme-metal complex, following the change in absorbance at 500 nm (106; 108). In the study by Gonzalez et al., PAR assay was used to determine the binding constant for the second zinc site of the two double mutants of BcII MBL, BcII-R121H/C221S (BcII-HS) and BcII-R121H/C221D (BcII-HD), in the presence of the substrate nitrocefin (9). As they were unable to determine the value of the binding constant of the first zinc site, they have used the value obtained by de Seny in 2001 to fit the experimental data (97; 9). They evaluated the K_{D2} for the second site of both mutants to be 18.3±12.9 μM for the mutant BcII-HS and less than 0.2 nM for the mutant BcII-HD (see Table 1a) (9). In the study by Thomas et al. in 2011, PAR was used again to determine the affinities of the zinc ions to the B1 subclass enzyme NDM-1 (109). Their objective was to determine if one of the two zinc ions bound to the enzyme had a weaker affinity. In their study, the di-zinc enzyme was incubated with PAR and the absorbance was measured at the specific wavelength of 500 nm (109). The experiment was also conducted under denaturing conditions to evaluate the binding of the tightly bound zinc ion (109). The metal ion binding constants for the second zinc site in NDM-1 MBL is reported to be 2 μM, but it was not possible to evaluate the value of the metal binding constant of the first zinc site (109) (see Table 1a). According to the reported values of the metal ion binding constants for various MBLs using PAR assays (see Table 1a), there seems to be a rather large discrepancy in the values of binding constants obtained experimentally. Therefore, PAR assay can only be used reasonably well to estimate the concentration of the metal ions bound within the enzyme.

1.4 Absorption Spectroscopy Studies

The electronic spectroscopy, or UV/Vis absorption spectroscopy, typically follows the change in the absorption spectra between 300 nm and 700 nm of the protein upon titration with the metal ion species (97; 110; 116; 104). The addition of metal ions to the apo-enzyme perturbs the UV/Vis spectra of the enzyme allowing the determination of the stoichiometry and binding constants of the process (110). The experimental data obtained are used to determine the extinction coefficient of the metal ions, which leads to the concentration of the metal ion bound to the enzyme that can be used to obtain the metal ion binding constant. In 2001 de Seny at al. measured the metal ion binding constants for Co(II) in BcII and several of its mutants, H86S, H88S, H149S, D90N, C168S, and H210S (97). During the Co(II) titration of the apo-enzyme, the appearance of different bands, the intensity was proportional to the metal ion concentration, allowed the determination of the metal ion binding constants (experimental data were fitted using a two-step binding model (Eq. 4), (see Table 1b) (97).

1.5 Kinetics of the metal ion binding monitoring fluorescence intensity

This methodology is based on the selection of a unique signal in the spectra that is proportional to the concentration of an individual component of the reaction studied, thereby directly allowing the change in the concentration of the selected component to be followed to determine the binding constant ${}^{c}K_{ML}$ (110). The fluorophore chosen as the indicator of the binding process can be a component of the biomolecule itself or an external compound that follows the reaction (110). Generally, two mechanisms are used to follow a biological process by fluorescence spectroscopy: i) the change (increase or decrease) in the fluorescence intensity of the fluorophore due to a conformational change in the biomolecule upon binding (117); and ii) the quenching of fluorescence (total or partial) by increased relaxation of the excited state, facilitated by a metal bound in the proximity of the fluorophore (117). Proteins have two intrinsic fluorophores which are the amino acids tyrosine and tryptophan. The first is less sensitive as a probe but the data collected are easier to analyse, because only the intensity of fluorescence is affected by the binding, not the emission wavelength (110; 117; 118). Conversely the tryptophan is more sensitive (ca. 5-fold stronger intensity) but both the intensity and the emission wavelength are affected by the binding process (118). Instead of using an intrinsic fluorophore, an extrinsic fluorophore can be added to the system as a competitor, to follow the conformational change upon metal ion binding (110; 117; 118). In the 2001 study by de Seny et al., the kinetics of metal ion binding was studied by measuring the change in the fluorescence intensity upon addition of metal ions, Zn(II), Co(II) and Cd(II) to BcII MBL. A mixture of the free-enzyme mixed with different metal ions concentrations were used to detect the fluorescence emission at wavelengths above 320 nm. They were able to determine the apparent association rate constants reported to be kon 1 14.1±0.3 µM-1 s-1 for the Zn(II), kon 1 0.28±0.01 µM-1s-1 for the Co(II), kon 1 26.0±1.3 µM-1s-1 and kon 2 0.50±0.01 µM-1s-1 for the Cd(II) (see Table 1c) (97).

Enzyme	Substrate	K_{D1} nM Zn(II)	K_{D1} nM Cd(II)	K_{D1} nM Co(II)	K_{D1} nM Cu(II)	K_{D2} μM Zn(II)	K_{D2} μM Cd(II)	K_{D2} μM Co(II)	K_{D2} μM Cu(II)
	No	0.62 (±0.08)[1]				1.50 (±0.71)[1]			
	No	0.66 μM[3]				890 μM[3]			
BcII WT	No	1.8 (±0.3) nM[5]	8.3 (±0.5)[1]			1.8 (±0.3) μM[5]	5.9 (±1.0)[1]		
		ND[6]				> 80 nM[6]			
	Imipenem	13.6 (±5) pM[5]				0.8 (±0.2) μM[5]			
H86S	No	5.30 (±2.34)[1]	ND			0.32 (±0.11)[1]	ND		
H88S	No	0.38 (±0.15)[1]	3.8 (±0.3)[1]			1.13 (±0.19)[1]	1.4 (±0.1)[1]		
H149S	No	3.11 (±0.05)[1]	ND			0.19 (±0.02)[1]	ND		
D90N	No	2.00 (±0.39)[1]	ND			5.02 (±2.39)[1]	ND		
C168S	No	0.61 (±0.19)[1]	ND			2.34 (±0.59)[1]	ND		
C168A	No	ND	ND			ND	ND		
H210S	No	0.43 (±0.11)[1]	ND			2.53 (±0.50)[1]	ND		
R121C	No	3.6 μM[3]				570 μM[3]			
BcII-HS	Nitrocefin	ND[120]				18.3 (±12.9) μM[120]			
BcII-HD	Nitrocefin	ND[120]				< 0.2 nM[120]			
BlaB	No	5.1 (±1.5) nM[5]				0.007 (±0.002) μM[5]			
	Nitrocefin	1.8 (±0.2) pM[5]				0.025 (±0.004) μM[5]			
NDM-1	No	ND	ND	ND	ND	2 μM[7]			
	No	7 (±2) pM[4] (pH 6.5)	60 (±10) pM[4] (pH 6.5)	220 (±25) pM[4] (pH 6.5)	620 (±55) pM[4] (pH 6.5)	40 (±6) μM[4] (pH 6.5)	82 (±8) μM[4] (pH 6.5)	>5 mM[4] (pH 6.5)	<10 μM[4] (pH 6.5)
CphA WT	No	6 (±2) pM[4] (pH 7.5)	80 (±72) pM[4] (pH 7.5)	330 (±40) nM[4] (pH 7.5)	550 (±58) nM[4] (pH 7.5)	10 (±3) μM[4] (pH 7.5)	4 (±2) μM[4] (pH 7.5)	500 (±48) μM[4] (pH 7.5)	<20 μM[4] (pH 7.5)
	Imipenem	1.2 (±0.2) pM[5]				1.9 (±0.3) μM[5]			
L1 WT	No	2.6 (±1.0) nM[5]				0.006 (±0.002) μM[5]			
	Imipenem	5.7 (±2.0) pM[5]				0.12 (±0.03) μM[5]			

Table 1a. Dissociation constants for the first (K_{D1}) and the second (K_{D2}) metal bound, obtained using competitive assays **(97; 9; 113; 112; 98; 114; 109)**

Enzyme	K_{D1} μM Co(II)	K_{D2} μM Co(II)
BcII WT	0.093 (± 0.015)[1]	66.7 (± 10.0)[1]
H86S	10.5 (± 1.5)[1]	ND
H88S	9.1 (± 1.1)[1]	ND
H149S	2.7 (± 0.3)[1]	ND
D90N	20.0 (± 3.5)[1]	ND
C168S	3.1 (± 0.4)[1]	ND
C168A	1.1 (± 0.1)[1]	ND
H210S	0.35 (± 0.05)[1]	ND

***Table 1b. Dissociation constants of Me1 and Me2 species of wild type and mutant BcII against Co(II)using absorption spectroscopy* (97)**

Zn(II)		Co(II)		Cd(II)	
κ_{on1} $\mu M^{-1}s^{-1}$	κ_{on2} $\mu M^{-1}s^{-1}$	κ_{on1} $\mu M^{-1}s^{-1}$	κ_{on2} $\mu M^{-1}s^{-1}$	κ_{on1} $\mu M^{-1}s^{-1}$	κ_{on2} $\mu M^{-1}s^{-1}$
14.1 (± 0.3)[1]	ND	0.28 (± 0.01)[1]	ND	26.0 (± 1.3)[1]	0.50 (± 0.01)

Table 1c. Comparison of Zn(II), Co(II), and Cd(II) metal ions

1.6 Kinetics of the metal ion binding using Isothermal Titration Calorimetry (ITC)

Isothermal titration calorimetry (ITC) is a very powerful tool which can be used to study small molecule interactions, such as the one occurring during the binding of a metal ion to a protein metal centre. During an ITC experiment, the instrument measures the heat generated from a reaction taking place in a sample cell and compares it with the heat of a reference cell (110; 119). This differential heat represents the change in enthalpy (ΔH) due to the reaction (119). The system maintains the temperature balance between sample and reference cells using a certain amount of power that leads to the heat released (exothermic reaction) or absorbed (endothermic reaction) by the process (119). Analysing the signals obtained which generates a thermogram, all thermodynamic parameters can be determined, such as the

stoichiometry of the reaction; the association constant (K_a); the change in the Gibbs free energy (ΔH) and the variation in enthalpy (ΔH) and entropy (ΔS) [Eq. 8 and Eq. 9] (119).

In contrast to the measurements of metal ion binding constants obtained using colorimetric assays and absorption spectroscopy, the thermodynamic parameters obtained using ITC are a direct measure of the binding process (110; 119). It is possible to evaluate the heat capacity of metal ion binding when performing experiments at different temperatures. The change in heat capacity (ΔC_p) can be calculated using Eq. 10. The principal contribution to the change in the heat capacity is due to displacement of the structured water molecules around non-polar region of the protein (119). For this reason, the information of the ΔC_p is useful in order to understand the nature and extent of the protein surface involved in the binding process (119). Surprisingly, even though the ITC technique is nowadays one of the most precise and specific methods to evaluate the thermodynamic parameters and the dissociation constants of a reaction, only one study has been published reporting the use of ITC to study the binding of the zinc metal ion to a mutant of the B1 subclass MBL, IMP-1 (100). In 2012 Horton et al. used the ITC technique to measure the dissociation constant of the Zn2 site of the mutant C221G of IMP-1, which was purified with the Zn1 site occupied by the first zinc ion (100). They evaluated a binding constant to be 17 μM, with the reaction driven by enthalpy energy. In the same work they used a thermofluor assay and an activity assay against nitrocefin as substrate to evaluate the binding constant for the same mutant (100). The experimentally obtained dissociation constants were found to be of the same order of magnitude as those obtained using ITC, 30 μM and 43 μM respectively.

Conclusions

Presented discussion of the available metal ion binding data so far for MBLs indicates that it is not easy to find common behaviours in the binding of the metal ions to the three subclasses of MBLs. Moreover, even within the same subclass, very different metal ion binding affinities are often found. In the literature there is considerable discrepancy about the affinity of the metal ions to these enzymes with K_d values ranging from the picomolar to the micromolar range (15; 97; 98). There is also significant inconsistency observed in the K_d values obtained for the same enzyme under different experimental conditions and using different techniques. Surprisingly, even though MBLs were first discovered around 40 years ago, there is still a lack of comprehensive study that compares the metal ion binding of the three MBL subgroups. To date, no attempt has been made to investigate the interactions between the metal ions and representatives of the three MBL subgroups under identical experimental conditions. A systematic approach in the study of the metal ion binding of the MBLs could significantly improve our knowledge of the catalytic mechanism and the biological relevance of the metal ion. Although we can speculate on the necessity of the metal ion centres for these enzymes to work, an in-depth knowledge of the behaviour of the metal ion(s) and its/their precise role(s) within the enzyme mechanism is essential. Thus, depending on how the metal ions bind/interact with MBLs it may be possible to find an optimum target to inhibit all the subclasses of the MBLs and develop potent universal inhibitors (7).

****

1.7 Since Publication of Review

To the author's knowledge no universal inhibitor has been discovered or engineered since the time of writing this review article in 2014. The number of researchers in this topical area has increased, and the knowledge base has increased regarding MBL's (120; 121; 122; 123; 124), and including NDM-1 and NDM-3 more specifically (6; 5; 125; 126).
Of this knowledge increase the most pertinent was an advancement made regarding the categorising of the MBL subgroups, more specifically, the discovery of a fourth subgroup. This new subgroup termed the B4 subgroup by the Ollis, Schenk, and Mitic groups (which includes the author of this thesis as a co-author) (127), was found when researching *Serratia Proteomaculans* (SPR-1) and a close homologue named *Cronobacter Sakazakii* (CSA-1). CSA-1 was found with 60% sequence identity with SPR-1. Both were compared with B1, B2, and B3 type MBL's using ClustalW2.1. B3 type was the closest group to SPR-1 and CSA-1 with ~30% sequence identity, and B1 and B2 types ~16% sequence identity with CSA-1. Hou et al., list the full table of CSA-1 comparison with representatives from B1, B2, and B3-type MBL's (127). The partial multiple sequence alignment carried out highlights the differences between the now B4 subgroup enzymes, and the other three subgroups. Contrastingly to the others, it is thought that the B4 subgroup contains only one Zn^{2+} ion when in resting form and then the second Zn^{2+} binds when in the presence of substrate, i.e., when in the active state. Hou et al, also highlighted the presence of different sequence motifs of residues around the metal binding sites making these two enzymes substantially different from the others. Generally, the residues around the metal binding sites in B1-B3 type MBL's are conserved. For B4-type subgroup SPR-1 differs in the M1 site where an arginine residue replaces His118. In the M2 site the Asp120 is conserved, but either Gln121/Ser 221 replaces Cys221/His121, and Asn262 replaces His263 (127). This was an interesting advancement on the classification of the metallo-β-lactamase subgroups, and the presence of the newer B4 subgroup is indeed a positive step towards learning more about these complex enzymes.

While plenty of research that has been undertaken is for MBL-like or non-pathogenic MBL's, congruently a lot of research has been going into investigating pathogenic MBL's which impact human health, most notably the superbug NDM-1 (128; 129; 130) and this is for very good reason. In the time since this publication and subsequently the generation of data for this research thesis, more focus has been placed on investigating inhibitors or potential inhibitors. Since 2019, a lot of promising inhibitor candidates have been discovered and are being investigated (131), for example Cefiderocol was approved by the FDA in 2019 and is in use for B1-type MBLs as a cephalosporin-based antibiotic (132). As NDMs are some of the most pathogenic of the MBLs a lot of inhibitor-based research has been conducted in recent years for NDM-1 (133; 134; 135; 136; 137), and the following focused on NDM-1 and its variants, including NDM-3 (138).

In 2022 an article was published taking into consideration what impact the Covid-19 pandemic may have had on antibiotic resistance and the threat it poses (139). The need for inhibitors and/or new treatment options for bacterial infections is still as important as ever.

1.8 NDM-1

NDM-1 (New Delhi metallo β- lactamase) is considered the most dangerous MBL because any bacterium that contains NDM-1 is classed as a superbug as it is highly resistant to all known antibiotics. NDM-1 is a B1-type MBL and has a molecular weight of 28.5kDa. At present it is considered the most virulent and pathogenic known MBL (43; 47; 48; 49; 50; 51; 52; 53). It consists of 270 amino acids, two metal ions in the metal centres, and contains the signature αββα sandwich. It has lower sequence identity to its nearest group member, VIM-2 than most members of a subgroup would have to their nearest group members. Its sequence similarity to VIM-2 is determined to be ~ 38%. It is an oligomer meaning it can exist as both a monomer and a dimer in solution. Interestingly it is alongside only L1 (a B3-type MBL) as an oligomer. Where NDM-1 differs from other known B1 type MBL's is the presence of an extra β-strand extension at the N-terminus and the elongated L3 loop (as seen in Figure 1h). It is a lipoprotein, meaning the protein is bound to lipids, which allows fats to move through the water inside and outside the cells. NDM-1's metal centres generally M1 occupancy is higher than M2. It is capable of spreading by horizontal gene transfer which makes it even more dangerous to human health as once a bacterium contains NDM-1 it is then resistant to all antibiotics. It is a major threat to human health, and by 2015 it had spread to sequence identity to other B1 type MBL's, but contains the signature motifs and αββα sandwich. It has now spread to more than 70 countries, and is widespread in India, where it got its name (140; 52; 141).

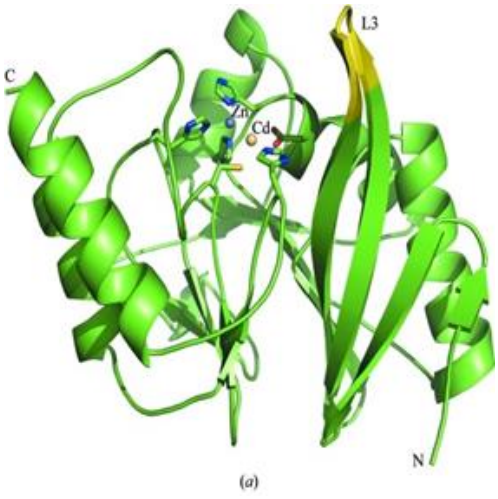

Figure 1h. The structure of NDM-1 shows that the protein contains the αβ/βα sandwich common to all MBLs despite the low sequence identity between NDM-1 and other metallo-β-lactamases. The metal-chelating residues within the active site are displayed as sticks. The zinc ion is coloured blue and the cadmium ion is coloured fawn. Flexible loop L3, which is proposed to play a role in substrate binding, is highlighted in yellow (141).

1.9 NDM-3

NDM-3 is a variant of NDM-1, differing from NDM-1 by a single amino acid. NDM-3 has a molecular weight of 28498 Da. The single amino acid substitution from NDM-1 is an asparagine replaces an aspartic acid residue (negatively charged amino acid replaced by a hydrophilic, neutral amino acid). The substitution occurs on the surface of the protein and alters the interactions with the side chains of various β-lactam antibiotics. As evident below in Figure 1i, the active site structure of NDM-3 is very similar to that of NDM-1 shown in Figure 1h above. This active site structure was developed during this research and is detailed in Section 3.3 of this thesis. At the time of authors research, very little was known about this variant of NDM-1, and so all characterisation works have been detailed in Chapters 3 and 4 of this thesis.

Figure 1i. Active site structure of NDM-3

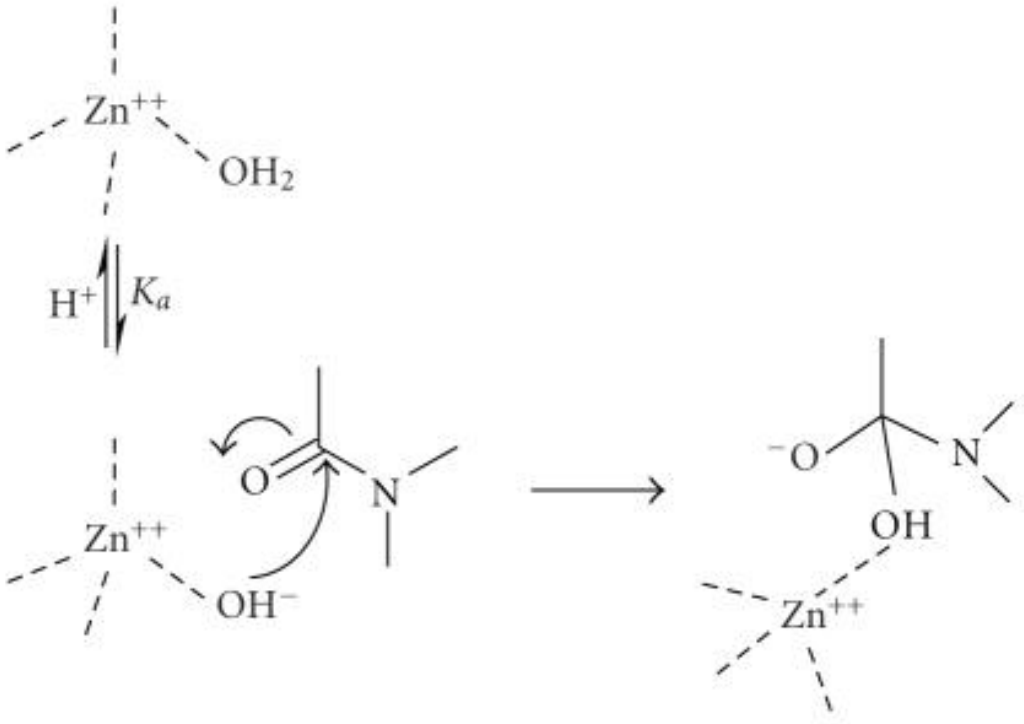

Figure 1j. Proposed mechanism for MBL's containing 2 metal ions (41).

Figure 1j is from ‘The Mechanisms of Catalysis by Metallo β-Lactamases’ by Page and Badarau from 2008 (41). As NDM-3 is a B1-type MBL and therefore contains 2 metal ions, this is the proposed mechanism of action for NDM-3 (41).

Chapter 2 – Materials and Methodologies

This chapter outlines the experimental materials and methods used for this research. The expression and purification of NDM-3, followed by the cleavage of ubiquitin tag, and the kinetic assays and pH profile, required an understanding of the enzyme microbiology, protein purification, and enzyme kinetics.

2.1. Materials

The materials used are sub-divided into two further sections

1. Chemicals, Reagents, and Solutions
2. Instrumentation and Software

2.1.1. Chemicals, Reagents, and Solutions

Chemicals were purchased from Sigma Aldrich unless stated otherwise. All chemicals were of analytical grade or higher.

Vectors

Two NDM-3 mutants were used during this research project – NDM-3 with the ubiquitin tag, henceforth denoted as NDM-3+Ub, and NDM-3 without the ubiquitin tag, denoted for clarity as NDM-3(NC), which denotes newer construct. Both were cloned into the commercial vector pHUE. NDM-3+Ub was expressed as a hexa-histidine-ubiquitin fusion protein and NDM-3(NC) was expressed with a hexa-histidine tag alone. Hexa-histidine tags aid in purification process (142; 143) and are based on the pET15b vector. Ubiquitin tags aid in increasing expression, and purification yield (144). USP2cc protease was expressed on pET15b vector. NDM-3+Ub, NDM-3(NC), and USP2cc are all selectively resistant to ampicillin (100 µg/mL). The three enzymes were obtained from a lab in University of Queensland, Brisbane, Australia, from Prof. Gary Schenk.

Expression

Cells

E. coli BL21(DE3) Competent Cells [purchased from Agilent] were used for recombinant expression of each protein.

LB Agar

10 g Tryptone, 5 g Yeast Extract, 10 g Sodium Chloride, 15 g Agarose was made up to 1 L dH_2O

LB Media

10 g Tryptone, 5 g Yeast Extract, 10 g Sodium Chloride made up to 1 L dH_2O

Ampicillin Stock Solution

100 mg/mL solution made up by adding 1 g of ampicillin to 10 mL dH_2O

Isopropyl β-D-1-thiogalactopyranoside (IPTG) Stock Solution
1 M solution of IPTG was made up by adding 2.38 g to 10 mL dH_2O.
Ten 1 mL aliquots were frozen at -20°C.

Magnesium Chloride Standard Solution
100 mM solution of $MgCl_2$ was made by adding 4.7605 g to 250 mL dH_2O.

Zinc Chloride Standard Solution
0.5 M $ZnCl_2$ Solution made up by adding 0.6815 g to 10 mLs dH_2O

Purification Standard Solutions
Imidazole Standard Solution
1 M Standard was made up by adding to 500 mLs of dH_2O

HEPES Standard Solution
0.5 M Standard was made up by adding to 500 mLs of dH_2O

Sodium Chloride Standard Solution
4 M Standard Solution was made up by adding to 500 mLs of dH_2O

Buffers – Optimised Buffer Conditions
Lysis Buffer
50 mM HEPES, 500 µM $ZnCl_2$

Binding Buffer
50 mM HEPES, 500 mM NaCl, 20 mM Imidazole

Elution Buffer
50 mM HEPES, 500 mM NaCl, 100 mM Imidazole

Dialysis Buffer 1
50 mM HEPES, 500 mM NaCl, 50 mM Imidazole

Dialysis Buffer 2
50 mM HEPES, 500 mM NaCl

Assay Buffer
50 mM HEPES, 50 mM NaCl, and 0 mM $ZnCl_2$

pH Standard Solutions
Hydrochloric Acid
1M solution was made up by adding 3.65 g HCl to 100 mL dH_2O

Sodium Hydroxide
1 M solution was made up by adding 10 g NaOH to 250 mL dH_2O

SDS-PAGE Solutions/Reagents

Staining Solution
Coomassie Brilliant Blue R-250 Staining Solution [purchased from Bio-Rad].

De-staining Solution
Solution made up by mixing dH_2O: Methanol: Acetic acid in a 50: 40: 10 ratios.

Marker
Precision Plus Protein Dual Xtra Standard Marker was used [purchased from Bio-Rad].

Loading Dye
2X SDS Loading dye [purchased from Bio-Rad]. Working solution of loading dye was made up by adding 5 mL of stock 2 X loading dye to 5 mL dH_2O.

SDS Running Buffer
Pre-mixed 10X electrophoresis buffer [purchased from Bio-Rad] was used. Running Buffer was made up by adding 100 mL of purchased buffer to 900 mL dH_2O.

Antibiotic Stock Solutions

Each of the antibiotic stocks were made up into 10X 1mL aliquots.

Ampicillin 10 mM
0.037139 g was added to 10 mL dH_2O.

PenicillinG 10 mM
0.035637 g was added to 10 mL dH_2O.

Meropenem 10 mM
0.043751 g was added to 10 mL dH_2O.

Imipenem 10 mM
0.031736 g was added to 10 mL dH_2O.

Cefoxitin 10 mM
0.044943 g was added to 10 mL dH_2O.

Cephalothin 10 mM
0.041842 g was added to 10 mL dH_2O.

N-3-oxo-octanoyl-L-Homoserine Lactone 10 mM
0.012065g was added to 10mL dH_2O.

Phenol Red Solution 10 mM
0.035438g was added to 10mL dH_2O.

2.1.2. Instruments and Software

The instruments used during the experiments included

- AKTAPurifier UPC10 FPLC
- Mason Technology UV-2550 Spectrophotometer
- Mason Technology Autoclave
- Thermo Scientific Incubator
- Bio-Rad Protean Tetra System and Power Pack
- Thermo Scientific MaxQ Shaker
- Thermo Scientific Centrifuge
- DELL desktop computer

Software used included

- UNICORN for FPLC,
- UVProbe for UV-Vis,
- Multiple Dell computers were used to analyse and collect the data.

Data Recording and Analysis

Microsoft Excel and Kaleidagraph were used to analyse the raw data from the UV-Probe and apply Michaelis-Menten curve to them.
The assays were performed in duplicate or triplicate generally in order to obtain accurate results.

2.2 Methodologies

The methodologies used to carry out the experiments are outlined below.

Transformation

Plasmid (5 µL) and 100 µL of *E. coli* BL21(DE3) Competent Cells were mixed and placed on ice for 30 minutes. Subsequently the solution underwent heatshock for 45 seconds at 42 °C, and again was placed on ice for a further 2 minutes (145). The solution was then either plated directly onto previously made-up LB Agar plates containing 100 µg/mL ampicillin, or 750 µL of autoclaved LB Media was added prior to plating. This only occurred when the colonies were too numerous or clustered when plated directly. The solution was then incubated for 16-18 hours at 37 °C. Once colonies had formed, plates were stored at 4 °C.

Expression of Proteins

Starter Culture

A colony was selected and added to 10 mL of autoclaved LB Medium and 100 µg/mL of ampicillin. This was shaken at 37 °C and 200 rpm for 15 hours (146; 147).

Cultures

Recombinant NDM-3 for both NDM-3+Ub and NDM-3(NC) was expressed by transferring the starter culture above into flasks containing 500 mLs of autoclaved LB Broth and 100 µg/mL ampicillin. The cultures were left to shake at 200 rpm at 37 °C for 1 hour with 0.1M $ZnCl_2$. IPTG (1 mM) was added once OD600 reached between 0.5-0.8 and the temperature was reduced to 18°C for 48 hours.

Centrifugation

Samples were centrifuged at 5000 x g for 20 minutes at 4 °C. The pellet contained the enzyme. Enzyme can be stored at -80 °C at this point if necessary.

Sonication and Centrifugation

The sample was re-suspended in the smallest volume of lysis buffer possible (15 ml to 20 mL). Lysozyme was added (1 mg/mL) to improve the lysis process and the resuspended pellet was incubated for 30 minutes at room temperature with gentle agitation. Following this, 5 mM MgCl2 and 20 µg/mL DNAse I was added and the sample was incubated on ice for 15 minutes.

The cells were then disrupted by 3 rounds of sonication for 30 seconds at 20% power. The cells were kept on ice to avoid overheating.

The lysate was centrifuged at 10000 x g for 25 minutes at 4 °C and filtered through a Millipore 0.22 µm membrane to remove any remaining impurities (147).

FPLC – Fast Protein Liquid Chromatography

Supernatant was loaded onto HisTrap FF Crude 5mL Column (GE Healthcare) and the method was run on an AKTAPurifier UPC10 in a cold room (between 4°C – 8°C). The column was pre-equilibrated with binding buffer (50 mM HEPES, 500 mM NaCl, 20 mM imidazole, pH 7.5) and the protein was eluted as a single peak in a step gradient of imidazole concentration going from 20 mM to 100 mM and eluted as a single narrow peak. The relevant fraction(s) were pooled and SDS-PAGE analysis was run. The protein eluted as a single peak, in a single step going from 0% Elution Buffer to 100% Elution Buffer (148).

Affinity Chromatography

Affinity Chromatography is a chromatography method that uses highly specific interactions to separate biochemical mixtures. These highly specific interactions include; antigens and antibodies, receptors and ligands, or enzyme and substrate.

Nickel Affinity Chromatography

Immobilized Metal Affinity Chromatography (IMAC), an enzyme and substrate type of affinity chromatography, was used during this experiment with Nickel as the metal. IMAC works particularly well for purification of histidine-tagged proteins and allows for a 'one step' purification step (142; 149; 150). The hexa-histidine tagged protein binds to the Nickel resins in the column, and imidazole is used as the eluting agent in the Elution buffer at high concentrations – 100 mM in this instance. The imidazole is used as a competitor to the histidine tagged protein and so when added in higher concentrations of imidazole in the elution buffer, imidazole replaces the protein at the binding sites and the protein elutes from the column.

USP2cc Protease - Expression, Chromatography and Cleavage of NDM-3+Ub

Methodologies were purposefully kept as like the steps listed above for NDM-3 expression as possible for the sake of consistency.

Transformation

Plasmid (2 µL) and 100 µL of BL21 (DE3) Competent Cells were mixed and placed on ice for 30 minutes. The solution then underwent Heatshock for 45 seconds at 42 °C, and was placed on ice for a further 2 minutes. Autoclaved LB Media (750 µL) was added, and the sample thoroughly mixed. The solution was then incubated for 16-18 hours at 37 °C. Once colonies had formed, plates were stored at 4 °C.

Expression of USP2cc Protease

Starter Culture

As per NDM-3 protocol outlined above.

Cultures

Recombinant USP2cc was expressed by transferring the starter culture above into a flask containing 500 mLs of autoclaved LB Broth and 100 ug/mL ampicillin. The cultures were left to shake at 200 rpm at 37 °C for 1 hour.
IPTG (0.4 mM) was added once OD600 reached between 0.5-0.8 and the temperature was reduced to 18 °C for 6 hours.

Centrifugation, Sonication, and FPLC

As per NDM-3 protocols outlined above.

SDS-PAGE

Samples for SDS-PAGE were prepared by mixing the enzyme and loading dye together in a 1:1 ratio. The samples were heated at 100 °C for 5 minutes and then loaded onto Mini Protean TGX Precision Gels (Bio-Rad).
Electrophoresis was run at 140 V for 1 hour using Mini PROTEAN Tetra System (Bio-rad). Precision Plus Protein Dual Xtra Standard Marker was used (Bio-rad).
When electrophoresis was finished gels were placed in fresh dh_20 three times for 5 minutes. The gel was placed in Coomassie Brilliant Blue R-250 staining solution (Bio-rad) for 1-2 hours, and then placed in fresh de-staining solution (dH_2O: Methanol: acetic acid - 50: 40: 10 ratio) two or three times until bands were clearest and visible (147; 150).
Gels were then analysed by comparison to marker. The images of these gels are included in Chapter 3 – Expression and Purification of NDM-3.

Principles of SDS-PAGE

SDS-PAGE is an electrophoresis technique that separates molecules using an electric field. The full name is Sodium Dodecyl Sulfate Polyacrylamide Gel Electrophoresis (SDS-PAGE) is one of the most commonly used electrophoresis techniques (151).
The effectiveness of the method is based on the fact that SDS is anionic, and when dissolved its molecules have a net negative charge over a large pH range. The negative charges on SDS are strongly attracted to and move towards the positively charged electrode (anode) in an electric field. The protein sample binds to the SDS proportionally to its mass, so the larger molecules take longer to reach the anode. This means the sample – protein or polypeptides – are separated on their relative molecular masses. A marker protein ladder is used as a comparison in order to assign molecular weights to the bands the desired sample has shown.

Cleavage of NDM-3+Ub using USP2cc Protease

The protein concentrations of both NDM-3+Ub, and USP2cc were estimated using theoretical extinction coefficients at 280 nm (as per table 3d), which were calculated from their sequences using the ProtParam Web tool, and using the Beer Lambert Law with their absorbance values at 280 nm.

Cleavage of ubiquitin tag using USP2cc protease was attempted at different conditions as outlined in Chapter 3 – Expression and Purification of NDM-3. The samples containing different concentration ratios were incubated for differing lengths of time at different temperatures as outlined in Table 2a below. To determine which conditions were most successful for cleavage, SDS-PAGE analysis was carried out in Chapter 3 – Expression and Purification of NDM-3 (152).

Temperature	Concentration Ratio (NDM-3+Ub: USP2cc)
4 °C	200: 1
4 °C	100: 1
4 °C	50: 1
25 °C	200: 1
25 °C	150: 1
25 °C	100: 1
25 °C	50: 1
37 °C	200: 1
37 °C	100: 1
37 °C	50: 1

Table 2a. Outlining Concentration Ratio and Temperature Conditions Tested for optimal cleavage conditions

Dialysis Exchange of Buffer

Due to instability of the protein in buffer containing imidazole, a buffer exchange step was carried out from Elution Buffer (100 mM imidazole), to Dialysis Buffer 1 (50 mM imidazole), to Dialysis Buffer 2 (0 mM imidazole) using SnakeSkin Dialysis Tubing (Thermo Scientific).

The buffer exchange process took place in the cold room (4 °C - 8 °C) over minimum of 4 hours in each buffer, stirring constantly. The ratio of enzyme to buffer volume was 1:100.

UV/Vis assays and optimisation

The β-lactamase activity of the NDM-3 enzymes towards different substrates were measured spectrophotometrically by monitoring substrate depletion (153). The substrates measured were ampicillin, penicillin G, imipenem, meropenem, cefoxitin, and cephalothin. Their respective extinction coefficients and wavelengths are listed in table 2b below.

Optimisation of salt, buffer, and $ZnCl_2$ concentrations for assay buffer was carried out by measuring the increasing values of each, outlined in Chapter 4 – Enzymatic characterisation of NDM-3's resistance to β-lactam antibiotics.

Antibiotic	**Wavelength (nm)**	**E ($M^{-1}cm^{-1}$)**
Imipenem	300	9000
Meropenem	300	6500
Ampicillin	235	820
PenicillinG	235	560
Cephalothin	260	6500
Cefoxitin	260	7700

Table 2b. Table generated listing antibiotics used, and their extinction coefficients and wavelengths.

pH Profile

The effect of pH on rate of reaction of NDM-3(NC) was measured for representatives of each of the major B-lactam groups. Activity was determined for ampicillin, imipenem, meropenem, and cefoxitin over a pH range of 4.5 to 11.0 (153; 147).

Lactonase Activity

A preliminary experiment was carried out to determine if NDM-3(NC) had lactonase activity. N-3-oxo-octanoyl-L-homoserine lactone was the representative lactone used in this experiment. It was carried out as per methodology in the paper (154), adopted from previous descriptions of the method (155; 156; 157; 158; 159; 160). The methodology is synopsised below.

The activity of NDM-3(NC) toward AHL was determined by first ascertaining how much methanol needed to be included in the assay mixture, by assessing the sensitivity of NDM-3(NC) towards methanol when working with a buffer of HEPES 50 mM at pH 7.5, and using 50 mM NaCl, and 15 nM NDM-3(NC).

The AHL hydrolysis was determined by measuring proton concentration during the reaction while using an appropriate pH indicator, in this case Phenol Red in HEPES buffer.

The assay was carried out at 25 °C and at 557 nm, using 100 – 150 nM of NDM-3(NC).

To ensure an accurate reflection of enzymatic activity towards this AHL, the auto-hydrolysis of the lactone was subtracted from the enzyme-catalysed reaction. The usual catalytic parameters, V_{max} and k_{cat}, were determined using the Michaelis Menten equation as outlined in Chapter 1 – Research Background., and the results of this assay are in Chapter 4 - Enzymatic characterisation of NDM-3's resistance to β-lactam antibiotics.

Chapter 3 – Expression and Purification of NDM-3

3.1 NDM-1

As outlined in Chapter 1 in the research background section, NDM-1 is the parent MBL to NDM-3, the variant studied in these works. Comparisons of characterisation work will be used from literature. In Table 3a, the results are show for a BLAST Multiple Sequence Alignment that was carried out during this research works for query sequence NDM-1 against VIM-2, IMP-1, CphA, and AIM-1 in order to get the sequence identity percentage between NDM-1 and representatives of each subgroup. VIM-2 is noted as the closest in sequence alignment to NDM-1, although relatively low at 38% evidencing that while NDM family is part of B1, it is very different from its closest homologue VIM-2. It is also evident that the B1 types (IMP-1 and VIM-2) are more closely related to NDM-1, followed by the other di-metallo type B3 with AIM-1 having 29% sequence identity with NDM-1. The least similar, as expected is the mono-metallo B2 type CphA MBL with 25% sequence identity.

Sequence comparison between NDM-1, VIM-2, IMP-1, CphA, and AIM-1

Enzyme for comparison	Identity %	Accession code	Max Score	Total Score	Query Cover	E value
NDM-1 (C7C422)	99	189940	554	554	100	0.0
VIM-2 (4BZ3)	38	189938	155	155	81	1.00E-50
IMP-1 (1DDK)	34	189937	134	134	81	2.00E-42
CphA (1X8G)	25	189939	60.5	76.2	69	8.00E-15
AIM-1 (4AWY)	29	189941	28.1	45.8	49	7.00E-04

Table 3a. Blast Comparison with NDM-1 as the query sequence using accession code 189940. This comparison was conducted to ascertain the similarity between NDM-1 as a B1 type MBL to the other types of MBLs (B2 and B3) and also within the B1 type MBLs.

3.2 NDM-1 vs NDM-3

As seen from Figure 3a below, a BLAST multiple sequence alignment tool was used to compare NDM-3 to representatives of each MBL subgroup. NDM-1 (140; 141), VIM-2 (43; 69), and IMP-1 (22) were the B1-types selected, CphA (25) was the B2-type, and AIM-1 (87) was B3-type selected. As VIM-2 was the closest MBL in identity to NDM-1 evidenced from Table 3a above, it was chosen for the comparison with NDM-3.

Figure 3a. Blast Multiple Sequence Alignment for NDM-3 with NDM-1, VIM-2, IMP-1, CphA, and AIM-1 to show sequence identities

Legend	Enzyme	MBL Subgroup	Sequence Identity
A	NDM-3	B1	Query Sequence
B	NDM-1	B1	99
C	VIM-2	B1	38
D	IMP-1	B1	34
E	CphA	B2	25
F	AIM-1	B3	29

Table 3b. BLAST multiple sequence alignment legend and information for NDM-3 with NDM-1, VIM-2, IMP-1, CphA, and AIM-1.

In Table 3b, the results are shown for a BLAST Multiple Sequence Alignment that was carried out for query sequence NDM-3 against NDM-1, VIM-2, IMP-1, CphA, and AIM-1 in order to get the sequence identity percentage between NDM-3 and representatives of each subgroup. As expected, the results showed the same sequency identity percentages as for NDM-1, with NDM-1 and NDM-3 having 99% sequence identity with each other. VIM-2 is the closest of those assessed to NDM-3 (with the exception of NDM-3 parent MBL NDM-1) with 38% As per NDM-1 assessment above in Table 3a, the least similar is the mono-zinc B2 type CphA MBL with 25% sequence identity, with B3-type MBLs fall in between. In figure 3b the structure of NDM-1 from literature and structure of NDM-3 was generated through PDB for comparison. As expected, the structures are similar.

NDM-1 **NDM-3**

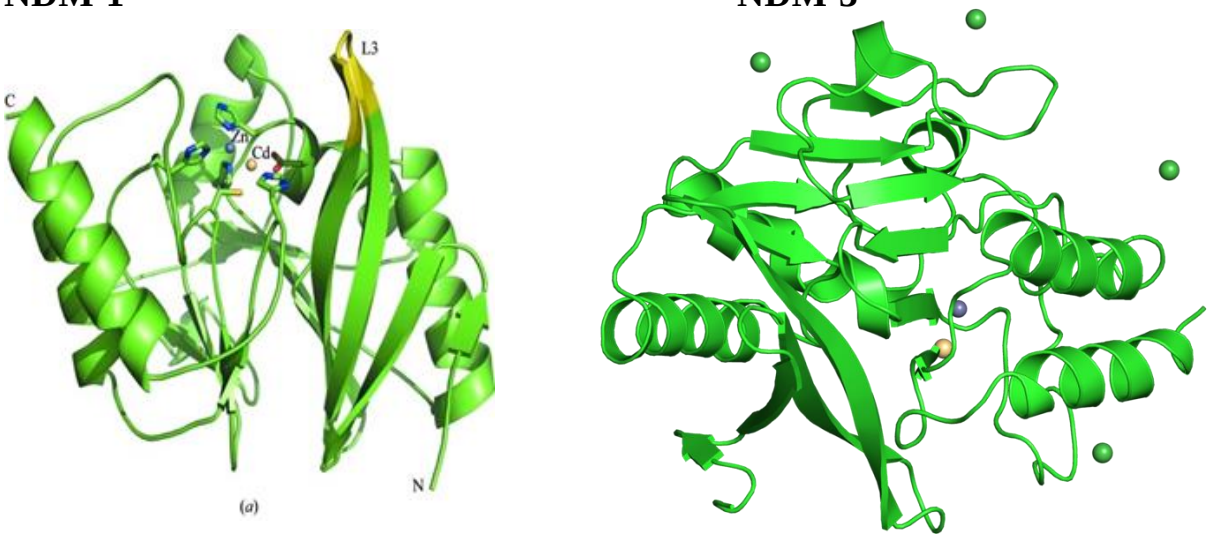

Figure 3b. NDM-1 Structure (141) *and NDM-3 Structure (PDB 4TZ9) with two metal ions in centre. Both contain Zinc in M1 and Cadmium in M2.*

3.3 NDM-3 – Characterisation using ProtParam and BLAST

From the research background outlined in chapter 1, it is known that NDM-3 is a mutant of well-known superbug, NDM-1. NDM-1 is a B1 type MBL and perhaps the most prevalent and dangerous MBL known thus far (129; 138; 128; 44; 52). NDM-3 was isolated originally from *Klebsiella pnuemoniae* and differs in one amino acid from NDM-1 at residue 95 as seen in figure 3c. This substitution is an aspartic acid that is replaced by an asparagine, as can be seen below in the sequence comparison (figure 3c). This replacement occurs on the protein surface, and not within the active site. The location of the replacement alters the interactions with the side chains of various β-lactam antibiotics. The difference in enzymatic activity between NDM-1 and NDM-3 with that single residue mutation is shown and discussed in section 4.6 - Enzymatic characterisation of NDM-3's resistance to β-lactam antibiotics. In the sequence alignment below in figure 3c the differences between NDM-1 and NDM-3 are shown. Protein Data Base (PDB) was used to find enzyme sequences and available structural images.

Uniprot Sequence C7C422: NDM-1

```
                10                  20                  30                  40                  50
MELPNIMHPV AKLSTALAAA LMLSGCMPGE IRPTIGQQME TGDQRFGDLV
                60                  70                  80                  90          95      100
FRQLAPNVWQ HTSYLDMPGF GAVASNGLIV RDGGRVLVVD TAWTDDQTAQ
            110                 120                 130                 140                 150
ILNWIKQEIN LPVALAVVTH AHQDKMGGMD ALHAAGIATY ANALSNQLAP
            160                 170                 180                 190                 200
QEGMVAAQHS LTFAANGWVE PATAPNFGPL KVFYPGPGHT SDNITVGIDG
            210                 220                 230                 240                 250
TDIAFGGCLI KDSKAKSLGN LGDADTEHYA ASARAFGAAF PKASMIVMSH
            260                 270
SAPDSRAAIT HTARMADKLR
```

Uniprot Sequence I3VKD5: NDM-3

```
                10                  20                  30                  40                  50
MELPNIMHPV AKLSTALAAA LMLSGCMPGE IRPTIGQQME TGDQRFGDLV
                60                  70                  80                  90          95      100
FRQLAPNVWQ HTSYLDMPGF GAVASNGLIV RDGGRVLVVD TAWTNDQTAQ
            110                 120                 130                 140                 150
ILNWIKQEIN LPVALAVVTH AHQDKMGGMD ALHAAGIATY ANALSNQLAP
            160                 170                 180                 190                 200
QEGMVAAQHS LTFAANGWVE PATAPNFGPL KVFYPGPGHT SDNITVGIDG
            210                 220                 230                 240                 250
TDIAFGGCLI KDSKAKSLGN LGDADTEHYA ASARAFGAAF PKASMIVMSH
            260                 270
SAPDSRAAIT HTARMADKLR
```

Figure 3c: Sequences of NDM-1 and NDM-3 respectively with the single amino acid difference highlighted – residue 95.

Sequence Comparison of known NDM mutants

Legend	Enzyme	Sequence Identity	Identifier
A	NDM-1	Query Sequence	Uniprot C7C422*
B	NDM-3	99	AFK80349
C	NDM-4	99	5WIG (PDB)*
D	NDM-5	99	4TZE (PDB)*
E	NDM-8	99	4TZF (PDB)*
F	NDM-12	99	5WIH (PDB)*

Table 3c. Sequence Comparison of known NDM mutants
*All used Fasta Sequences found on Uniprot or PDB as noted.

Figure 3d. Blast Multiple Sequence Alignment for NDM-1 (141) *with NDM-3(this works), NDM-4* (161), *NDM-5* (128), *NDM-8* (162), *NDM-12* (163) *to show sequence identities and amino acid differences*

As seen in Table 3c and Figure 3d above, a sequence comparison was performed using BLAST for all known variants of NDM-1 by 2016, using NDM-1 as the query sequence. As expected, all variants had 99% sequence identity with NDM-1. The variants used in the comparison included NDM-3 (as per section 3.2 above), NDM-4 (161), NDM-5 (128), NDM-8 (162), and NDM-12 (163).

3.4 Transformation and Expression of NDM-3

NDM-3 – both NDM-3(NC) and NDM-3+Ub - were transformed and expressed as per section 2.2 with procedures being adopted and where relevant, adapted from the literature (145; 146; 147; 150; 152). They were both transformed onto an agar plate containing 100 µg/mL ampicillin using *E. coli* BL21 (DE3) competent cells. The cells were streaked across the plate and incubated for 16 – 18 hours at 37 °C. It was found through this works that 5 µL of plasmid was needed per 100 µL of competent cells. It was determined that when between 20 µL and 50 µL of the undiluted solution was directly streaked onto the agar it was the most successful for producing colonies. An ampicillin concentration of 100 µg/mL was used throughout transformation and expression of NDM-3. During expression the IPTG (147) was added once OD_{600} was reached. This took approximately 1.5 – 2 hours each time. The purpose of IPTG is to induce expression of the *lac* operon in *E. coli*. It works by preventing the repression of the β-galactosidase coding gene *lacZ* by binding to and altering the *lacI* repressor. IPTG (1 mM) was added for NDM-3+Ub and NDM-3(NC) expression. For USP2cc expression 0.4 mM of IPTG was added. $ZnCl_2$ (0.1 mM) was added to ensure enough metal ions were available for utilisation if required.

Centrifugation Yields

After centrifugation at 5000 x g for 20 minutes at 4 °C the pellet contains the NDM-3 enzyme (either NDM-3+Ub or NDM-3(NC)). The supernatant was stored until SDS-PAGE confirmed the presence of enzyme in pellet, in case of any errors in centrifugation. The average pellet weight during this research was 5.1 g. Following this step, the pellet was resuspended in lysis buffer. Lysozyme, $MgCl_2$, and DNAse I were added to the resuspended solution which then underwent sonication (164). Sonication is the process of agitating particles in a sample using sound energy (164). The settings used for sonication were 20% power for 3 rounds of 30 seconds with the protein on ice to ensure it did not overheat.

FPLC Procedure

Fast Protein Liquid Chromatography (FPLC) was used to purify proteins (148). The FPLC system consists of many components – namely the system pumps, UV detector, Fraction Collector, and Column. The columns used in this works were the HisTrap FF 5 mL and the HisTrap FF Crude 5 mL (142; 149). During the optimisation of this process for NDM-3, it was found that both NDM-3+Ub and NDM-3(NC) were sensitive to high imidazole concentrations. Imidazole was used in the elution buffer as a competitor to the histidine

molecules bound to the nickel packed in the column. A general recommendation for starting off is to use 200 mM imidazole in the elution buffer (165). In the case of both NDM-3 constructs however this caused precipitation of the protein and in some cases an inactive protein and so the concentration of imidazole was gradual reduced during these works. When the concentration of imidazole was determined to be optimised at 100 mM in the elution buffer and the FPLC process was consistent, a pure and active NDM-3 enzyme was produced.

During FPLC, the elution method employed was stepwise elution, meaning the system jumped from using 100% loading buffer to 100% elution buffer (142). When this occurred for both NDM-3+Ub and NDM-3(NC) it was approximately 5 mLs after the buffer changeover from loading buffer containing 20 mM imidazole to elution buffer containing 100 mM imidazole.

As can be seen from figure 3e below, both proteins (NDM-3+Ub and NDM-3(NC)) consistently eluted in fractions 23 – 25 in this case and always between 5 – 7 mLs after loading buffer was replaced by elution buffer. The green line in the image from the UNICORN FPLC software below denotes changeover from loading buffer to elution buffer. The blue line represents UV readings.

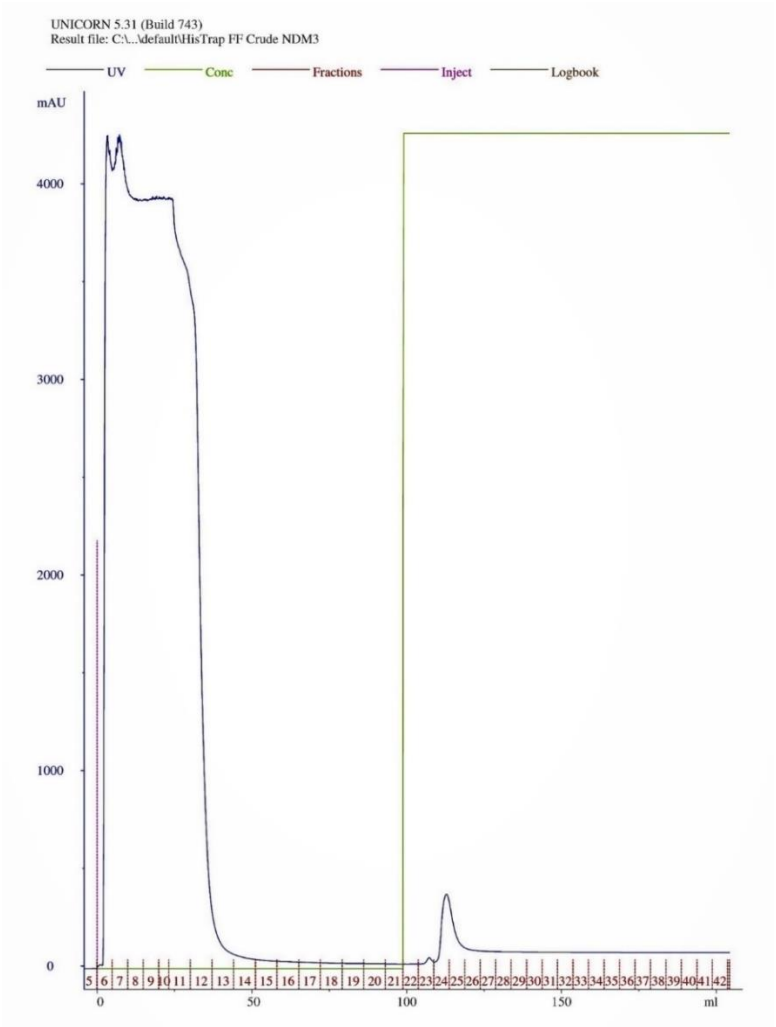

Figure 3e - Full elution graph of NDM-3(NC) and NDM-3+Ub.

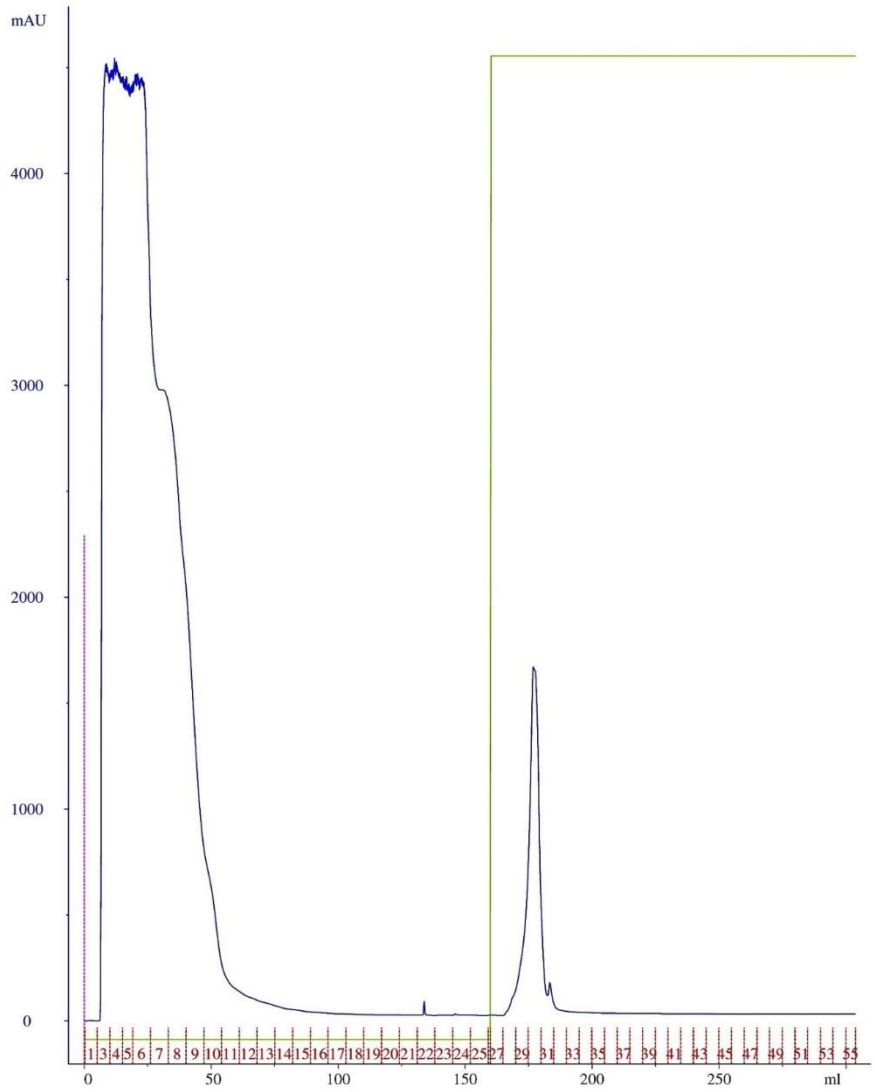

Figure 3f - FPLC Elution graph for USP2cc, similar to NDM-3 above. Green line denotes changeover from loading buffer to elution buffer. Blue lines are UV readings. USP2cc eluted in fractions 28 - 31.

As can be seen from figure 3f above, protease USP2cc consistently eluted in fractions 28 – 31 in this case. The green line in the image from the UNICORN FPLC software below denotes changeover from loading buffer to elution buffer while the blue line represents UV readings.

All three proteins, NDM-3+Ub, NDM-3(NC), and USP2cc eluted at the same point in the FPLC process due to the presence of the hexa-histidine tag (149).

3.5 Buffer Exchange

As described in section 2.2, neither NDM-3(NC) nor NDM-3+Ub constructs remained stable in the elution buffer. The reason a dialysis/buffer exchange step was introduced was due in large part to the precipitation evident in both NDM-3+Ub and NDM-3(NC) (166). It was also noted at other times for NDM-3+Ub only it was evident through a lack of activity of the protein in others only when stored in elution buffer for longer than 24 hours, that something was not correct in the isolation/purification process. Through trial and error the precipitation event was determined to have been because the concentration of imidazole was too high for the proteins to remain in. The buffer exchange step was introduced to the process to allow the proteins to go from Elution Buffer containing 100 mM imidazole, to Dialysis Buffer 1 containing 50 mM imidazole, and finally to Dialysis Buffer 2 containing 0 mM imidazole using SnakeSkin Dialysis Tubing (Thermo Scientific). A 2-step process was required as a single step also caused precipitation (i.e., from Elution Buffer containing 100 mM imidazole to Dialysis Buffer 2 containing 0 mM imidazole).

The buffer exchange process optimised for NDM-3(NC) or NDM-3+Ub took place in the cold room (4 °C - 8 °C) for a minimum of 4 hours in each buffer, with constant stirring. More than 4 hours of constant stirring for the dialysis in each subsequent buffer was acceptable and had no impact on the protein or activity. The ratio of enzyme to buffer volume was 1:100. These parameters were optimised throughout the research works to largely reduce the risk of precipitation. Once the dialysis & buffer exchange steps were conducted within 24 hours of the chromatography step, and therefore not stored in the elution buffer with high concentrations of imidazole for any length of time, and was performed in 2-step manner described above, there was no further precipitation.

3.6 Confirmation of NDM-3

In order to confirm the presence of NDM-3 in the pooled fractions collected from FPLC purification, SDS-PAGE gels were run and an activity assay was carried out against ampicillin to confirm activity/active protein was isolated (151). Below are the gels and the marker which was used to compare the bands visible and determine their molecular weight. The molecular weight of NDM-3+Ub was determined to be 37kDa using ProtParam, as listed in Table 3d below.

Enzyme Name	**Extinction Co-efficient**	**Molecular Weight**	**pI**
NDM-3+Ub + H6	29575 M^{-1} cm^{-1}	37868	6.11
NDM-3 + H6	28085 M^{-1} cm^{-1}	29321	6.02
Ubiquitin tag	1490 M^{-1} cm^{-1}	8565	6.56

Table 3d. The ProtParam information given when sequences entered. Extinction coefficients are used to accurately measure concentration at Abs 280 nm. Molecular weights of NDM-3 constructs include the hexa-histidine tag.

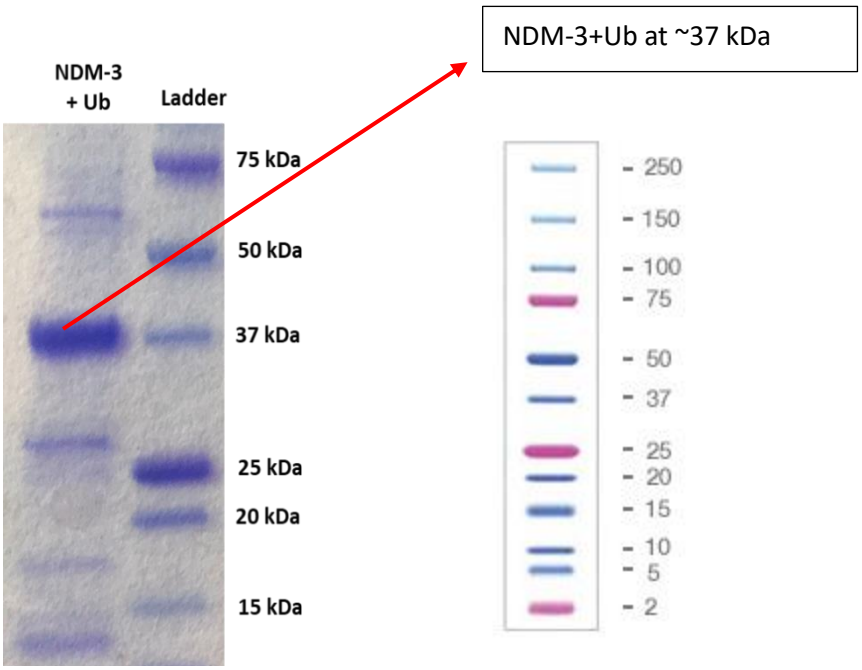

Figure 3g. SDS Gel showing NDM-3+Ub at 37kDa and the Protein Marker used for all SDS Gels

From Table 3d and Figure 3g above we can see that the NDM-3+Ub was present at approximately 37kDa less the histidine tag. This is aligned with the projected molecular weight of the NDM-3+Ub molecular weight as noted in table 3d. This provided evidence that NDM-3+Ub was indeed isolated.

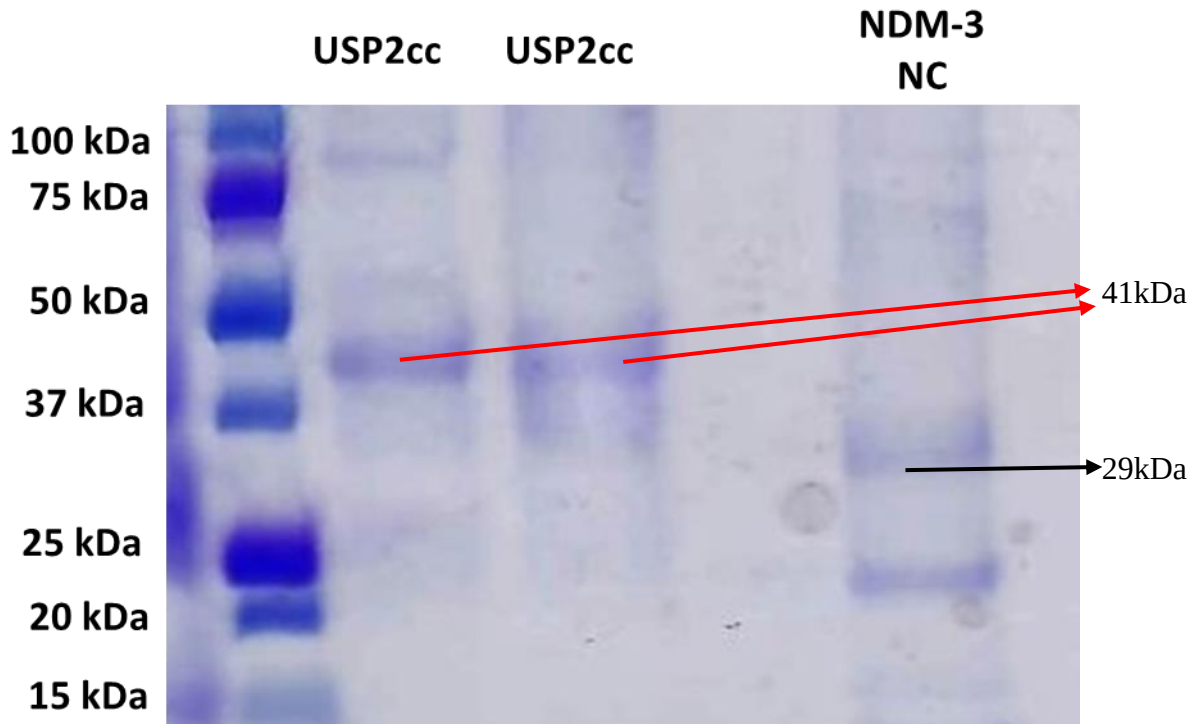

Figure 3h. SDS Gel showing NDM-3(NC) in well 6 at ~29 kDa, and USP2cc protease in wells 3 and 4 at ~41 kDa. SDS marker is in well 2.

As is evident from figure 3h and table 3d, the USP2cc protease was present in wells 3 & 4 beside the marker in well 2. This clearly shows the presence of a band at approximately 41kDa (167), approximately aligning with the predicted molecular weight in table 3d.

NDM-3(NC) is shown in well 6 in figure 3h with a band at approximately 28/29 kDa, clearly shown between marker (well 2) 25 kDa and 37 kDa bands. This aligns with table 3d and provides evidence that NDM-3(NC) is indeed isolated and present.

3.7 Protparam

In order to determine ε, an online tool called ExPASy ProtParam was used. This allows one to input a protein sequence and computes physical and chemical parameters for said protein. These parameters include extinction coefficient, as can be seen in Table 3d above. In this instance the Extinction coefficient, molecular weight, and pI are listed. pI is the isoelectric point and is the pH of the protein that at which it has no net charge. When pH > pI the net charge is negative, and conversely when pH < pI a protein has a positive net charge.

3.8 Determining the concentration using the Beer-Lambert Law

(168; 169)

The concentration (c) of the protein was determined using the Beer-Lambert Law, which is:

$$A = \varepsilon c l$$

Where A = Absorbance, ε = extinction coefficient of protein, and l = path length = 1 cm in this case.

Therefore;

$$c = A/\varepsilon$$

Using the online tool ProtParam at this link: https://web.expasy.org/protparam/

$c = A/29{,}575$ (1) $c = M^{-1}$ ~~cm^{-1}~~ ~~cm~~; c = M (units)

Many batches of said proteins were made up but for this example: A = 0.896 (unit-less).

Absorbance was measured at 280 nm.

$c = 0.896/29{,}575$

$c = 3.029 \times 10^{-5}$ M

To convert to mg/mL = 3.029×10^{-5} M x 37868 (mw from ProtParam tool)

c = 1.14724355 mg/mL of protein

In 6 mLs collected = 6.88 mg of NDM-3+Ub protein.

After the concentration of the protein was found and the SDS-PAGE gels confirmed presence of protein, the samples were concentrated to approximately 1 mL from 6 mL to have a more concentrated stock solution and then aliquoted into small amounts for use in activity assays to a concentration of 1 mg/mL. These aliquots were then stored at -20 °C. NDM-3 was expressed on a Pet vector (47) but due to low solubility and low expression yields it was then expressed on a pHUE vector as a hexahistidine-ubiquitin fusion protein, which allows for a one step purification. However, for the NDM-3+Ub protein, the ubiquitin tag still needs to be cleaved off using the USP2cc protease.

3.9 Cleavage of Ubiquitin tag using USP2cc

Ubiquitination is a post-translational modification of attaching ubiquitin to a protein which affects the protein by signalling for their degradation (170). The proteasome alters cellular locations by affecting their activity or by promoting or preventing protein interactions (144; 152; 171). It is a small regulatory protein found in almost all tissues. In this case USP2cc is a deubiquitinating enzyme. It works by formation of non-covalent complex with the ubiquitin using two sites for interaction. Further information about this binding can be found in Structural Basis of Ubiquitin Recognition by the Deubiquitinating Protease USP2 by Renatus et al., (172). The method for deubiquitination was kept similar to approach taken in Catanzariti et al., (152) and is outlined in Chapter 2 – Materials and Methods. When USP2cc was purified and the concentration measured, using the Beer-Lambert Law as outlined above for NDM-3 and concentrated to and separated into 0.5 mg/mL aliquots.

Cleavage Conditions

A scientific approach to the optimisation of cleavage conditions was taken, whereby a range of concentration ratios of NDM-3+Ub: USP2cc were attempted, at different temperatures, with the time being the one parameter that remained constant. The conditions are outlined below;

Temperature	Concentration Ratio (NDM-3+Ub: USP2cc)
4 °C	200: 1
4 °C	100: 1
4 °C	50: 1
25 °C	200: 1
25 °C	150: 1
25 °C	100: 1

25 °C	50: 1
37 °C	200: 1
37 °C	100: 1
37 °C	50: 1

Table 3e. Outlining Concentration Ratio and Temperature Conditions experiment for optimal cleavage conditions

The results of said experiment are shown below in the SDS Page gel. It can be clearly seen between figure 3i and table 3e, that well 9 containing 200:1 ratio of NDM-3+Ub: USP2cc had the most successful cleavage, with the entire NDM-3+Ub band at 37kDa appearing to be gone. Therefore, room temperature and a ratio of 200:1 was determined to be the most appropriate temperature for the cleavage process.

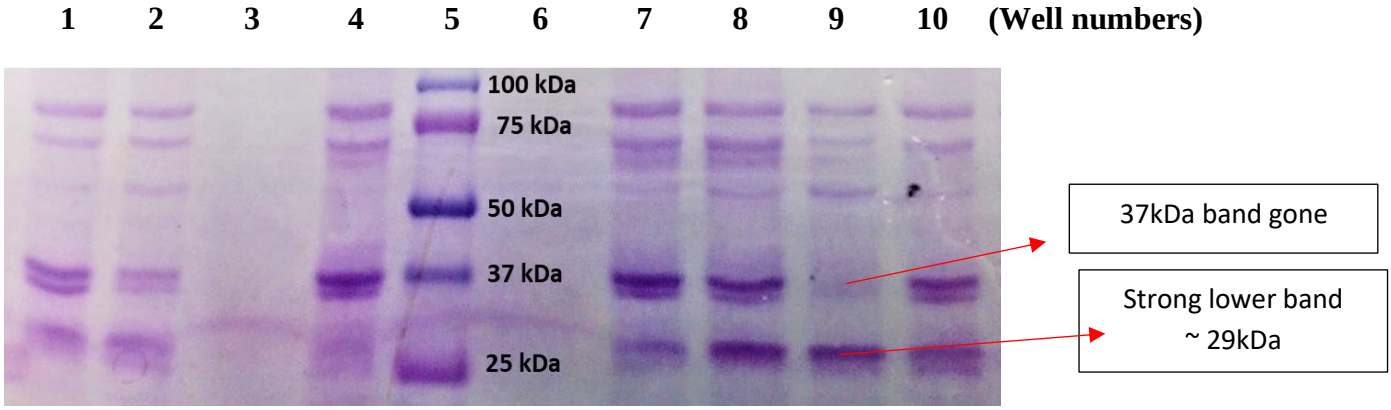

Figure 3i. Well #9 contains 200:1 concentration of NDM-3+Ub: USP2cc

Well 1: 37C 200:1 ratio

Well 2: 37C 100:1 ratio

Well 3: 37C 50:1 ratio

Well 4: 4C 200:1 ratio

Well 5: Marker

Well 6: Concentrated NDM-3+Ub

Well 7: 4C 100:1 ratio

Well 8: 4C 50:1 ratio

Well 9: Room Temperature 200:1 ratio

Well 10: Room Temperature 150:1 ratio

With the now isolated and purified enzymes of both NDM-3 (NDM-3+Ub cleaved) and NDM-3(NC), in the next chapter, chapter – 4 'Enzymatic characterisation of NDM-3 resistance to β-lactam antibiotics', these proteins will be tested for activity against multiple beta lactam antibiotics to determine kinetic activity data for NDM-3 and compare it to both NDM-1 and other NDM variants from the literature. It was also intended to compare NDM-3 (cleaved from NDM-3+Ub) and NDM-3(NC) to each other and determine if the ubiquitin tag and cleavage stages had any effect on the activity of the NDM-3 protein or interferes with the rate of reaction for the different substrates.

Chapter 4 – Enzymatic characterisation of NDM-3 resistance to β-lactam antibiotics

Introduction

Enzymatic assays are a widely used and important analytical technique that provides invaluable information about the activity of an enzyme. This activity is either a measure of the appearance of the product that appears, or the disappearance (depletion) of a substrate as a result of the reaction (173). In the case of NDM-3 it is the depletion of the substrate that is measured. The assay allows for the measurement of the enzyme's activity in the presence of substrates as they deplete. In these studies' ampicillin, penicillinG, meropenem, imipenem, cefoxitin, and cephalothin are used. The most common analysis of enzyme kinetics data is based on the model developed by Michaelis and Menten (174; 175). A full breakdown of this model is available on the following page in this chapter. In this analysis the measurement of catalytic rates as a function of substrate concentration provides an estimate for the K_m value and the V_{max} for a specific substrate where V_{max} represents the maximal rate possible and K_m is the Michaelis constant of a substrate and is equivalent to the concentration of substrate at which the enzyme achieves half V_{max}. In most cases V_{max} is the reaction rate when the enzyme is saturated with substrate, which is also the maximum speed of reaction rate of substrate molecules catalysed. The relationship between the rate of the reaction and substrate concentration is dependent on the affinity the enzyme has for the substrate, K_m. K_m provides an estimate of the substrate affinity; a high K_m value indicates low affinity, while a low K_m is indicative of high affinity. The k_{cat} value can then be defined as the turnover number of the enzyme for a specific substrate, i.e., the number of substrate molecules that are converted to product per unit time (seconds generally) for each enzyme site. The k_{cat}/ K_m ratio thus corresponds to the catalytic efficiency for the substrate conversion by the enzyme. In the equations below E stands for enzyme and S for substrate (174; 175).

Below the breakdown of the Michaelis Menten kinetics and the steady-state assumptions are outlined along with the equations used throughout (174; 175).

Michaelis Menten Kinetics and the Steady-State Assumption (174; 175)

Eq. 1 $$E + S \underset{-1}{\overset{1}{\rightleftharpoons}} ES \overset{2}{\rightleftharpoons} E + P$$

Eq. 2 Rate of 1 = $k_1[E][S]$

Eq. 3 Rate of 2 = $k_2[ES]$

When the enzyme concentration is kept constant, under the Steady-State assumption [ES] is constant, as the limiting factor is the enzyme concentration as there is more than enough substrate. Therefore;

Eq. 4 Formation [ES] = Loss [ES]

Rate of [ES] formation is also equal to Rate 1 plus Rate -2

Rate of [ES] loss is also equal to Rate -1 plus Rate 2

Therefore;

Eq. 5 $Rate_1 + Rate_{-2} = Rate_{-1} + Rate_2$

However, as products do not tend to revert to the intermediate complex [ES], we can change the original equation 1 to:

Eq. 6 $$E + S \underset{-1}{\overset{1}{\rightleftharpoons}} ES \overset{2}{\rightarrow} E + P$$

And so, equation 5 can be re-written as:

Eq. 7 $Rate_1 = Rate_{-1} + Rate_2$ and;

Eq. 8 $k_1[E][S] = k_{-1}[ES] + k_2[ES]$

Total enzyme in the reaction;

Eq.9 $[E]_T = [E] + [ES]$ therefore;

Eq. 10 $[E] = [E]_T - [ES]$

And when equation 10 is incorporated with equation 8;

Eq.11 $k_1([E]_T - [ES])\,[S] = k_{-1}[ES] + k_2[ES]$

= $k_1([E]_T - [ES])\,[S] = [ES]\,(k_{-1} + k_2)$

Multiply out = $k_1[E]_T\,[S] - k_1[ES][S] = [ES]\,(k_{-1} + k_2)$

Divide by k_1 = $[E]_T\,[S] - [ES][S] = [ES]\,(k_{-1} + k_2)/\,k_1$

The value for $(k_{-1} + k_2)/\,k_1$ is therefore assigned a constant value. This is termed K_m

$K_m = (k_{-1} + k_2)/\,k_1$

Using this new K_m term, we can update the previous equation to state:

Eq. 12 $[E]_T\,[S] = [ES]\,K_m + [ES][S]$

Eq. 13 $[E]_T\,[S] = [ES]\,(K_m + [S])$

So; $[ES] = [E]_T\,[S]/\,(K_m + [S])$

The speed of an enzymatic reaction is denoted V_0;

Eq. 14 $V_0 = dP/dt = k_2[ES]$

Inputting equation 14 with equation 13, we see that;

Eq. 15 $k_2\,[ES] = k_2\,[E]_T\,[S]/\,(K_m + [S])$

So, if $V_0 = V_{max}$, when the substrate concentration is very high, then the total Enzyme concentration, $E_T = [ES]$. This means there is no 'free' enzyme at any point.

Therefore;

Eq. 16 $k_2\,[E]_T = V_{max}$

Eq. 17 $V_o = (V_{max}\,[S])\,/\,K_m + [S]$

Equation 17 is known as the **Michaelis Menten Equation.**

If K_m = the Michaelis constant for the particular enzyme being targeted, and is a substrate concentration whereby K_m = [S] (assumption for practical purposes) then;

Eq. 18 $V_o = (V_{max}\,[S]) / 2[S]$ (Substituting Km for [S])

= $V_o = (V_{max}\,\cancel{[S]}) / 2\cancel{[S]}$

Eq. 19 $V_o = V_{max}/ 2$

So, K_m is the substrate concentration where the reaction speed is half of V_{max}, = $V_o = 0.5\,(V_{max})$

Catalytic Efficiency

K_m is the affinity that an enzyme has for the substrate it is interacting with.

A high K_m value indicates an enzyme with a low affinity for its substrate, and that a much higher concentration of substrate will be needed to achieve V_{max}

Another measure of enzymatic activity is the k_{cat}.

The k_{cat} is the measure of how many substrates an enzyme can turn into product at the maximum speed per second. A higher k_{cat} means the enzyme is more efficient at catalysis.

Eq. 20 $k_{cat} = V_{max} / [ES]$

Because when $[E]_T$ = when enzyme is the limited reactant = [ES]

The final rate constant determined is the Catalytic Efficiency. It is the value or score for enzymes for their ability to speed up reactions. It is specific to the enzyme.

This catalytic efficiency rating is;

Eq. 21 k_{cat} / K_m

These calculations, equations, and principles are the basis of the results shown in this chapter (174; 175).

Aims of Chapter Four: NDM-3 Characterisation

Kinetic assays were performed for the following studies;

1. Determine the optimised assay buffer for all further characterisation studies
2. Outline enzymatic assays best practices
3. Determine the k_{cat} and K_m values of NDM-3+Ub for various substrates
4. Determine the k_{cat} and K_m values of cleaved NDM-3+Ub
5. Determine the k_{cat} and K_m values for NDM-3(NC)
6. Compare the above parameters to values published for NDM-1 and other NDM variants
7. Carry out preliminary kinetic assays at different pH values for four substrates with a view to discovering the difference pH makes on enzymatic activity
8. Ascertain if NDM-3(NC) exhibits any lactonase activity by carrying out preliminary kinetic assays with representative lactone substrates (154)

4.1 The Optimisation of the Assay Buffer

Determining the conditions required for the assay buffer was an important step as the buffer has an impact on every assay carried out. The three conditions for optimisation were HEPES concentration, Sodium Chloride concentration, and Zinc Chloride concentration. ΔAbsorbance (delta) is indicative of the change activity in these cases as it is correlated to the rate of depletion of substrate when an assay is occurring (173), meaning that as substrate concentration reduces due to forming into product, the change in absorbance measurements can be utilised to determine rate of activity/rate of reaction. Enzymatic assays are a widely used and important analytical technique that provides invaluable information about the activity of an enzyme. This activity is either a measure of the appearance of the product that appears, or the disappearance (depletion) of a substrate as a result of the reaction (173). In this case it is the depletion of the substrate that is measured. The assay allows for the measurement of the enzyme's activity in the presence of substrates as they deplete

4.1.1 HEPES Buffer Concentration

HEPES was chosen as the buffering agent for these NDM-3 studies as it is used widely in cell culture and is generally considered a good buffer for physiological pH ranges (47). As these were initial assays, a starting buffer containing the HEPES concentration being tested, and 500 mM NaCl and 0.1 mM $ZnCl_2$ was used. NaCl (500 mM) was used as a starting point for these assays as this was the dialysis buffer concentration of NaCl. $ZnCl_2$ (0.1 Mm) was used initially for this test as a starting point.

Table of data for HEPES in Assay Buffer

Hepes Concentration (mM)	ΔAbsorbance 1	ΔAbsorbance 2	ΔAbsorbance 3	ΔAbsorbance 4	ΔAbsorbance Mean	n	SD	RSD (%)	RSD (%)
0	0.3414	0.346	0.3229	0.3135	0.331	4	0.01533	1.53298	1.5
50	0.2364	0.1872	0.1848	0.1924	0.200	4	0.02434	2.43409	2.4
100	0.1432	0.1031	0.1318	0.1372	0.129	4	0.01777	1.77708	1.8
150	0.1763	0.1742	0.1828	0.1631	0.174	4	0.0082	0.81963	0.8
200	0.0054	0.0007	0.0008	N/A	0.002	3	0.00269	0.26851	0.3

Table 4a. Data measured for HEPES assay buffer experiments

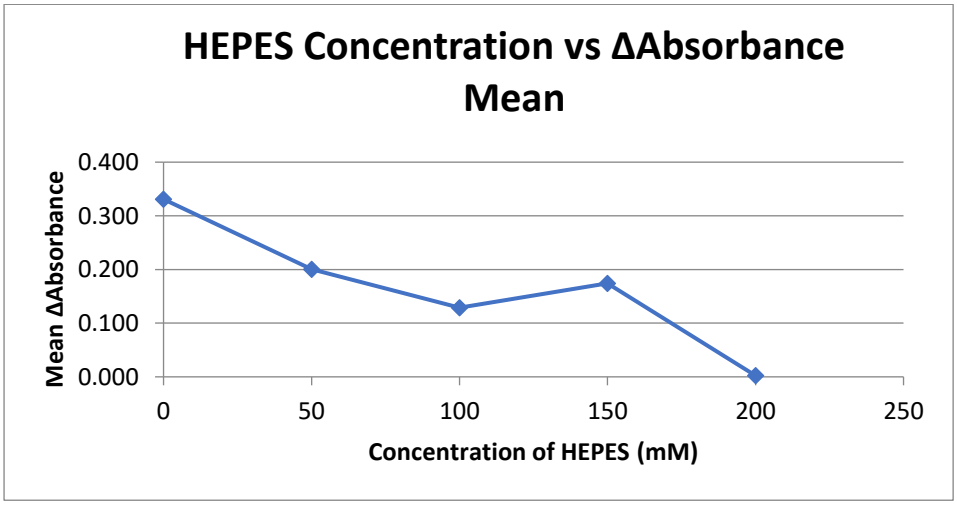

Figure 4a. Graph plotting HEPES concentration vs mean of delta absorbance

Conclusion

It was determined that 50 mM HEPES was the optimal concentration to use during the kinetic assays. All assays were run in triplicate. As evident from the data in table 4a and the graph in figure 4a, the best activity was seen for preliminary NDM-3(NC) enzyme assays against ampicillin when HEPES 50 mM was in use. This concentration was then used for the following optimisation tests for NaCl and $ZnCl_2$.

4.1.2 NaCl Buffer Concentration

NaCl was the chosen salt for the assay buffer. Salt can affect the activity of enzymes, as well as the folding, conformation, and the stability of enzymes. NaCl is one of the most commonly used salts as it is relatively inexpensive and Na^+ and Cl^- are compatible ions. When salt concentration is too high or too low it can cause denaturation of an enzyme or lower enzymatic activities (176). Finding the optimum concentration of NaCl is therefore of high import. Based on 4.1.1 50 mM HEPES was used, the NaCl concentration being tested, and 0.1 mM $ZnCl_2$ using NDM-3(NC) against ampicillin to ascertain the best NaCl concentration in the assay buffer.

Table of data for NaCl in Assay Buffer - Optimisation of NaCl

NaCl Concentration (mM)	ΔAbsorbance 1	ΔAbsorbance 2	ΔAbsorbance 3	ΔAbsorbance Mean	n	SD	RSD (%)	RSD (%)
0	0.1581	0.1258	0.144	0.143	3	0.016193	1.619331	1.6
50	0.1928	0.1838	0.1789	0.185	3	0.00705	0.705006	0.7
100	0.1562	0.1563	0.1566	0.156	3	0.000208	0.020817	0.0
200	0.1504	0.1436	0.1328	0.142	3	0.008875	0.887543	0.9
500	0.1028	0.1027	0.1028	0.103	3	5.77E-05	0.005774	0.0
700	0.1217	0.0884	0.0893	0.100	3	0.018971	1.897129	1.9
1000	0.0867	0.0774	0.0632	0.076	3	0.011835	1.183484	1.2

Table 4b. Data measured for NaCl Assay Buffer experiments

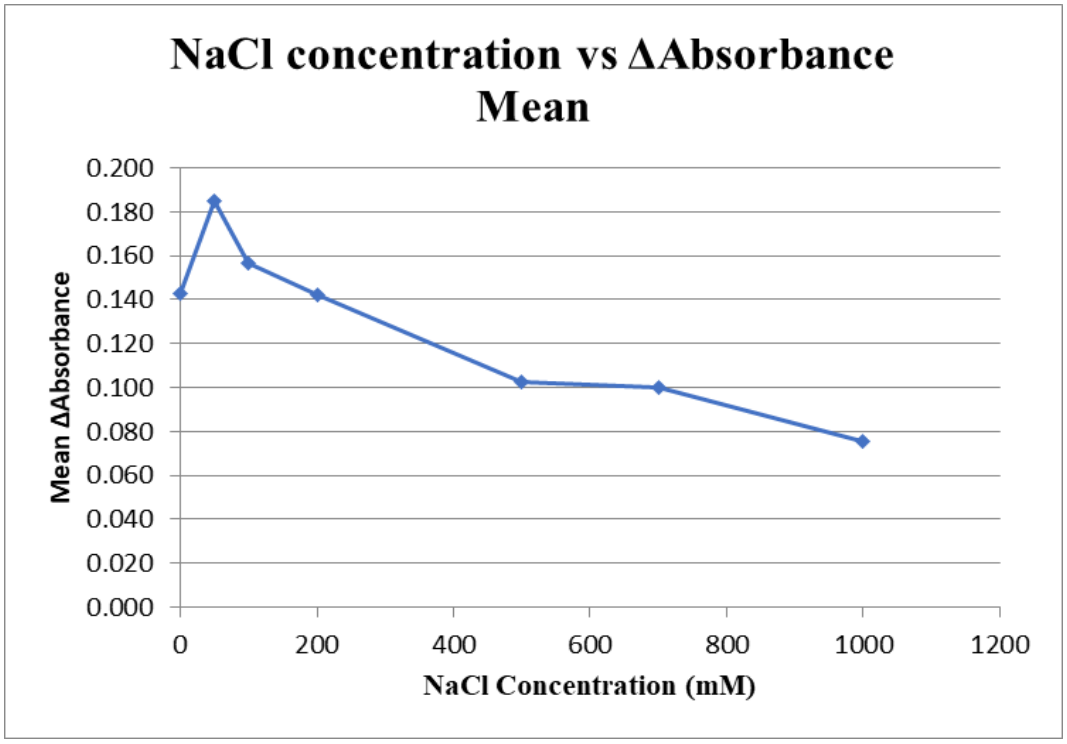

Figure 4b. Graph plotting NaCl concentration vs mean of delta absorbance

Conclusion

As evident from table 4b and figure 4b, the activity assays showed the highest activity in NaCl concentrations of 50 mM. This 50 mM NaCl along with 50mM HEPES was deemed the optimal concentrations to use during the kinetic assays. These concentrations were used for the determination of optimal $ZnCl_2$ concentration as described in the next section.

4.1.3 Zinc Chloride Buffer Concentration

This final part of the assay buffer study was conducted to find the optimal concentration of $ZnCl_2$ in the assay buffer. It was also to determine if the enzyme needed to have metal ions available in abundance when interacting with the different substrates. As seen in section 4.1.1 and 4.1.2 above, the optimal concentrations of NaCl was 50 mM and the optimal concentration of HEPES was 50mM HEPES. Buffers made of these concentrations and $ZnCl_2$ concentrations being tested were made up.

Table of data for $ZnCl_2$ in Assay Buffer - Optimisation of $ZnCl_2$

$ZnCl_2$ (µM)	ΔAbsorbance 1	ΔAbsorbance 2	ΔAbsorbance 3	ΔAbsorbance Mean	n	SD	RSD (%)	RSD (%)
0	0.1506	0.1313	0.1393	0.140	3	0.009697	0.969691	1.0
100	0.0837	0.0756	0.066	0.075	3	0.008861	0.886059	0.9
150	0.0651	0.054	0.062	0.060	3	0.005727	0.572742	0.6
200	0.0532	0.0482	0.0415	0.048	3	0.005871	0.587055	0.6
500	0.0337	0.0416	0.04	0.038	3	0.004177	0.417652	0.4
700	0.0079	0.0052	0.0069	0.007	3	0.001365	0.136504	0.1

Table 4c. Data measured for Zinc Chloride Assay Buffer experiments

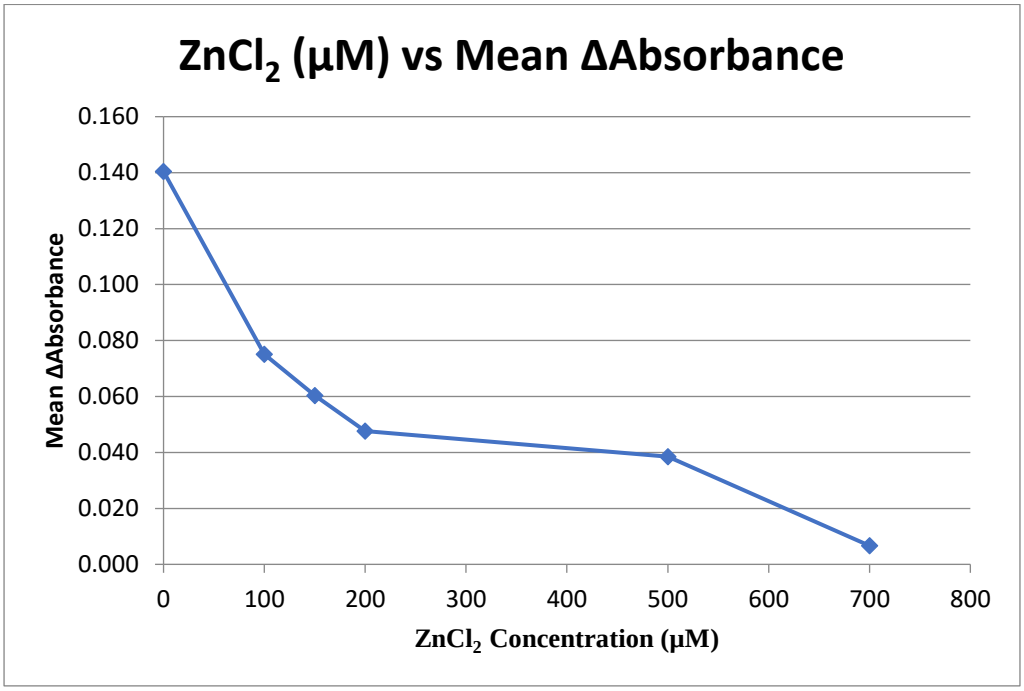

Figure 4c. Graph plotting Zinc Chloride concentration vs mean of delta absorbance

Conclusion

As seen from table 4c and figure 4c, it was determined that 0 µM $ZnCl_2$ was the best concentration to use during the kinetic assays. It was evident that the assays worked

considerably better without $ZnCl_2$. It is possible perhaps that the $ZnCl_2$ molecules were interfering in some way, or perhaps restricting access of the substrate to enzyme.

Optimisation of Assay Buffer – Conclusion

From the evidence presented above a 50 mM HEPES, 50 mM NaCl, and 0 mM $ZnCl_2$ was determined to be the optimal assay buffer for all of the following enzymatic assays for NDM-3. The solution, heretofore called 'Assay Buffer,' was prepared and used for all of the following enzymatic assays for NDM-3 (both NDM-3+Ub cleaved or uncleaved, and NDM-3(NC)).

4.2 Enzymatic Assays for NDM-3

Assays were carried out as per methodologies section 3.2. The optimised assay buffer determined in section 4.1 was used for all future enzymatic assays.

General Assay Practices for NDM-3 Enzymatic Assays (153)

The lowest amount of NDM-3(NC) and NDM-3+Ub enzyme were used during these assays, for two reasons;

1. To ensure consistency in enzyme concentrations of a stable protein.
2. To conserve the protein due to the difficult nature of expression and purification of NDM-3. Conservation was important as it had proven difficult to express, purify, and isolate active enzyme.

Provisional assays were done with both NDM-3 enzymes (NDM-3+Ub, and NDM-3(NC)) and each substrate initially to determine their general range of activity and to find the lowest amount of enzyme that could be used for successful assays while conserving enzyme as stated above.

4.3 NDM-3+Ub – k_{cat} and K_m values

As outlined in chapter 3 – Expression and Purification of NDM-3; NDM-3+Ub was expressed as a ubiquitin-histidine fusion protein. In order to compare activities of NDM-3 with and without the ubiquitin tag (i.e. cleaved and uncleaved), kinetic assays were carried out on the uncleaved enzyme against ampicillin, penicillinG, imipenem, meropenem, and cefoxitin. All assays in this section were carried out at pH 7.5. The results are reported below in figure 4d showing the concentration of the substrate vs the rate of reaction per second of the enzyme in the presence of said substrate. The k_{cat} values represent the turnover rate per second of substrate molecules by the enzyme. K_m is the concentration of substrate where half of V_{max} is achieved. The k_{cat} and K_m principles and values can be determined using the equations at the beginning of this chapter.

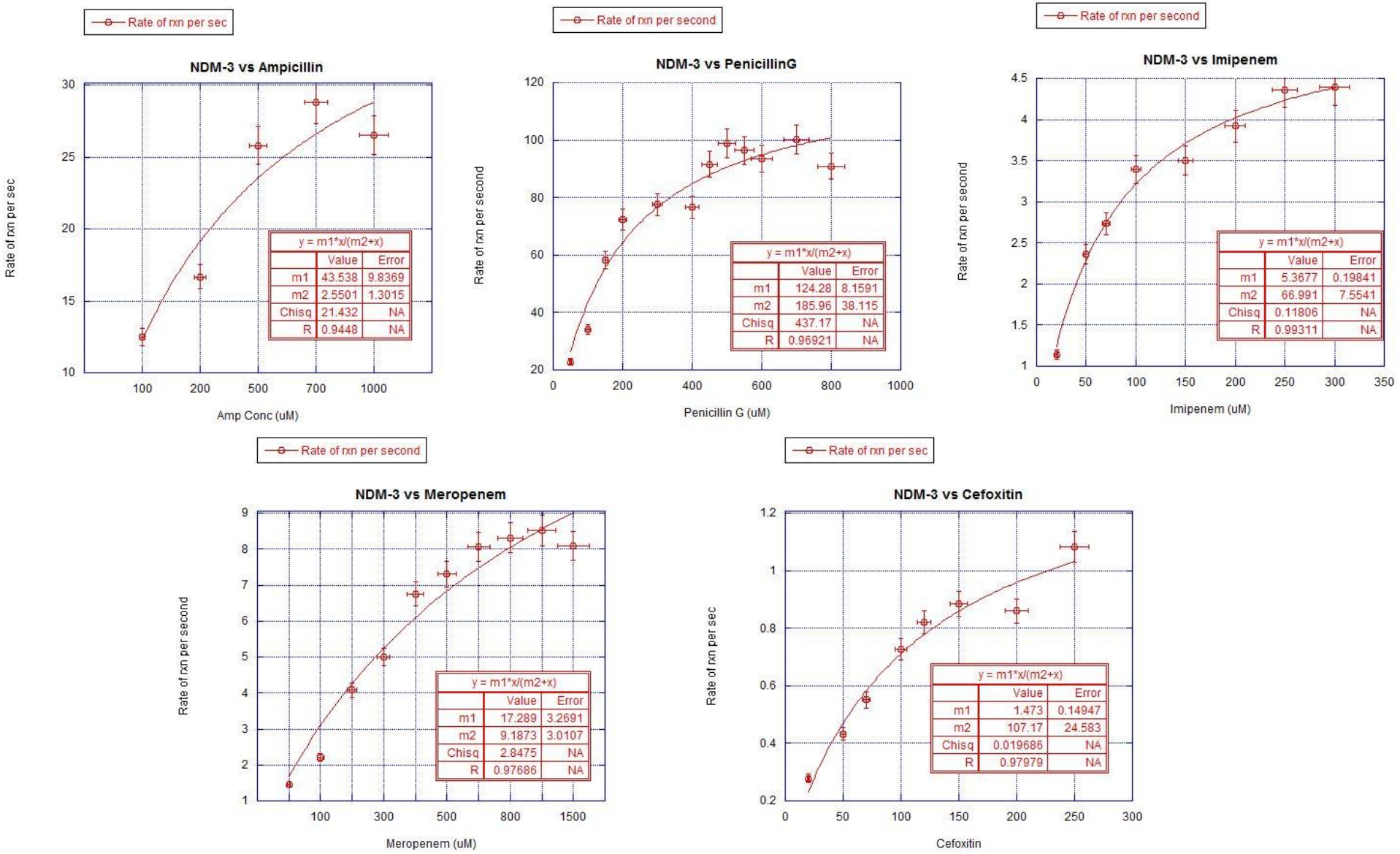

Figure 4d. Graphs showing the rate of reaction per second of NDM-3+Ub vs ampicillin, penicillinG, imipenem, meropenem, and cefoxitin.

4.3.1 NDM-3+Ub vs Representative Substrates

As shown above in the graphs (figure 4d), NDM-3+Ub enzyme was assayed against ampicillin, penicillinG, imipenem, meropenem, and cefoxitin. The concentrations tested for each substrate were dependent on the preliminary assays done for each as outlined in 4.2. PenicillinG was assayed at varying concentrations from 50 µM to 800 µM, and ampicillin from 100 µM to 1000 µM. For both substrates 700 µM exhibited the greatest activity from NDM-3+Ub. NDM-3+Ub was then assayed against imipenem and meropenem from the carbapenem family of antibiotics. Imipenem was tested between 20 µM and 350 µM, and its highest activity was shown to be 300 µM. Meropenem was tested between 50 µM and 1500 µM, with 1000 µM showing the highest activity.
Finally, NDM-3+Ub was assayed against cefoxitin at varying concentrations from 20 µM to 250 µM. As shown above NDM-3+Ub activity against cefoxitin is highest at 250 µM.

4.3.2 Table of Results for NDM-3+Ub against β-lactam antibiotics

	k_{cat} (s^{-1})	K_m (µM)	k_{cat} (s^{-1})/K_m (µM)
Ampicillin	22	3	8.54
PenicillinG	62	186	0.33
Imipenem	3	67	0.04
Meropenem	9	9	0.94
Cefoxitin	1	107	0.01

Table 4d. Summary of results for NDM-3+Ub vs various substrates experiments at pH 7.5

Evident from table 4d above, NDM-3+Ub uncleaved exhibited activity against all five β-lactam antibiotics at pH 7.5 to varying degrees. The V_{max} values and K_m values are taken directly from the graph and accompanying equation where the data were fit with the Michaelis-Menten model. The k_{cat} values represent the turnover rate per second of substrate molecules by the enzyme. PenicillinG activity against NDM-3+Ub is considerably higher than that of even its closest analogue, ampicillin, with ampicillin having almost one third of the activity.

As can also be seen, the binding affinity between ampicillin and NDM-3+Ub was the highest (lowest K_m value), while meropenem showed high binding affinity too. Interestingly when comparing the 'catalytic efficiency' rates or scores (k_{cat}/K_m) ampicillin scores highest, followed by meropenem, penicillinG, imipenem, and finally cefoxitin. Despite penicillinG showing a stronger k_{cat} value to all the other substrates, its high K_m value, and therefore low affinity for the enzyme means its catalytic efficiency rating is lower than ampicillin and meropenem in this instance.

4.4 Cleaved NDM-3+Ub

While cleavage conditions of NDM-3+Ub were determined and optimised as outlined in section 3.9, no enzymatic assay data was obtained on the cleaved enzyme. The cleaved enzyme was isolated as shown in the SDS Page Gels in Figure 3i, but no activity was measured on numerous assay occasions testing the cleaved NDM-3+Ub enzyme, at wide ranges of cleaved NDM-3+Ub and substrate concentrations. Unfortunately, none of the five substrates tested for the uncleaved enzyme as per section 4.3 and additional substrates such as cephalothin showed activity and therefore, no activity data are available for this cleaved enzyme.

Following these results, at this point the decision was made to order a new construct without the ubiquitin tag attached to aid research of activity of NDM-3. This new construct (denoted NDM-3(NC)) also contained the hexa-histidine tag in order to aid in one step purification as before, and the purification process was completed as outlined in section 2.2 and 3.4. The conditions of optimising this process were also outlined in chapter 3. The intended comparison was between the cleaved and uncleaved NDM-3+Ub construct. Due to the lack of activity of the cleaved enzyme, it was decided to change the comparison study to compare the uncleaved NDM-3+Ub enzyme with the NDM-3(NC) enzyme and see the difference in activities. The same substrates were used in order to make a direct comparison. For the sake of clarity between the experiments using uncleaved NDM-3+Ub and the newer construct of NDM-3, the latter was denoted NDM-3(NC).

4.5 Activity Assays of NDM-3(NC)

Following on from Section 4.4, the enzymatic assays were carried out for NDM-3(NC) against ampicillin, penicillinG, imipenem, meropenem, cefoxitin, and cephalothin in this case. All assays were carried out at room temperature and at pH 7.5 and using the assay buffer as determined in section 4.1. These data were also used in section 4.7 for the pH profile experiments.

4.5.1 NDM-3(NC) vs Representative Substrates

In this section the NDM-3(NC) enzyme was assayed against ampicillin, penicillinG, imipenem, meropenem, cefoxitin, and cephalothin (see figure 4e). Ampicillin was assayed at increasing concentrations from 100 µM to 1500 µM and NDM-3(NC) activity was highest in the presence of 1000 µM of ampicillin. NDM-3(NC) enzyme was assayed against penicillinG at increasing concentrations from 100 µM to 1250 µM and again activity was highest in the presence of 1000 µM of penicillinG. Both substrates highest activity at 1000 µM is interesting as for NDM-3+Ub the highest activity was the same between the two substrates, but was lower at 700 µM.

NDM-3(NC) enzyme was then assayed against imipenem from 50 µM to 480 µM and activity can be seen to be highest at 450 µM of imipenem. Against meropenem, activity was measured from 50 µM to 1500 µM and activity was highest in the presence of 1500 µM of meropenem. Above this concentration of meropenem however, no activity was measured for NDM-3(NC).

When assayed against cefoxitin at increasing concentrations from 20 µM to 200 µM and NDM-3(NC) activity was highest in the presence of 200 µM of cefoxitin. NDM-3(NC) was inactive at concentrations above 200 µM of cefoxitin. Finally, when assayed against cephalothin at increasing concentrations from 5 µM to 200 µM activity was highest in the presence of 150 µM of cephalothin.

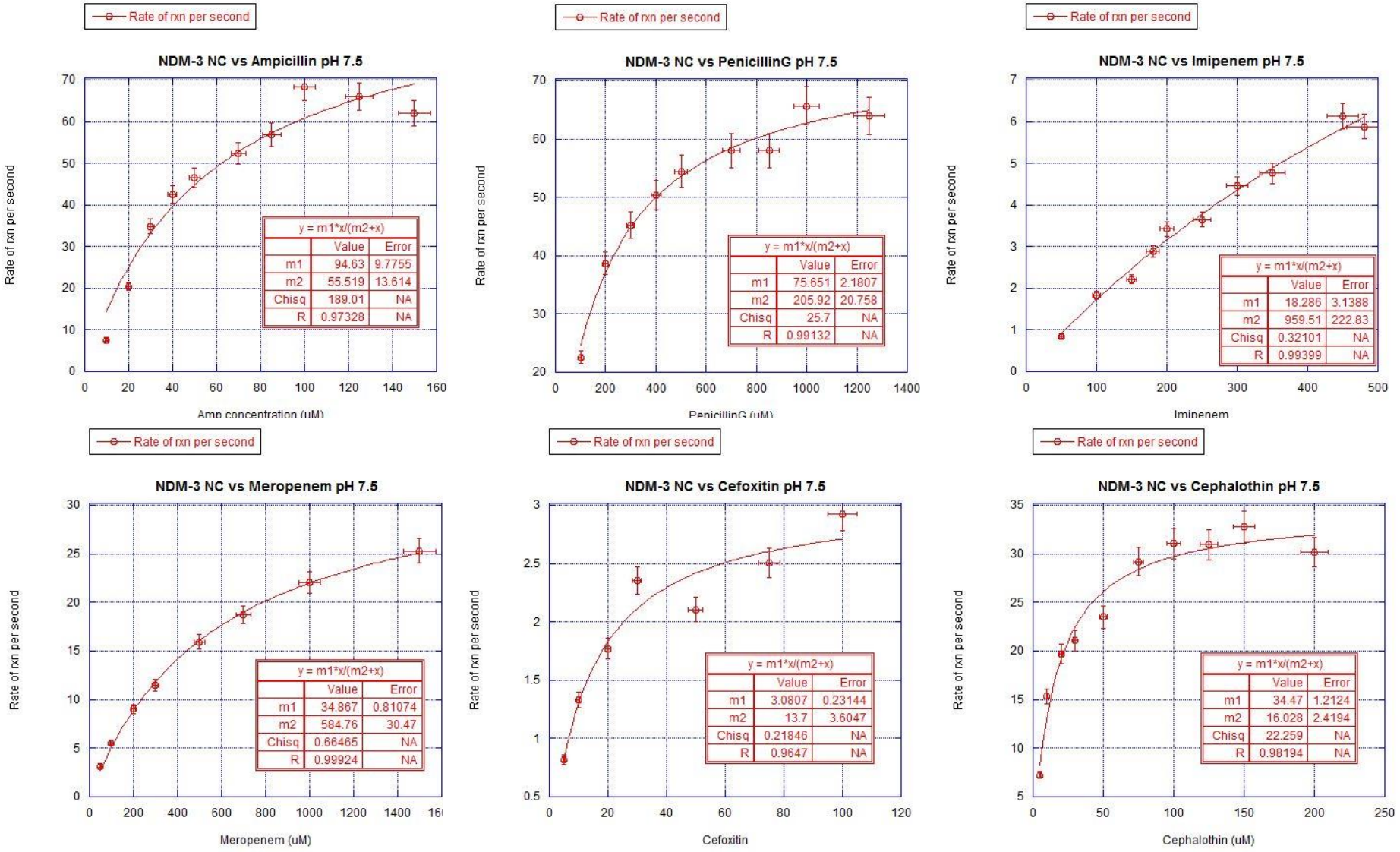

Figure 4e. Graphs showing the rate of reaction per second of NDM-3(NC) vs ampicillin, penicillinG, imipenem, meropenem, cefoxitin, and cephalothin at pH 7.5.

4.5.2 Table of Results for NDM-3(NC) against β-lactam antibiotics

	k_{cat} (s^{-1})	K_m (μM)	k_{cat} (s^{-1})/K_m (μM)
Ampicillin	47	56	0.85
PenicillinG	38	206	0.18
Imipenem	9	960	0.01
Meropenem	17	585	0.03
Cefoxitin	2	14	0.11
Cephalothin	17	16	1.08

Table 4e Summary of results for NDM-3(NC) vs various substrates experiments at pH 7.5

As can be seen from table 4e, the summary table of results for NDM-3(NC) vs various β-lactam antibiotics, activity was present for all five substrates at pH 7.5. The K_m and k_{cat} numbers were calculated from the plots above, and the equations given within the plot and at the beginning of this chapter. The k_{cat} values shown above represent the turnover rate per second of substrate molecules by the enzyme, NDM-3(NC) while the K_m value represents the binding affinity of the enzyme for the substrate.
Contrastingly to uncleaved NDM-3+Ub before, ampicillin has a higher rate of activity than penicillinG does for NDM-3(NC). Also determined is that the binding affinity between ampicillin, cefoxitin, and cephalothin is lower (and therefore better binding affinity), with meropenem having a very high K_m value for NDM-3(NC), different to its lower one for NDM-3+Ub.

Evident from these results are that ampicillin and penicillinG elicit the highest activity, with ampicillins binding affinity being much better than penicillinG's in this case. As can be clearly seen, NDM-3(NC) alone had higher k_{cat} values for the majority of the substrates, with penicillinG being the one notable exception.

For NDM-3(NC) the catalytic efficiency 'ratings' are in the following order;
Cephalothin, ampicillin, penicillinG, cefoxitin, meropenem, and imipenem.

4.5.3 Comparison of NDM-3+Ub and NDM-3(NC) activities against five representatives from the β-lactam antibiotic families

Substrate	Enzyme	kcat (s^{-1})	Km (μM)	kcat (s^{-1})/Km (μM)
Ampicillin	*NDM-3+Ub*	22	3	8.54
	NDM-3(NC)	47	56	0.85
PenicillinG	*NDM-3+Ub*	62	186	0.33
	NDM-3(NC)	38	206	0.18
Imipenem	*NDM-3+Ub*	3	67	0.04
	NDM-3(NC)	9	960	0.01
Meropenem	*NDM-3+Ub*	9	9	0.94
	NDM-3(NC)	17	585	0.03
Cefoxitin	*NDM-3+Ub*	1	107	0.01
	NDM-3(NC)	2	14	0.11

Table 4f. Table of k_{cat}, K_m, *and* k_{cat} / K_m *values for NDM-3+Ub and NDM-3(NC) for comparison of results.*

What can be seen from summary table 4f, is that NDM-3(NC) has higher K_m values to NDM-3+Ub for all substrates with the exception of cefoxitin. The affinity of NDM-3+Ub is higher than the construct without the ubiquitin tag. What this tells us is that the ubiquitin tag makes this construct (NDM-3+Ub) less active generally, but actually increases the affinity the substrates have for the enzyme, therefore increasing the 'catalytic efficiency' number. It is worth noting that the ubiquitin tag must be altering the conformation of the enzyme significantly and allowing a different or improved access for the substrate and enzyme to bind. However, despite aiding in access it seems to hinder the activity of the enzyme too. In this instance, NDM-3(NC) construct that does not contain the ubiquitin tag seems to be better than the construct with the ubiquitin tag(NDM-3+Ub), as it is a truer representation of the enzymatic ability of the enzyme.

For NDM-3(NC) the catalytic efficiency 'ratings' are in the following order;

Cephalothin, ampicillin, penicillinG, cefoxitin, meropenem, and imipenem*.

For NDM-3+Ub, it was;

Ampicillin, meropenem, penicillinG, imipenem, and cefoxitin.

*Not tested for NDM-3+Ub

From this information we can ascertain that imipenem is not a substrate that is catalysed as readily by NDM-3 as others in general, and that ampicillin and penicillinG appear to deplete faster and bind better to the enzyme. Meropenem seems to have undergone the greatest change between the two enzymes, ranking second for NDM-3+Ub, to second last for NDM-3(NC). This all appears to be as a result of a much higher K_m value for the latter.

4.6 Comparison of NDM-3(NC) to NDM-1, NDM-4, NDM-8, NDM-14

NDM-3				NDM-1		
kcat (s^{-1})	**Km (μM)**	**kcat (s^{-1})/Km (μM)**	**Substrate**	**kcat (s^{-1})**	**Km (μM)**	**kcat (s^{-1})/Km (μM)**
47.32	55.52	0.85	**Ampicillin**	182	154	1.18
37.83	205.92	0.18	**Penicillin**	142	58	2.45
9.14	959.51	0.01	**Imipenem**	58	108	0.54
17.43	584.76	0.03	**Meropenem**	72	69	1.04
1.54	13.70	0.11	**Cefoxitin**	Data N/A	Data N/A	Data N/A
NDM-4						**NDM-14**
kcat (s^{-1})	**Km (μM)**	**kcat (s^{-1})/Km (μM)**	**Substrate**	**kcat (s^{-1})**	**Km (μM)**	**kcat (s^{-1})/Km (μM)**
ND	ND	ND	**Ampicillin**	102	80	1.28
ND	ND	ND	**Penicillin**	230	186	1.24
40	86	0.47	**Imipenem**	42	90	0.47
30	95	0.32	**Meropenem**	60	53	1.13
Data N/A	Data N/A	Data N/A	**Cefoxitin**	**Data N/A**	**Data N/A**	**Data N/A**
NDM-8						
kcat (s^{-1})	**Km (μM)**	**kcat (s^{-1})/Km (μM)**	**Substrate**			
158	193	0.82	**Ampicillin**			
91	74	1.23	**Penicillin**			
167	46	3.63	**Imipenem**			
127	169	0.75	**Meropenem**			
34	3	11.33	**Cefoxitin**			

Table 4g. Comparison of NDM-3(NC) to NDM-1 (177), *NDM-4* (161), *NDM-8* (162), *and NDM-14* (177)

4.6.1 NDM-3(NC) vs NDM-1; Enzymatic assays comparison

As can be determined from the table 4g above, NDM-3(NC) has lower affinity (higher K_m values) and lower turnover rates (k_{cat}) than the other NDM mutants. This could be attributed to the position of the substitution which as described in Chapter 2 and 3 that it is on the surface of the protein, at residue 95. As can be seen from table 4g, NDM-3(NC) has weaker activity rates than NDM-1 for all antibiotic substrates when data were available for NDM-1. No data were available for NDM-1 activity against cefoxitin, but the activity for NDM-3(NC) for that substrate was very low. There is sufficient evidence that NDM-3(NC), similar to NDM-1, appears to hydrolyse all β-lactam antibiotics. NDM-3(NC) had lower k_{cat} values than NDM-1 for all substrates tested, and had higher K_m values (and therefore lower affinity) for all excepting ampicillin. This suggest that the substitution on the surface of the protein, from aspartic acid to asparagine (Asp to Asn) aids in some way for the ampicillin substrate binding to the active site of NDM-3(NC). Perhaps it can be attributed to the change in charge, from negatively charged to uncharged/neutral at pH 7.0. Overall, however, due to the lower k_{cat} numbers for NDM-3(NC) - between 16% and 26% activity of NDM-1 was measured - the catalytic efficiency of NDM-1 is far superior than NDM-3(NC). The substitution location is not in the active site nor is it involved in the active site area so the decrease of activity for a single amino acid substitution indicates that there is much about these enzymes and their mechanisms of action that we do not yet know.

4.6.2 NDM-1, NDM-3, NDM-4, NDM-8, and NDM-14 comparisons

Generally NDM-1 shows the greatest activity in the hydrolysis of β-lactam antibiotics than NDM-3(NC), NDM-4, NDM-8, and NDM-14. The few exceptions are NDM-8's higher carbapenemase activity, and NDM-14's higher activity against penicillin. The increased NDM-8 imipenem and meropenem activity is again perhaps attributable to the substitutions of two amino acids, at position 130 and 154 from Asp to Gly and Met to Leu respectively. Like NDM-3, these residues are not present in the two important loops – L3 and L10 – further suggesting that unknown to us as yet residues must indirectly affect the binding site or the binding affinity the enzyme has with the antibiotic not in the active site. For these substitutions, at pH 7.0; at 130 there is a negatively charged aspartic acid replaced by a neutrally charged glycine, and at 154 there is an uncharged methionine residue replaced by a positively charged leucine residue. Interestingly the same replacement occurs in NDM-4 at 154 only (not at 130 too) and the increased carbapenemase activity is not evident.

For NDM-14's increased activity against penicillin, its residue substitution occurs at 130 and is the same as NDM-8. It appears that the substitution at 154 alone does not increase enzyme activity against carbapenems or penicillin (such as NDM-4 mentioned above). However, a substitution at residue 130 alone shows increased penicillin activity for NDM-14, and when aided by the substitution of 154 in NDM-8 appears to lead to increased carbapenem activity.

This is interesting due to the nature of where the substitutions lie. The substitution for all NDM-1 mutants as listed above do not occur in the active site in either the L3, or L10 loops. It is telling that a single substitution far enough away from the active site can impact on

certain substrates activity so greatly. It tells us that this amino acid residue must indirectly affect the substrate's interaction with the active site of the enzyme.

4.6.3 Enzymatic assays comparison - Conclusion

NDM-3(NC) shows lower activity than all of the other NDM mutants listed above. This could mean that residue 95 being substituted as outlined above makes a significant difference to the binding and the hydrolysing activity of the enzyme for each substrate. While further study on this area could further illuminate the reasons behind this, it is interesting to see how one, and in some cases two, single amino acid substitutions can widely affect an enzyme's ability to hydrolyse β-lactam antibiotics.

It is as yet unclear which residues and residue positions play an integral role in their enzymatic activity, but it is also clear that NDM-1 followed by NDM-8 seem to have the highest all-around activities. NDM-1 also shows the best 'catalytic efficiency score' out of all of the NDM mutants listed above, which must aid in its robust and virulent nature.

4.7 pH profile study for NDM-3(NC)

Aim of the pH profile study

For these experiments NDM-3(NC) was used in assays against four antibiotics – ampicillin, imipenem, meropenem, and cefoxitin. Assays were performed across a range of pH 4.5 to pH 11.0 for each substrate. The aim was to find the optimal pH range for NDM-3(NC) for the four substrates below, and to analyse and compare the results.

4.7.1 Ampicillin

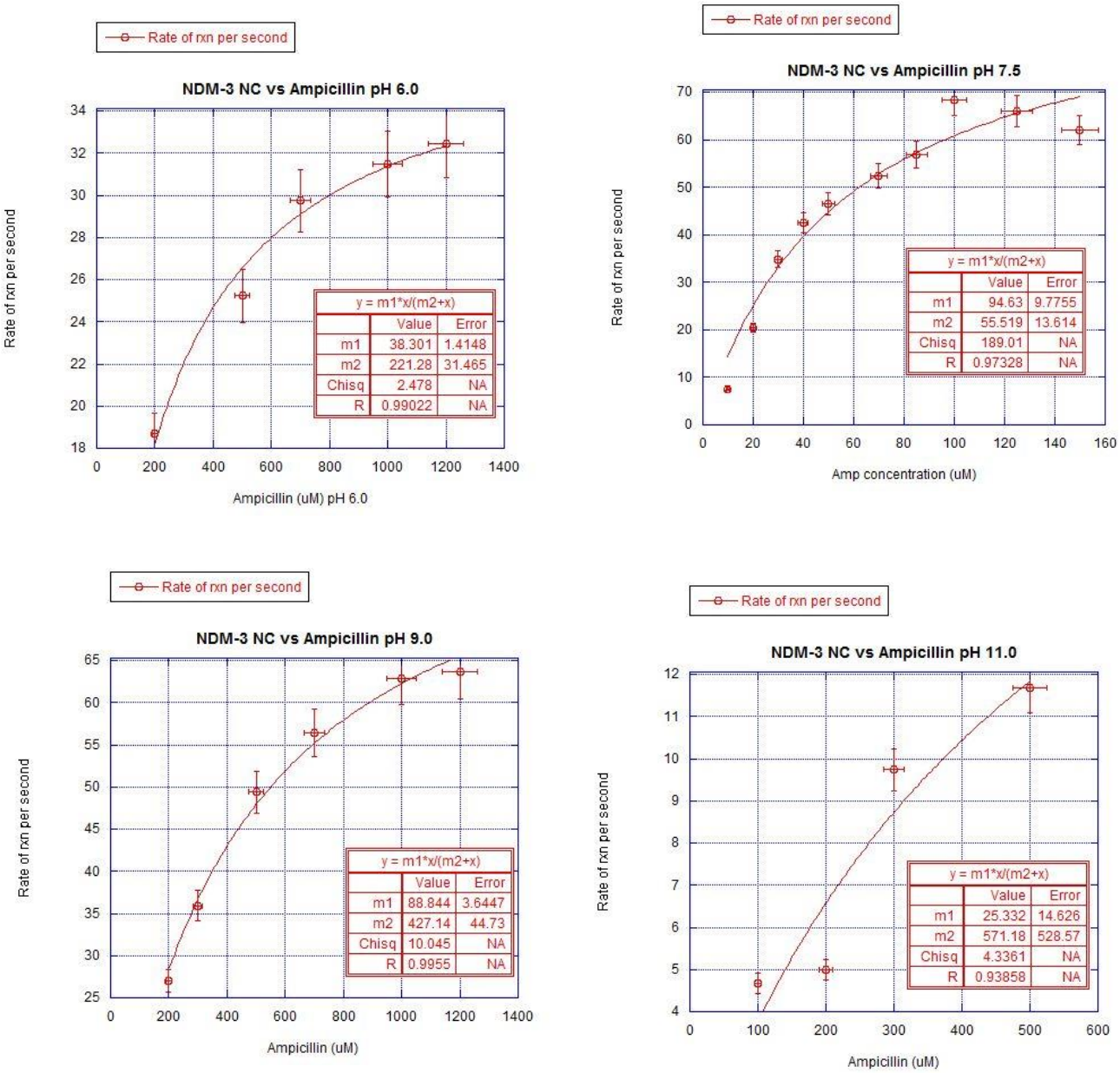

Figure 4f. Graphs showing results of NDM-3(NC) vs ampicillin at pH 6.0, 7.5, 9.0, and 11.0. No data could be measured at pH 4.5

4.7.1 Table of Results showing activity of NDM-3(NC) against ampicillin substrate over range of pH values from 4.5 to 11.0

Ampicillin	kcat (s^{-1})	Km (µM)	kcat (s^{-1})/Km (µM)
4.5	ND	ND	ND
6.0	19	221	0.09
7.5	47	56	0.85
9.0	44	427	0.10
11.0	13	571	0.02

Table 4h. Summary of results for NDM-3(NC) against ampicillin at multiple pH points

As can be seen from the plots (figure 4f) and the table of results (table 4h), at pH 4.5 no data was measured. At pH 6.0 only low activity was measured. Unsurprisingly, at physiological pH 7.5 the highest activity was measured. This was consistent until pH 9.0 after which point the activity dwindled. The substrate had much higher affinity (a low Km value) for the NDM-3(NC) enzyme at pH 7.5 compared to pH 9.0, therefore the catalytic efficiency value is highest here. At pH 9.0 the K_m value is much higher which means that a higher concentration of substrate is necessary at this pH in order to achieve V_{max}. At pH 11.0 the lowest measurable activity was shown, showing the lowest affinity and turnover rate at this pH. This physiological pH preference on the part of NDM-3 makes sense. pH 7.5 is definitely the optimal pH point for ampicillin hydrolysis for NDM-3(NC), but between pH 7.5 and 9.0 appears to remain highly active.

4.7.2 Imipenem

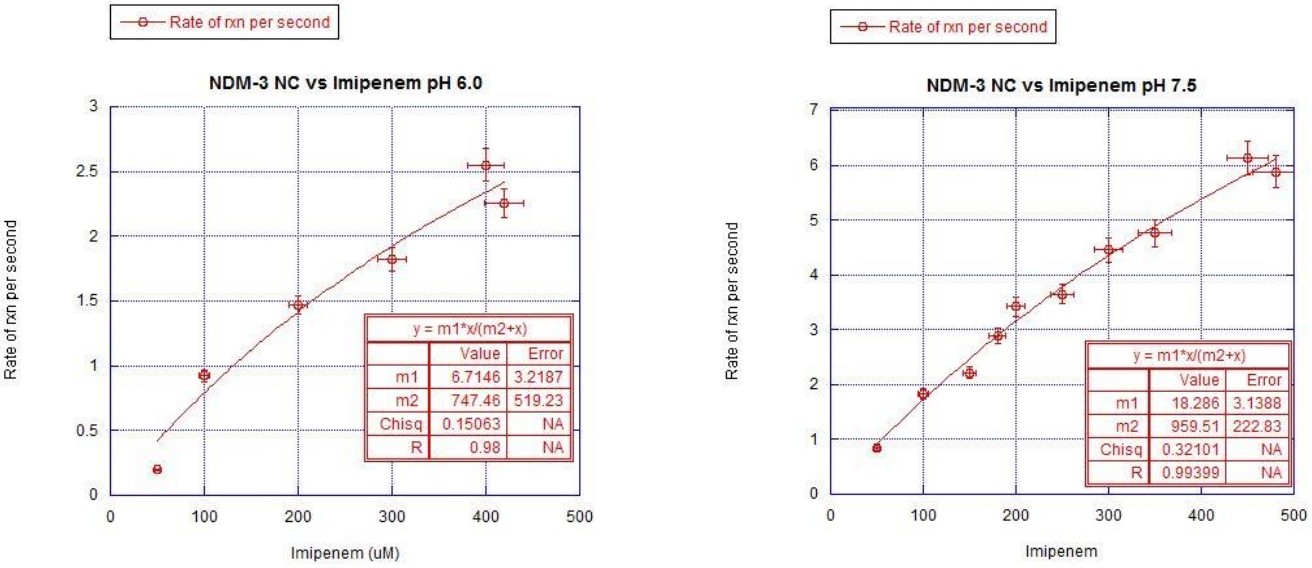

Figure 4g. Graphs showing results of NDM-3(NC) vs imipenem at pH 6.0, and 7.5. No data could be measured at pH 4.5, 9.0, or 11.0.

4.7.2 Table of Results showing activity of NDM-3(NC) against imipenem Substrate over range of pH values from 4.5 to 11.0

Imipenem	kcat (s^{-1})	Km (µM)	kcat (s^{-1})/Km (µM)
4.5	ND	ND	ND
6.0	3	747	0.00
7.5	9	960	0.01
9.0	ND	ND	ND
11.0	ND	ND	ND

Table 4i. Summary of results for NDM-3(NC) against imipenem at multiple pH points

As can be seen from the plots (figure 4g) and table 4i, at pH 4.5, 9.0, and 11.0 no data were able to be measured. At pH 6.0 very low activity was measured. Again, unsurprisingly physiological pH of 7.5 showed the greatest activity, specifically three times that of pH 6.0. However, for both pH points the affinity of the substrate for the enzyme was very low, as can be seen by the high Km value. Overall imipenem appears to be hydrolysed poorly by NDM-3(NC) and the pH study shows a much narrower pH range of imipenem usefulness, compared to the other substrates. The optimal range is pH 7.5, or more probably pH 7.0 to 7.5.

4.7.3 Meropenem

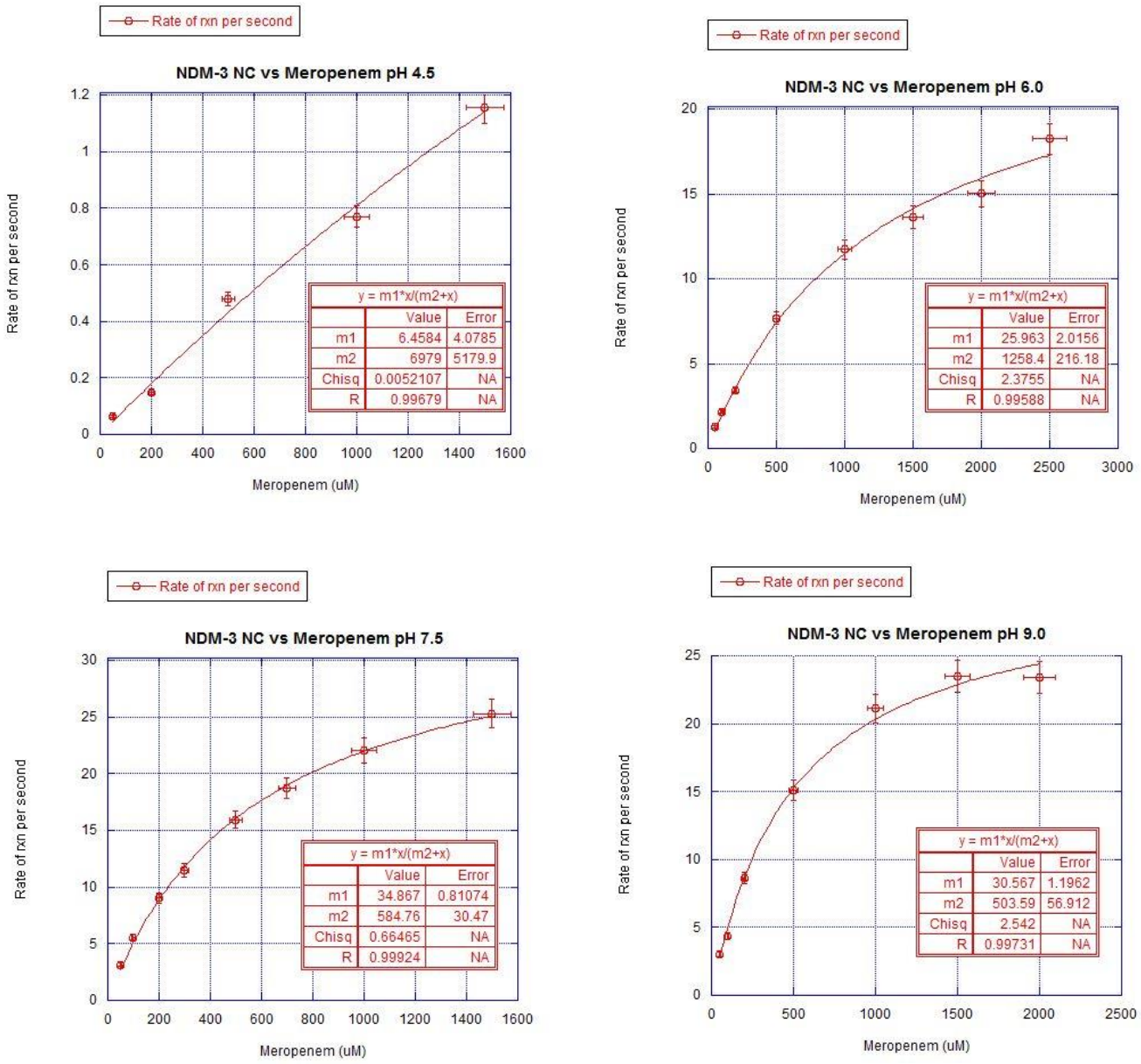

Figure 4h. Graphs showing results of NDM-3(NC) vs meropenem at pH 4.5 ,6.0, 7.5, and 9.0. No data could be measured at pH 11.0

4.7.3 Table of Results of activity of NDM-3(NC) against meropenem for pH range 4.5 to 11.0

Meropenem	kcat (s^{-1})	Km (µM)	kcat (s^{-1})/Km (µM)
4.5	3	6979	0.00
6.0	13	1258	0.01
7.5	17	585	0.03
9.0	15	504	0.03
11.0	ND	ND	ND

Table 4j. Summary of results for NDM-3(NC) against meropenem at multiple pH points

As can be seen from the plots (figure 4h) and table (table 4j) data were available at pH 4.5, 6.0, 7.5, and 9.0 for meropenem. At pH 4.5 very low activity was measured which when added to an extremely high K_m value signifying very low affinity means realistically it is not part of the optimal range of pH for meropenem and NDM-3(NC). It was noted however that meropenem and imipenem have very different activity profiles at different pH values. Unsurprisingly, the physiological pH of 7.5 showed the greatest activity, and pH 9.0 very similar. The catalytic efficiency value for pH 9.0 is actually superior to pH 7.5 due to a slightly improved K_m value for pH 9.0. No data could be recorded at pH 11.0, but thus far meropenem appears to have a wider optimal pH range than imipenem. Interestingly the K_m values decrease rather quickly between pH 4.5 and eventually pH 9.0. This again shows the optimal range for meropenem is pH 7.5 - 9.0.

4.7.4 Cefoxitin

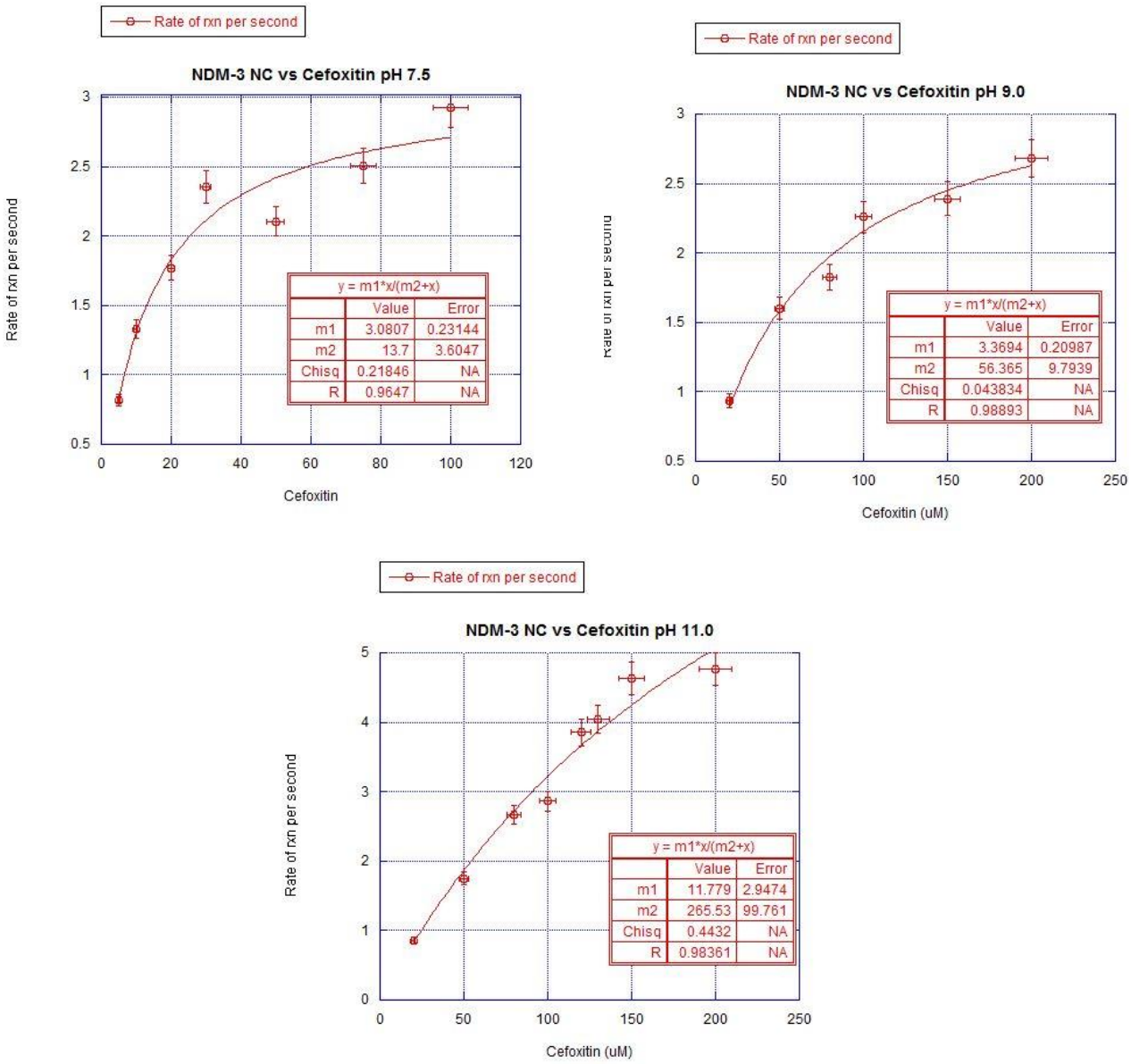

Figure 4i. Graphs showing results of NDM-3(NC) vs cefoxitin at pH 7.5, 9.0, and 11.0
No data could be measured at pH 4.5, or 6.0

4.7.4 Table of Results showing activity of NDM-3(NC) against cefoxitin Substrate over range of pH values from 4.5 to 11.0

Cefoxitin	kcat (s^{-1})	Km (μM)	kcat (s^{-1})/Km (μM)
4.5	ND	ND	ND
6.0	ND	ND	ND
7.5	2	14	0.11
9.0	2	56	0.03
11.0	6	266	0.02

Table 4k Summary of results for NDM-3(NC) against cefoxitin at multiple pH points.

As can be seen from the plots (figure 4i) and table (table 4k) data were available at pH 7.5, 9.0, and 11.0 for cefoxitin. For all three pH points rather low activity was measured, and increasing K_m values from pH 7.5 to pH 11.0 means that pH 7.5 is the best pH point of the three measured. Unsurprisingly again the physiological pH of 7.5 showed the greatest activity, while pH 9.0 had the same k_{cat} value but a higher K_m value meaning it was not quite as efficient at this pH point. The catalytic efficiency value for pH 7.5 is superior to pH 9.0. which is superior to pH 11.0, but they are relatively close in values. The K_m values for all three are relatively low, indicating good binding between enzyme and substrate, in comparison to values obtained for some of the other substrates. At pH 4.5 and 6.0 no data were recorded.

4.7.5 Overall pH ranges of the substrates; ampicillin, imipenem, meropenem, and cefoxitin

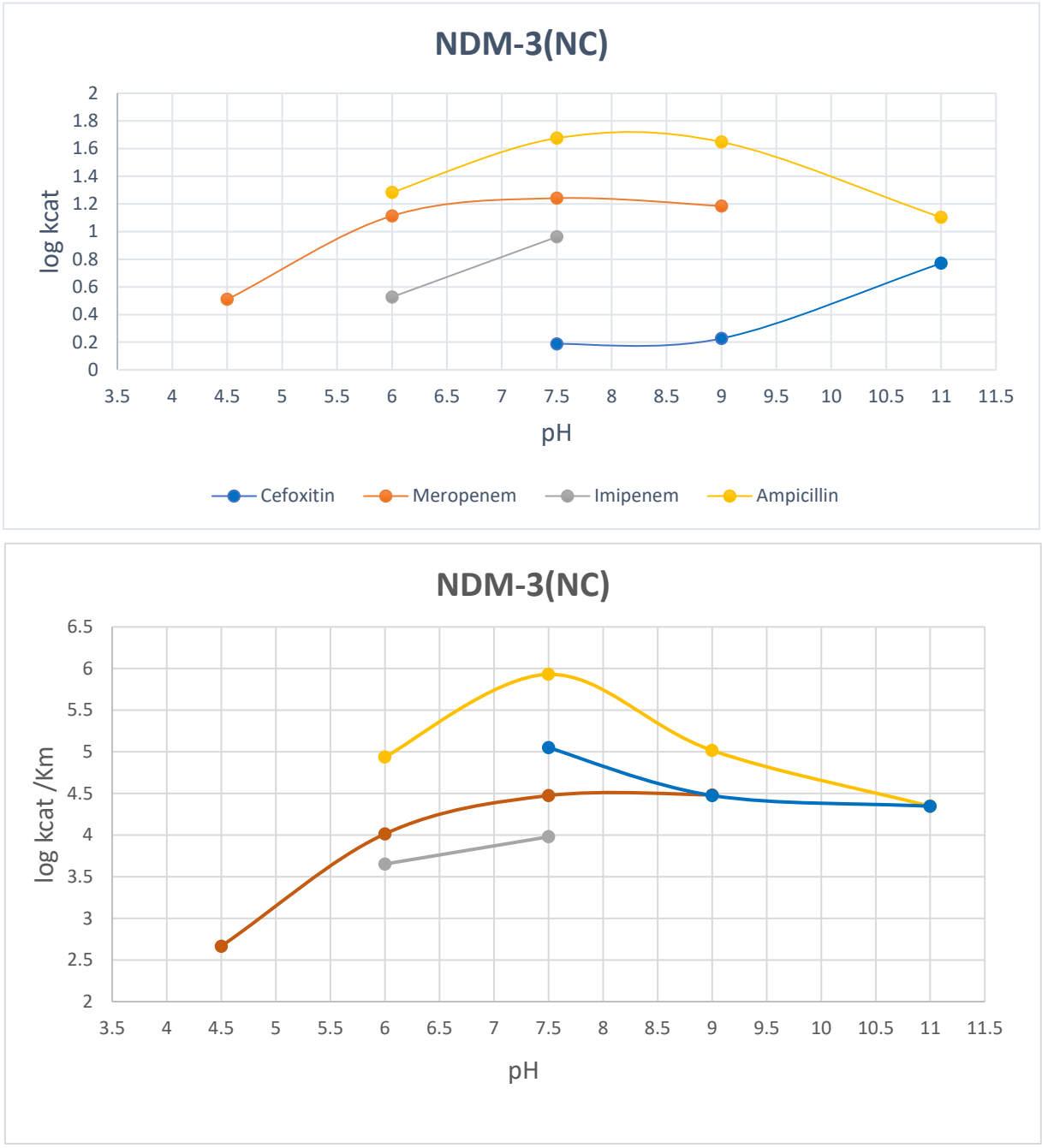

Figure 4j. The two graphs plot (a) pH vs log k_{cat} and (b) pH vs log k_{cat} / K_m

4.7.5 What information this pH study can tell us

As seen in the data above and in the summary graphs in figure 4j, the optimal pH for each substrate when interacting with NDM-3(NC) can be measured from graphing log k_{cat} vs pH and log k_{cat}/K_m vs pH.
In this example it can be clearly seen that the optimal pH ranges for each substrate are as follows;

Substrate	Optimal pH range
Ampicillin	7.5 – 8.5
Imipenem	7.5
Meropenem	7.5 – 9.0
Cefoxitin	7.5

Table 4l. Table showing optimal pH point or range for NDM-3(NC) with each substrate.

From table 4l we can deduce that all four of the chosen substrates show some, but more importantly, the highest activity is at physiological pH. This would contribute to the virulent nature of NDM, as its most active form is at the neutral pH range, between 7.3 to 7.8, which is the physiological pH range.
These plots (figure 4j) also tell us over what pH range NDM-3(NC) is capable of hydrolysing specific β-lactam antibiotics, as well as the optimum range for its hydrolysis of each enzyme. We learn from this that imipenem has the narrowest range of activity over pH.
It can be inferred from this that the pH range of 7.0 – 8.0 is most appropriate for NDM-3(NC) to thrive against all of the antibiotics tested.
Meropenem and ampicillin were the widest ranging, while cefoxitin was capable of showing activity at more pH points than imipenem but less than meropenem or ampicillin.
Interestingly, meropenem has a wider optimal pH range than ampicillin, and despite have some activity at pH 4.5, still has the optimal activity at pH 7.5 and above.
Despite having preferred pH ranges, NDM-3(NC) shows activity over the entire range for different substrates, which is a huge pH range of activity.

4.8 Lactonase Experiment

As outlined in the experimental section in chapter 3, NDM-3(NC) underwent assays to test if it had activity against lactonases. Following procedures previously determined as per Miraula in "Promiscuous metallo-β-lactamases: MIM-1 and MIM-2 may play an essential role in quorum sensing networks" (154). Initial assays were carried out to determine the correct methanol percentage required for the buffer. This was carried out using 50 μM penicillin as the enzyme has been proven to be active in the presence of penicillin. Increasing amounts of methanol were added to each assay to see the effect it had on the enzyme activity. A concentration of 15% methanol was found to be the optimum percentage (155; 156; 157; 158; 159; 160).

Two AHL's were used in the experiment, namely N-(β-ketocaproyl)-L-homoserine lactone and N-3-oxo-octanoyl-L-homoserine lactone. No activity was found for either lactone for NDM-3(NC). Preliminary assays determined that NDM-3(NC) had no lactonase activity, however it would be interesting in the future for other groups to test NDM-1 in the same way.

4.9 Conclusion

NDM-3 was a sensitive and difficult enzyme to work with, giving problems during purification and isolation of active enzyme. Once this had occurred, enzymatic assays for both NDM-3+Ub and NDM-3(NC) were carried out.

The assay buffer used for all of the enzymatic assays was determined through optimisation experiments outlined in section 4.1, which was 50 mM HEPES and 50 mM NaCl.

From section 4.3 to 4.5 the k_{cat} and K_m values for both enzymes (NDM-3+Ub, and NDM-3(NC)) were determined and reported. Through this process we saw that no activity could be measured for the cleaved NDM-3+Ub construct when isolated after successful cleaving with USP2cc protease. A new construct (NDM-3(NC)) substituted then as outlined in 4.5, and the two sets of results were outlined at the end of section 4.5. Ultimately it has been determined that NDM-3 (both constructs) has a wide range of hydrolytic activity for all the substrates tested. While binding affinities and therefore catalytic efficiencies altered, the turnover numbers were generally consistent between the two NDM-3 constructs.

In section 4.6 the results reported from section 4.5 for NDM-3(NC) were used for a comparison with literature data available for NDM-1, NDM-4, NDM-8, and NDM-14. This was an effort to see where NDM-3(NC) activity ranked in relation to these other mutants which had kinetic data available. NDM-3(NC) proved to show the lowest activities of all the mutants listed above.

From the pH profile study for NDM-3(NC) against ampicillin, imipenem, meropenem, and cefoxitin, we can see that at physiological pH (pH 7.3 – 7.8) NDM-3(NC) has the highest activity rates. This absolutely contributes to the virulence NDM-3(NC), and by extension NDM-1 would have as it can flourish at physiological pH levels. Adding to this, this study also showed the wide pH range that NDM-3(NC) can hydrolyse β-lactam antibiotics over.

No inhibitor was available for testing at the time of these experiments but future work in this area involving potential inhibitors whether universal or specific to NDM MBLs with NDM-3 or NDM-1 would be advantageous. This is a topic and area of research where there is no end to the amount of work to do, with the biggest task being to find an antibiotic that evades most evolutions the enzymes could adapt and evolve to. Alternatively, finding an inhibitor, similar to clavulanic acid for SBLs, that would inhibit or cause the mechanisms the MBLs employ to inactivate the lactamase antibiotics to fail would be the goal. This seems to be the most viable option but there is still much work to do before that happens.

Thesis Conclusion

As discussed in Chapter One – 'Introduction and research background' the main aim of this research work was to isolate and optimise the expression, purification, and characterisation of novel enzyme NDM-3 and to compare it to well-known and better characterised NDM-1 enzyme. NDM-3 is currently just one of up to 15 mutants of NDM-1 which have been discovered. The NDM-3 plasmid originally acquired was a ubiquitin-hexa histidine fusion protein denoted NDM-3+Ub, which aided in expression and purification yields but required the addition of a cleavage step in order to isolate the NDM-3 protein on its own. NDM-3 has a single amino acid difference from NDM-1, and the placement of said substitution is not directly involved with the active site or the residues around it. The native NDM-1 enzyme along with its mutants are of high importance for further investigation by research due to their significant impact to human health. At the time this research project began no published papers or documents were available on NDM-3. Since completing experimental work on this enzyme similar results were found by another group, which showed similar enzymatic characterisation results with some of the same substrates (5).

NDM-3 was a sensitive and at times problematic enzyme to work with. It was highly sensitive to changes in environment, including salt concentrations, imidazole concentrations, temperature changes, and unfortunately it was common that despite having it isolated the enzyme did not show or have any activity against any of the β-lactam antibiotics (in the case of NDM-3+Ub only). The data shown are the result of many failed attempts to isolate a pure, active, and (in the case of the construct with the ubiquitin tag) cleaved enzyme for NDM-3+Ub. As the research project developed, the need for an NDM-3 construct without the ubiquitin tag was required as no activity was shown for the cleaved enzyme, that construct denoted NDM-3(NC). As shown in chapter three, even though the cleavage was quite clear on the SDS gel, the enzyme was not active when assays were carried out. For this reason, only results with NDM-3+Ub tag were available.

When the second NDM-3 construct was made available, NDM-3(NC), the same expression and purification steps were utilised as both constructs had hexa-histidine tags attached, allowing for a 'one-step' purification using IMAC (chromatography) and using imidazole as the eluting agent. The appropriate imidazole concentrations were also a scientific discovery due to the sensitivity of the enzyme. The maximum imidazole concentration that worked best for my enzyme was 100 mM and this was determined to work best for my enzyme compared to the usual/suggested higher concentrations due to precipitation issues when higher concentrations were used (165).

The uncleaved NDM-3+Ub and NDM-3(NC) underwent similar enzymatic assay testing and the data were fit with steady-state kinetics plot fitting. Michaelis Menten (174) equations were used to determine the k_{cat} and K_m values of each construct for each substrate and a comparison carried out between the results of each. The results were as expected mostly, in that the NDM-3(NC), the construct without the ubiquitin tag, had higher k_{cat} values than the ubiquitin tagged protein, but interestingly the K_m values showed higher binding affinity for the enzymes in the construct with the ubiquitin tag. This suggests perhaps a structural

difference which allows the substrate to access the enzyme sites more easily, and yet not aid in the rate of reaction.

The cleaved NDM-3+Ub protein never showed activity for any of the substrates that it did when uncleaved, and indeed than the new construct did when tested afterwards. The cause for the inactivity of the protein is unknown to the author. It was not caused by precipitation of the protein or lack of cleavage by the protease (evidence of cleavage is in the SDS gel in chapter 3- Figure 3i).

The NDM-3(NC) underwent enzymatic assay testing and was compared to NDM-1 and other NDM mutants where the data were publicly available. The comparison showed that NDM-3(NC) is approximately 40% as active as NDM-1 against the substrates it has the highest activity against, namely ampicillin and penicillinG. Other NDM mutants showed significant increases in activity for certain antibiotics especially carbapenems. Ideally in the future further research will be undertaken to attribute the changes in activities for substrates based on the residue differences between all of the mutants. Currently potentially deterring this however is the wide range of reported results for NDM-1, and of course the knowledge gap surrounding NDM-1 in general due to it being more dissimilar to the other B1 type MBLs than members of the groups are usually. Ideally using all the information about the mutants in the future it will be easier to determine which residues specifically are vital for high affinity and low k_{cat} numbers.

Further kinetic assays were carried out on NDM-3(NC) against one representative from each β-lactam antibiotic family at different pH points. I chose ampicillin, imipenem, meropenem, and cefoxitin to assess. This experiment found the rate of reaction for pH 4.5, 6.0, 7.5, 9.0, 11.0 and plotted the log of the k_{cat} and the k_{cat}/K_m to see what pH range suits NDM-3(NC) best for each substrate. Generally, it was found that physiological pH range was most suited for NDM-3(NC), between 7.0 and 8.0 (human pH levels would be 7.3 – 7.6). This further adds to the reasons behind NDM-1's ability to flourish in humans.

Throughout this thesis error bars or RSDs are shown. Within plots/graphs (such as optimisation of buffers) the RSD and %RSD were calculated. For the data that were fit by Michaelis Menten kinetics the errors are included in the graph legend, which can be found beside each result.

The final aim of this project was to carry out initial assays to see if NDM-3(NC) had any lactonase activity which could be the basis for future work. Unfortunately, when tested the enzyme against two different AHLases neither showed activity against NDM-3(NC) from the proven active NDM-3(NC) batches previously used in lactamase activity assays.

Therefore, I can conclude that all of the aims of this research project were carried out where possible during the research time of this degree, and that hopefully the results found here could be useful to the scientific community in the future if all NDM mutants kinetic characterisation results are pooled together to attribute conformation and amino acid substitutions in order to better understand the way NDM's work. This would be done with an aim to finding or developing an inhibitor or new type of antibiotic that these enzymes would be unable to evolve past.

With the work currently going on in this field I am confident that with further research it will be possible to overcome this challenge we face. The sooner this particular enzyme is overcome the better due to the potential it has to cause death and illness.

Figures and Tables List

4c	*Zinc Chloride optimisation plot*
4d	*Graphs of reaction rates of NDM-3+Ub v substrates*
4e	*Graphs of reaction rates of NDM-3(NC) v substrates*
4f	*pH plots for ampicillin*
4g	*pH plots for imipenem*
4h	*pH plots for meropenem*
4i	*pH plots for cefoxitin*
4j	*pH comparison plots (a) pH vs log* k_{cat} *and (b) pH vs log* k_{cat} / K_m

Table Name	Information
1a	*Dissociation constants for the first (K_{D1}) and the second (K_{D2}) metal bound, obtained using competitive assays*
1b	*Dissociation constants of Me1 and Me2 species of wild type and mutant BcII against Co(II)using absorption spectroscopy (1)*
1c	*Comparison of Zn(II), Co(II), and Cd(II) metal ions*
2a	*Optimal cleavage conditions*
2b	*Antibiotics used with their extinction coefficients and wavelengths.*
3a	*BLAST Comparison with NDM-1 as the query sequence*
3b	*BLAST multiple sequence alignment legend and information for NDM-3 with NDM-1, VIM-2, IMP-1, CphA, and AIM-1.*
3c	*Sequence Comparison of known NDM mutants*
3d	*ProtParam information*
3e	*Optimal cleavage conditions*
4a	*Data measured for HEPES Assay Buffer experiments*
4b	*Data measured for NaCl Assay Buffer experiments*
4c	*Data measured for Zinc Chloride Assay Buffer experiments*
4d	*Summary of results for NDM-3+Ub vs various substrates experiments at pH 7.5*
4e	*Summary of results for NDM-3(NC) vs various substrates experiments at pH 7.5*
4f	*Table of* k_{cat}, K_m, *and* k_{cat} / K_m *values for NDM-3+Ub and NDM-3(NC) for comparison of results.*
4g	*Comparison of NDM-3 to NDM-1 (156), NDM-4 (158), NDM-8 (157) and NDM-14 (156)*
4h	*Summary of results for NDM-3(NC) against ampicillin at multiple pH points*

4i	*Summary of results for NDM-3(NC) against imipenem at multiple pH points*
4j	*Summary of results for NDM-3(NC) against meropenem at multiple pH points*
4k	*Summary of results for NDM-3(NC) against cefoxitin at multiple pH points.*
4l	*Table showing optimal pH point or range for NDM-3(NC) with each substrate.*

References

1. **Organisation, World Health.** https://www.who.int/news-room/fact-sheets/detail/antibiotic-resistance. *World Health Organisation.* [Online]

2. *The Antibiotic Resistance Crisis.* **Ventola, CL.** 4, s.l. : National Library of Medicine, 2015, Vol. 40.

3. *Antibiotics: past, present and future.* **Hutchings, MI. , Truman, AW., Wilkinson, B.** s.l. : Current Opinion in Microbiology, 2019, Vol. 51.

4. *β-Lactamases and β-Lactamase Inhibitors in the 21st Century.* **Tooke, C., et al.** 18, s.l. : Journal of Molecular Biology, 2019, Vol. 431.

5. *Biochemical analysis of metallo-β-lactamase NDM-3 from a multidrug-resistant Escherichia coli strain isolated in Japan.* **Tada, T., Miyoshi-Akiyama, T., Shimada, K., Kirikae, T.** s.l. : Antimicrobial Agents Chemotherapy, 2014, Vols. 58(6) 3538 – 3540.

6. *Detection of NDM Variants (blaNDM-1, blaNDM-2, blaNDM-3) from Carbapenem-Resistant Escherichia coli and Klebsiella pneumoniae: First Report from Nepal.* **Thapa, A., Upreti, KM, Bimali, NK, Shrestha, B, Sah, AK, Nepal, K., Dhungel, B., Adhikari, S., Adhikari, N., Lekhak, B., Rijal, KR.** s.l. : Infection and Drug Resistance, 2022, Vol. 15.

7. *Metallo-β-lactamases: a major threat to human health.* **Phelan, E. K., Miraula, M., Schenk, G., Mitic, N.** s.l. : American Journal of Molecular Biology, 2014, Vols. 4, 89-104 .

8. *The importance of efflux pumps in bacterial antibiotic resistance .* **Webber, M. A., and Piddock, L. J. V.** 9-11, s.l. : Journal of Antimicrobial Chemotherapy, 2003, Vol. 51.

9. *The Zn2 position in metallo-β-lactamases is critical for activity: a study on chimeric metal sites on a conserved protein scaffold.* **Gonzalez, J. M., Medrano Martin, F. J., Costello, A. L., Tierney, D. L., and Vila, A. J.** s.l. : Journal of molecular biology, 2007, Vols. 373, 1141-1156.

10. *Inactivation of antibiotics and the dissemination of resistance genes.* **Davies, J.** 375-382, s.l. : Science, 1994, Vol. 264.

11. *Updated functional classification of β-lactamases.* **Bush, K., and Jacoby, G. A. (2010) Antimicrobial Agents and chemotherapy 54, 969-976.** 969-976, s.l. : Antimicrobial Agents and chemotherapy, 2010, Vol. 54.

12. *ß-Lactamase: mechanism of action.* **Waley, S. G.** s.l. : Springer Netherlands, 1992, Vols. 198-228.

13. *Characterization of beta-lactamases.* **Bush, K.** 259, s.l. : Antimicrobial Agents and chemotherapy, 1989, Vol. 33.

14. *The structure of β-lactamases.* **Ambler, R. P.** 321-331, s.l. : Philosophical Transactions of the Royal Society of London. B, Biological Sciences, 1980, Vol. 289.

15. *Metallo-β-lactamases (classification, activity, genetic organization, structure, zinc coordination) and their superfamily.* **Bebrone, C.** s.l. : Biochemistry Pharmacology, 2007, Vols. 74, 1686-1701.

16. *The identification of new metallo-β-lactamase inhibitor leads from fragment-based screening.* **Vella, P., Hussein, W. M., Leung, E. W., Clayton, D., Ollis, D. L., Mitic, N., Schenk, G., and McGeary, R. P.** s.l. : Bioorganic & Medicinal Chemistry Letters, 2011, Vols. 21, 3282-3285.

17. *Rapid identification of metallo-and serine beta-lactamases.* **Payne, D. J., Cramp, R., Bateson, J. H., Neale, J., and Knowles, D.** s.l. : Antimicrobial Agents and chemotherapy, 1994, Vols. 38, 991-996.

18. *Catalytic mechanism of active-site serine β-lactamases: role of the conserved hydroxy group of the Lys-Thr(Ser)-Gly triad.* **Dubus, A., Wilkin, J.-M., Raquet, X., Normark, S., and Frere, J.-M.** s.l. : Biochemistry. J, 1994, Vols. 301, 485-494.

19. *Interactions between active-site-serine β-lactamases and compounds bearing a methoxy side chain on the α-face of the β-lactam ring: kinetic and molecular modelling ….* **Matagne, A., Lamotte-Brasseur, J., Dive, G., Knox, J., and Frère, J.-M.** s.l. : Biochemistry. J, 1993, Vols. 293, 607-611.

20. *β-lactamase inhibitors. The inhibition of serine β-lactamases by specific boronic acids.* **Crompton, I., Cuthbert, B., Lowe, G., and Waley, S.** s.l. : Biochemistry. J, 1988, Vols. 251, 453-459.

21. *The 3-D structure of a zinc metallo-beta-lactamase from Bacillus cereus reveals a new type of protein fold.* **Carfi, A., Pares, S., Duee, E., Galleni, M., Duez, C., Frere, J. M., and Dideberg, O.** s.l. : Embo Journal, 1995, Vols. 14, 4914-4921.

22. *Crystal Structure of the IMP-1 Metallo β-Lactamase from Pseudomonas aeruginosa and Its Complex with a Mercaptocarboxylate Inhibitor: Binding Determinants of a Potent, Broad-Spectrum Inhibitor.* **Concha, N. O., Janson, C. A., Rowling, P., Pearson, S., Cheever, C. A., Clarke, B. P., Lewis, C., Galleni, M., Frère, J.-M., Payne, D. J., Bateson, J. H., and Abdel-Meguid, S. S.** s.l. : Biochemistry, 2000, Vols. Concha, N. O., Janson, C. A., Rowling, P., Pearson, S., Cheever, C. A., Clarke, B. P., Lewis, C., Galleni, 39, 4288-4298.

23. *The crystal structure of the L1 metallo-β-lactamase from Stenotrophomonas maltophilia at 1.7 Å resolution.* **Ullah, J. H., Walsh, T. R., Taylor, I. A., Emery, D. C., Verma, C. S., Gamblin, S. J., and Spencer, J.** s.l. : Journal of Molecular Biology, 1998, Vols. 284, 125-136.

24. *Expansion of the zinc metallo-hydrolase family of the β-lactamase fold.* **Daiyasu, H., Osaka, K., Ishino, Y., and Toh, H.** s.l. : FEBS Letters, 2001, Vols. 503, 1-6.

25. *The structure of the dizinc subclass B2 metallo-β-lactamase CphA reveals that the second inhibitory zinc ion binds in the histidine site.* **Bebrone, C., Delbrück, H., Kupper, M. B., Schlömer, P., Willmann, C., Frère, J.-M., Fischer, R., Galleni, M., and Hoffmann, K. M.** s.l. : Antimicrobial Agents and chemotherapy, 2009, Vols. 53, 4464-4471.

26. *Zinc and antibiotic resistance: metallo-β-lactamases and their synthetic analogues.* **Tamilselvi, A., and Mugesh, G.** s.l. : JBIC Journal of Biological Inorganic Chemistry, 2008, Vols. 13, 1039-1053.

27. *Crystal structure of Serratia fonticola Sfh-I: activation of the nucleophile in mono-zinc metallo-β-lactamases.* **Fonseca, F., Bromley, E. H. C., Saavedra, M. J., Correia, A., and Spencer, J.** s.l. : Journal of Molecular Biology, 2011, Vols. 411, 951-959.

28. *A Demetallation Method for IMP-1 Metallo-β-Lactamase with Restored Enzymatic Activity Upon Addition of Metal Ion(s).* **Yamaguchi, Y., Ding, S., Murakami, E., Imamura, K., Fuchigami, S., Hashiguchi, R., Yutani, K., Mori, H., Suzuki, S., Arakawa, Y., and Kurosaki, H.** s.l. : Chembiochem , 2011, Vols. 12, 1979-1983.

29. *Metal preference of Zn(II) and Co(II) for the dinuclear metal binding site of IMP-1 metallo-β-lactamase and spectroscopic properties of Co(II)-substituted IMP-1 with mercaptoacetic acid.* **Yamaguchi, Y., Imamura, K., Sasao, A., Murakami, E., Arakawa, Y., and Kurosaki, H.** s.l. : MedChemComm, 2011, Vols. 2, 720-725.

30. *Purification, Characterization, and Kinetic Studies of a SolubleBacteroides fragilis Metallo-β-lactamase That Provides Multiple Antibiotic Resistance.* **Wang, Z., and Benkovic, S. J.** s.l. : Journal of Biological Chemistry, 1998, Vols. 273, 22402-22408.

31. *Metallo-β-lactamases: novel weaponry for antibiotic resistance in bacteria.* **Crowder, M. W., Spencer, J., and Vila, A. J.** s.l. : Accounts of Chemical Research, 2006, Vols. 39, 721-728.

32. *Global Challenge of Multidrug-Resistant Acinetobacter baumannii.* **Perez, F., Hujer, A. M., Hujer, K. M., Decker, B. K., Rather, P. N., and Bonomo, R. A. (2007) Antimicrobial Agents and chemotherapy 51, 3471-3484.** s.l. : Antimicrobial Agents and chemotherapy, 2007, Vols. 51, 3471-3484.

33. *The threat of antibiotic resistance in Gram-negative pathogenic bacteria: β-lactams in peril!* **Thomson, J. M., and Bonomo, R. A.** s.l. : Current opinion in microbiology, 2005, Vols. 8, 518-524.

34. *European communicable disease bulletin.* **Vatopoulos, A.** s.l. : Euro surveillance: bulletin européen sur les maladies transmissibles, 2008, Vol. bulletin 13.

35. *Cloning and Characterization of blaVIM, a New Integron-Borne Metallo-β-Lactamase Gene from a Pseudomonas aeruginosa Clinical Isolate.* **Lauretti, L., Riccio, M. L., Mazzariol, A., Cornaglia, G., Amicosante, G., Fontana, R., and Rossolini, G. M.** s.l. : Antimicrobial Agents and chemotherapy, 1999, Vols. 43, 1584-1590.

36. *Dissemination in distinct Brazilian regions of an epidemic carbapenem-resistant Pseudomonas aeruginosa producing SPM metallo-β-lactamase.* **Gales, A. C., Menezes, L. C., Silbert, S., and Sader, H. S.** s.l. : Journal of Antimicrobial Chemotherapy , 2003, Vols. 52, 699-702.

37. *Molecular Characterization of a β-Lactamase Gene, blaGIM-1, Encoding a New Subclass of Metallo-β-Lactamase.* **Castanheira, M., Toleman, M. A., Jones, R. N., Schmidt, F. J., and Walsh, T. R.** s.l. : Antimicrobial Agents and chemotherapy, 2004, Vols. 48, 4654-4661.

38. *Multifocal outbreaks of metallo-beta-lactamase-producing Pseudomonas aeruginosa resistant to broad-spectrum beta-lactams, including carbapenems.* **Senda, K., Arakawa, Y., Nakashima, K., Ito, H., Ichiyama, S., Shimokata, K., Kato, N., and Ohta, M.** s.l. : Antimicrobial Agents and chemotherapy, 1996, Vols. 40, 349-353.

39. *Plasmid-mediated dissemination of the metallo-beta-lactamase gene blaIMP among clinically isolated strains of Serratia marcescens.* **Ito, H., Arakawa, Y., Ohsuka, S., Wacharotayankun, R., Kato, N., and Ohta, M.** s.l. : Antimicrobial Agents and chemotherapy, 1995, Vols. 39, 824-829.

40. *Molecular characterization of an enterobacterial metallo beta-lactamase found in a clinical isolate of Serratia marcescens that shows imipenem resistance.* **Osano, E., Arakawa, Y., Wacharotayankun, R., Ohta, M., Horii, T., Ito, H., Yoshimura, F., and Kato, N.** s.l. : Antimicrobial Agents and chemotherapy, 1994, Vols. 38, 71-78.

41. *The Mechanisms of Catalysis by Metallo β-Lactamases.* **Page, M. I., and Badarau, A.** s.l. : Bioinorganic Chemistry and Applications, 2008, Vol. 2008.

42. *Metallo-β-lactamases—a new therapeutic challenge.* **Payne, D. J.** s.l. : Journal of Medicinal Microbiology, 1993, Vols. 39, 93-99.

43. *The three-dimensional structure of VIM-2, a Zn-β-lactamase from Pseudomonas aeruginosa in its reduced and oxidised form.* **Garcia-Saez, I., Docquier, J. D., Rossolini, G. M., and Dideberg, O.** s.l. : Journal of Molecular Biology, 2008, Vols. 375, 604-611.

44. *Emergence of Metallo-β-Lactamase NDM-1-Producing Multidrug-Resistant Escherichia coli in Australia.* **Poirel, L., Lagrutta, E., Taylor, P., Pham, J., and Nordmann, P.** s.l. : Antimicrobial Agents and chemotherapy, 2010, Vols. 54, 4914-4916.

45. *Amino acid substitutions in a variant of IMP-1 metallo-β-lactamase.* **Iyobe, S., Kusadokoro, H., Ozaki, J., Matsumura, N., Minami, S., Haruta, S., Sawai, T., and O'Hara, K.** s.l. : Antimicrobial Agents and chemotherapy, 2000, Vols. 44, 2023-2027.

46. *Biochemical Characterization of the Pseudomonas aeruginosa 101/1477 Metallo-β-Lactamase IMP-1 Produced byEscherichia coli.* **Laraki, N., Franceschini, N., Rossolini, G. M., Santucci, P., Meunier, C., de Pauw, E., Amicosante, G., Frère, J. M., and Galleni, M.** s.l. : Antimicrobial Agents and chemotherapy, 1999, Vols. 43, 902-906.

47. *Characterization of a New Metallo-β-Lactamase Gene, blaNDM-1, and a Novel Erythromycin Esterase Gene Carried on a Unique Genetic Structure in Klebsiella pneumoniae Sequence Type 14 from India.* **Yong, D., Toleman, M. A., Giske, C. G., Cho, H. S., Sundman, K., Lee, K., and Walsh, T. R.** s.l. : Antimicrobial Agents and chemotherapy, 2009, Vols. 53, 5046-5054.

48. *Crystal structure of NDM-1 reveals a common β-lactam hydrolysis mechanism.* **Zhang, H., and Hao, Q.** s.l. : The FASEB Journal, 2011, Vols. 25, 2574-2582.

49. *Dissemination of NDM-1 positive bacteria in the New Delhi environment and its implications for human health: an environmental point prevalence study.* **Walsh, T. R., Weeks, J., Livermore, D. M., and Toleman, M. A.** s.l. : The Lancet Infectious Diseases, 2011, Vols. 11, 355-362.

50. *Global spread of New Delhi metallo-β-lactamase 1.* **Poirel, L., Hombrouck-Alet, C., Freneaux, C., Bernabeu, S., and Nordmann, P. (2010) The Lancet Infectious Diseases 10, 832.** s.l. : The Lancet Infectious Diseases, 2010, Vols. 10, 832.

51. **Struelens, M., Monnet, D., Magiorakos, A., O'Connor, F. S., and Giesecke, Eurosurveillance.** New Delhi metallo-beta-lactamase 1–producing Enterobacteriaceae: emergence and response in Europe. *eurosurveillance.org.* [Online] 2010.

52. *New Delhi metallo-beta-lactamase (NDM-1): towards a new pandemia?* **Rolain, J. M., Parola, P. and Cornaglia, G.** s.l. : Clinical Microbiology and Infection, 2010, Vols. 16: 1699–1701.

53. *New Delhi metallo-β-lactamase and multidrug resistance: a global SOS?* **Bonomo, R. A.** s.l. : Clinical Infectious Diseases, 2011, Vols. 52, 485-487.

54. *Metallo-β-lactamases: a last frontier for β-lactams?* **Cornaglia, G., Giamarellou, H., and Rossolini, G. M.** s.l. : The Lancet Infectious Diseases, 2011, Vols. 11, 381-393.

55. *Crystal structure of Pseudomonas aeruginosa SPM-1 provides insights into variable zinc affinity of metallo-β-lactamases.* **Murphy, T. A., Catto, L. E., Halford, S. E., Hadfield, A. T., Minor, W., Walsh, T. R., and Spencer, J.** s.l. : Journal of Molecular Biology, 2006, Vols. 357, 890-903.

56. *Biochemical characterization of the metallo-beta-lactamase CcrA from Bacteroides fragilis TAL3636.* **Yang, Y., Rasmussen, B. A., and Bush, K.** s.l. : Antimicrobial Agents and chemotherapy, 1992, Vols. 36, 1155-1157.

57. *Hybrid QM/MM and DFT Investigations of the Catalytic Mechanism and Inhibition of the Dinuclear Zinc Metallo-β-Lactamase CcrA from Bacteroides fragilis.* **Park, H., Brothers, E. N., and Merz, K. M.** s.l. : Journal of the American Chemical Society, 2005, Vols. 127, 4232-4241.

58. *Mutational Analysis of Metallo-β-lactamase CcrA from Bacteroides fragilis.* **Yanchak, M. P., Taylor, R. A., and Crowder, M. W.** s.l. : Biochemistry, 2000, Vols. 39, 11330-11339.

59. *Crystal structure of the wide-spectrum binuclear zinc β-lactamase from Bacteroides fragilis.* **Concha, N. O., Rasmussen, B. A., Bush, K., and Herzberg, O.** s.l. : Structure, 1996, Vols. 4, 823-836.

60. *The 1.5-Å structure of Chryseobacterium meningosepticum zinc β-lactamase in complex with the inhibitor, D-captopril.* **García-Sáez, I., Hopkins, J., Papamicael, C., Franceschini, N., Amicosante, G., Rossolini, G. M., Galleni, M., Frère, J.-M., and Dideberg, O.** s.l. : Journal of Biological Chemistry, 2003, Vols. 278, 23868-23873.

61. *Structure of metallo-β-lactamase IND-7 from a Chryseobacterium indologenes clinical isolate at 1.65-Å resolution.* **Yamaguchi, Y., Takashio, N., Wachino, J., Yamagata, Y., Arakawa, Y., Matsuda, K., and Kurosaki, H.** s.l. : Journal of Biochemistry, 2010, Vols. 147, 905-915.

62. *Crystal structures of Pseudomonas aeruginosa GIM-1: active-site plasticity in metallo-β-lactamases.* **Borra, P. S., Samuelsen, O., Spencer, J., Walsh, T. R., Lorentzen, M. S., and Leiros, H. K.** s.l. : Antimicrobial Agents Chemotherapy, 2013, Vols. 57, 848-854.

63. *Genetic and biochemical characterization of the chromosome-encoded class B β-lactamases from Shewanella livingstonensis (SLB-1) and Shewanella frigidimarina (SFB-1).* **Poirel, L., Héritier, C., and Nordmann, P.** s.l. : Journal of Antimicrobial Chemotherapy, 2005, Vols. 55, 680-685.

64. *EBR-1, a Novel Ambler Subclass B1 β-Lactamase from Empedobacter brevis.* **Bellais, S., Girlich, D., Karim, A., and Nordmann, P.** s.l. : Antimicrobial Agents and chemotherapy, 2002, Vols. 46, 3223-3227.

65. *Escherichia coli with a Self-Transferable, Multiresistant Plasmid Coding for Metallo-β-Lactamase VIM-1.* **Miriagou, V., Tzelepi, E., Gianneli, D., and Tzouvelekis, L. S.** s.l. : Antimicrobial Agents and chemotherapy, 2003, Vols. 47, 395-397.

66. *Hospital Outbreak of Carbapenem-Resistant Pseudomonas aeruginosa Producing VIM-1, a Novel Transferable Metallo-β-Lactamase.* **Cornaglia, G., Mazzariol, A., Lauretti, L., Rossolini, G. M., and Fontana, R.** s.l. : Clinical Infectious Diseases, 2000, Vols. 31, 1119-1125.

67. *Outbreak of Infections Caused by Pseudomonas aeruginosa Producing VIM-1 Carbapenemase in Greece.* **Tsakris, A., Pournaras, S., Woodford, N., Palepou, M.-F. I., Babini, G. S., Douboyas, J., and Livermore, D. M.** s.l. : Journal of clinical microbiology, 2000, Vols. 38, 1290-1292.

68. *VIM-1 Metallo-β-Lactamase-Producing Klebsiella pneumoniae Strains in Greek Hospitals.* **Giakkoupi, P., Xanthaki, A., Kanelopoulou, M., Vlahaki, A., Miriagou, V., Kontou, S., Papafraggas, E., Malamou-Lada, H., Tzouvelekis, L., and Legakis, N.** s.l. : Journal of clinical microbiology, 2003, Vols. 41, 3893-3896.

69. *Hospital outbreak of multiple clones of Pseudomonas aeruginosa carrying the unrelated metallo-β-lactamase gene variants blaVIM-2 and blaVIM-4.* **Pournaras, S., Maniati, M., Petinaki, E., Tzouvelekis, L., Tsakris, A., Legakis, N., and Maniatis, A.** s.l. : Journal of Antimicrobial Chemotherapy, 2003, Vols. 51, 1409-1414.

70. *VIM-4 in a carbapenem-resistant strain of Pseudomonas aeruginosa isolated in Sweden.* **Giske, C. G., Rylander, M., and Kronvall, G.** s.l. : Antimicrobial Agents and chemotherapy, 2003, Vols. 47, 3034-3035.

71. *Emergence of Multidrug-Resistant Klebsiella pneumoniae Isolates Producing VIM-4 Metallo-β-Lactamase, CTX-M-15 Extended-Spectrum β-Lactamase, and CMY-4 AmpC β-Lactamase in a Tunisian University Hospital.* **Ktari, S., Arlet, G., Mnif, B., Gautier, V., Mahjoubi, F., Jmeaa, M. B., Bouaziz, M., and Hammami, A.** s.l. : Antimicrobial Agents and chemotherapy, 2006, Vols. 50, 4198-4201.

72. *Emergence in Klebsiella pneumoniae and Enterobacter cloacae Clinical Isolates of the VIM-4 Metallo-β-Lactamase Encoded by a Conjugative Plasmid.* **Luzzaro, F., Docquier, J.-D., Colinon, C., Endimiani, A., Lombardi, G., Amicosante, G., Rossolini, G. M., and Toniolo, A.** s.l. : Antimicrobial Agents and chemotherapy, 2004, Vols. 48, 648-650.

73. *Metallo beta lactamases in Pseudomonas aeruginosa and Acinetobacter species.* **Gupta, V.** s.l. : Expert Opinion on Investigational Drugs, 2008, Vols. 17, 131-143.

74. *Identification of a Plasmid Encoding SHV-12, TEM-1, and a Variant of IMP-2 Metallo-β-Lactamase, IMP-8, from a Clinical Isolate of Klebsiella pneumoniae.* **Yan, JJ., Ko, WC., and Wu, JJ.** s.l. : Antimicrobial Agents and chemotherapy, 2001, Vols. 45, 2368-2371.

75. *Novel Acquired Metallo-β-Lactamase Gene, blaSIM-1, in a Class 1 Integron from Acinetobacter baumannii Clinical Isolates from Korea.* **Lee, K., Yum, J. H., Yong, D., Lee, H. M., Kim, H. D., Docquier, J.-D., Rossolini, G. M., and Chong, Y.** s.l. : Antimicrobial Agents and chemotherapy, 2005, Vols. 49, 4485-4491.

76. *FIM-1, a new acquired metallo-β-lactamase from a Pseudomonas aeruginosa clinical isolate from Italy.* **Pollini, S., Maradei, S., Pecile, P., Olivo, G., Luzzaro, F., Docquier, J.-D., and Rossolini, G. M.** s.l. : Antimicrobial Agents and chemotherapy, 2013, Vols. 57, 410-416.

77. *A metallo-β-lactamase enzyme in action: crystal structures of the monozinc carbapenemase CphA and its complex with biapenem.* **Garau, G., Bebrone, C., Anne, C., Galleni, M., Frere, J. M., and Dideberg, O.** s.l. : Journal of molecular biology, 2005, Vols. 345, 785-795.

78. *Sfh-I, a Subclass B2 Metallo-β-Lactamase from a Serratia fonticola Environmental Isolate.* **Saavedra, M. J., Peixe, L., Sousa, J. C., Henriques, I., Alves, A., and Correia, A.** s.l. : Antimicrobial Agents and chemotherapy, 2003, Vols. 47, 2330-2333.

79. *Over-expression, purification, and characterization of metallo-β-lactamase ImiS from Aeromonas veronii bv. sobria.* **Crawford, P. A., Sharma, N., Chandrasekar, S., Sigdel, T., Walsh, T. R., Spencer, J., and Crowder, M. W.** s.l. : Protein Expression and Purification, 2004, Vols. 36, 272-279.

80. *Common mechanistic features among metallo-β-lactamases: a computational study of Aeromonas hydrophila CphA enzyme.* **Simona, F., Magistrato, A., Dal Peraro, M., Cavalli, A., Vila, A. J., and Carloni, P.** s.l. : Journal of Biological Chemistry, 2009, Vols. 284, 28164-28171.

81. *High specificity of cphA-encoded metallo-beta-lactamase from Aeromonas hydrophila AE036 for carbapenems and its contribution to beta-lactam resistance.* **Segatore, B., Massidda, O., Satta, G., Setacci, D., and Amicosante, G.** s.l. : Antimicrobial Agents and chemotherapy, 1993, Vols. 37, 1324-1328.

82. *Antibiotic Binding to Monozinc CphA β-Lactamase from Aeromonas hydropila: Quantum Mechanical/Molecular Mechanical and Density Functional Theory Studies.* **Xu, D., Zhou, Y., Xie, D., and Guo, H.** s.l. : Journal of Medicinal Chemistry, 2005, Vols. 48, 6679-6689.

83. *The Aeromonas hydrophila cphA gene: molecular heterogeneity among class B metallo-beta-lactamases.* **Massidda, O., Rossolini, G. M., and Satta, G.** s.l. : Journal of bacteriology, 1991, Vols. 173, 4611-4617.

84. *Molecular Heterogeneity of the L-1 Metallo-β-Lactamase Family from Stenotrophomonas maltophilia.* **Sanschagrin, F., Dufresne, J., and Levesque, R. C.** s.l. : Antimicrobial Agents and chemotherapy, 1998, Vols. 42, 1245-1248.

85. *Three-dimensional structure of FEZ-1, a monomeric subclass B3 metallo-β-lactamase from Fluoribacter gormanii, in native form and in complex with D-captopril.* **García-Sáez, I., Mercuri, P. S., Papamicael, C., Kahn, R., Frère, J. M., Galleni, M., Rossolini, G. M., and Dideberg, O.** s.l. : Journal of Molecular Biology, 2003, Vols. 325, 651-660.

86. *High-resolution crystal structure of the subclass B3 metallo-β-lactamase BJP-1: rational basis for substrate specificity and interaction with sulfonamides.* **Docquier, J.-D., Benvenuti, M., Calderone, V., Stoczko, M., Menciassi, N., Rossolini, G. M., and Mangani, S.** s.l. : Antimicrobial Agents and chemotherapy, 2010, Vols. 54, 4343-4351.

87. *Crystal structure of the mobile metallo-β-lactamase AIM-1 from Pseudomonas aeruginosa: insights into antibiotic binding and the role of Gln157.* **Leiros, H.-K. S., Borra, P. S., Brandsdal, B. O.,**

References

Edvardsen, K. S. W., Spencer, J., Walsh, T. R., and Samuelsen, Ø. s.l. : Antimicrobial Agents and chemotherapy, 2012, Vols. 56, 4341-4353.

88. *SMB-1, a Novel Subclass B3 Metallo-β-Lactamase, Associated with ISCR1 and a Class 1 Integron, from a Carbapenem-Resistant Serratia marcescens Clinical Isolate.* **Wachino, J., Yoshida, H., Yamane, K., Suzuki, S., Matsui, M., Yamagishi, T., Tsutsui, A., Konda, T., Shibayama, K., and Arakawa, Y.** s.l. : Antimicrobial Agents and chemotherapy, 2011, Vols. 55, 5143-5149.

89. *Molecular and Biochemical Heterogeneity of Class B Carbapenem-Hydrolyzing β-Lactamases in Chryseobacterium meningosepticum.* **Bellais, S., Aubert, D., Naas, T., and Nordmann, P.** s.l. : Antimicrobial Agents and chemotherapy, 2000, Vols. 44, 1878-1886.

90. *Carbapenem Resistance in Elizabethkingia meningoseptica Is Mediated by Metallo-β-Lactamase BlaB.* **Gonzalez L, J., Vila, A.,.** 1686-1692, s.l. : Antimicrobial Agents and Chemotherapy, 2012, Vol. 56 (4).

91. *Functional Diversity among Metallo-β-Lactamases: Characterization of the CAR-1 Enzyme of Erwinia carotovora.* **Stoczko, M., Frère, J.-M., Rossolini, G. M., and Docquier, J.-D.** s.l. : Antimicrobial Agents and chemotherapy, 2008, Vols. 52, 2473-2479.

92. *Metallo-β-Lactamase Producers in Environmental Microbiota: New Molecular Class B Enzyme inJanthinobacterium lividum.* **Rossolini, G. M., Condemi, M. A., Pantanella, F., Docquier, J.-D., Amicosante, G., and Thaller, M. C.** s.l. : Antimicrobial Agents and chemotherapy, 2001, Vols. 45, 837-844.

93. *Identification and characterization of an unusual metallo-β-lactamase from Serratia proteamaculans.* **Vella, P., Miraula, M., Phelan, E., Leung, E. W., Ely, F., Ollis, D. L., McGeary, R. P., Schenk, G., and Mitić, N.** s.l. : Journal of Biological Inorganic Chemistry, 2013, Vols. 18, 855-863.

94. *Identification and preliminary characterization of novel B3-type metallo-β-lactamases.* **Miraula, M., Brunton, C., Schenk, G. and Mitic, N.** s.l. : American Journal of Molecular Biology, 2013, Vols. 3, 198-203.

95. *Zn(II) Dependence of the Aeromonas hydrophila AE036 Metallo-β-lactamase Activity and Stability.* **Valladares, M. H., Felici, A., Weber, G., Adolph, H. W., Zeppezauer, M., Rossolini, G. M., Amicosante, G., Frere, J. M., and Galleni, M.** s.l. : Biochemistry, 1997, Vols. 36, 11534-11541.

96. *Engineered Mononuclear Variants in Bacillus cereus Metallo-β-lactamase BcII Are Inactive.* **Abriata, L. A., González, L. J., Llarrull, L. I., Tomatis, P. E., Myers, W. K., Costello, A. L., Tierney, D. L., and Vila, A. J.** s.l. : Biochemistry, 2008, Vols. 47, 8590-8599.

97. *Metal Ion Binding and Coordination Geometry for Wild Type and Mutants of Metallo-β-lactamase from Bacillus cereus569/H/9 (BcII).* **de Seny, D., Heinz, U., Wommer, S., Kiefer, M., Meyer-Klaucke, W., Galleni, M., Frere, J. M., Bauer, R., and Adolph, H. W.** s.l. : Journal of Biological Chemistry, 2001, Vols. 276, 45065-45078.

98. *Substrate-activated zinc binding of metallo-β-lactamases: Physiological importance of the mononuclear enzymes.* **Wommer, S., Rival, S., Heinz, U., Galleni, M., Frere, J. M., Franceschini, N.,**

References

Amicosante, G., Rasmussen, B., Bauer, R., and Adolph, H. W. s.l. : Journal of Biological Chemistry, 2002, Vols. 277, 24142-24147.

99. *Mono- and binuclear Zn-β-lactamase from Bacteroides fragilis: catalytic and structural roles of the zinc ions.* **Paul-Soto, R., Hernandez-Valladares, M., Galleni, M., Bauer, R., Zeppezauer, M., Frere, J. M., and Adolph, H. W.** s.l. : Febs Letters, 1998, Vols. 438, 137-140.

100. *Mutagenesis of zinc ligand residue Cys221 reveals plasticity in the IMP-1 metallo-β-lactamase active site.* **Horton, L. B., Shanker, S., Mikulski, R., Brown, N. G., Phillips, K. J., Lykissa, E., Venkataram Prasad, B. V., and Palzkill, T.** s.l. : Antimicrobial Agents Chemotherapy, 2012, Vols. 56, 5667-5677.

101. *Structural determinants of substrate binding to Bacillus cereus metallo-β-lactamase.* **Rasia, R. M., and Vila, A. J.** s.l. : Journal of Biological Chemistry, 2004, Vols. 279, 26046-26051.

102. *Loss of enzyme activity during turnover of the Bacillus cereus β-lactamase catalysed hydrolysis of β-lactams due to loss of zinc ion.* **Badarau, A., and Page, M. I. (2008) Journal of Biological Inorganic Chemistry 13, 919-928.** s.l. : Journal of Biological Inorganic Chemistry, 2008, Vols. 13, 919-928.

103. *Familial Mutations and Zinc Stoichiometry Determine the Rate-Limiting Step of Nitrocefin Hydrolysis by Metallo-β-lactamase from Bacteroides fragilis.* **Fast, W., Wang, Z. G., and Benkovic, S. J.** s.l. : Biochemistry, 2001, Vols. 40, 1640-1650.

104. *Structural and kinetic studies on metallo-β-lactamase IMP-1.* **Griffin, D. H., Richmond, T. K., Sanchez, C., Moller, A. J., Breece, R. M., Tierney, D. L., Bennett, B., and Crowder, M. W.** s.l. : Biochemistry, 2011, Vols. 50, 9125-9134.

105. *Differential Binding of Co(II) and Zn(II) to Metallo-β-Lactamase Bla2 from Bacillus anthracis.* **Hawk, M. J., Breece, R. M., Hajdin, C. E., Bender, K. M., Hu, Z. X., Costello, A. L., Bennett, B., Tierney, D. L., and Crowder, M. W.** s.l. : Journal of the American Chemical Society, 2009, Vols. 131, 10753-10762.

106. *The use of 4-(2-pyridylazo) resorcinol in studies of zinc release from Escherichia coli aspartate transcarbamoylase.* **Hunt, J. B., Neece, S. H., and Ginsburg, A.** s.l. : Analytical Biochemistry, 1985, Vols. 46, 150-157.

107. *Measurement of free Zn2+ ion concentration with the fluorescent probe mag-fura-2 (furaptra).* **Simons, T. J. B.** s.l. : Journal of biochemical and biophysical methods, 1993, Vols. 27, 25-37.

108. *Colorimetric and fluorimetric assays to quantitate micromolar concentrations of transition metals.* **McCall, K. A., and Fierke, C. A.** s.l. : Analytical Biochemistry, 2000, Vols. 284, 307-315.

109. *Characterization of purified New Delhi metallo-β-lactamase-1.* **Thomas, P. W., Zheng, M., Wu, S. S., Guo, H., Liu, D. L., Xu, D. G., and Fast, W.** s.l. : Biochemistry, 2011, Vols. 50, 10102-10113.

110. *Affinity of copper and zinc ions to proteins and peptides related to neurodegenerative conditions (Aβ, APP, α-synuclein, PrP).* **Zawisza, I., Rozga, M., and Bal, W.** s.l. : Coordination Chemistry Reviews, 2012, Vols. 256, 2297-2307.

111. *Application of isothermal titration calorimetry in bioinorganic chemistry.* **Grossoehme, N. E., Spuches, A. M., and Wilcox, D. E.** s.l. : Journal of Biological Inorganic Chemistry, 2010, Vols. 15, 1183-1191.

112. *Kinetic and spectroscopic characterization of native and metal-substituted beta-lactamase from Aeromonas hydrophila AE036.* **Valladares, M. H., Kiefer, M., Heinz, U., Soto, R. P., Meyer-Klaucke, W., Nolting, H. F., Zeppezauer, M., Galleni, M., Frere, J. M., Rossolini, G. M., Amicosante, G., and Adolph, H. W.** s.l. : FEBS Letter, 2000, Vols. 477, 285-285.

113. *Exploring the Role and the Binding Affinity of a Second Zinc Equivalent in B. cereus Metallo-β-lactamase.* **Rasia, R. M., and Vila, A. J.** 1853-1860, s.l. : Biochemistry, 2002, Vol. 41.

114. *Positively cooperative binding of zinc ions to Bacillus cereus 569/H/9 β-lactamase II suggests that the binuclear enzyme is the only relevant form for catalysis.* **Jacquin, O., Balbeur, D., Damblon, C., Marchot, P., De Pauw, E., Roberts, G. C. K., Frere, J. M., and Matagne, A.** s.l. : Journal of molecular biology, 2009, Vols. 392, 1278-1291.

115. *Enzyme deactivation due to metal-ion dissociation during turnover of the cobalt-β-lactamase catalyzed hydrolysis of β-lactams.* **Badarau, A., and Page, M. I.** s.l. : Biochemistry, 2006, Vols. 45, 11012-11020.

116. *Folding strategy to prepare Co (II)-substituted metallo-β-lactamase L1.* **Hu, Z., Periyannan, G. R., and Crowder, M. W.** s.l. : Analytical biochemistry , 2008, Vols. 378, 177-183.

117. *Fluorescence techniques for studying protein structure.* **Eftink, M. R.** s.l. : Method of Biochemical Analysis, 1991, Vols. 35, 127-205.

118. *Some characteristics of the fluorescence of quinine.* **Chen, R. F.** s.l. : Analytical Biochemistry, 1967, Vols. 19, 374-387.

119. *Survey of the year 2008: applications of isothermal titration calorimetry.* **Falconer, R. J., Penkova, A., Jelesarov, I., and Collins, B. M.** s.l. : Journal of molecular recognition, 2010, Vols. 23, 395-413.

120. *New Delhi Metallo-beta-lactamase around the world: an eReview using Google Maps.* **Berrazeg M, Diene S M, Medjahed L, Parola P, Drissi M, Raoult D, Rolain J M.** s.l. : Euro Surveillence, 2014 , Vol. 19(20):.

121. *High prevalence of metallo-beta-lactamase producing Acinetobacter baumannii isolated from two hospitals of Tehran, Iran.* **Noori M, Karimi A, Fallah F, Hashemi A, Alimehr S.** s.l. : Paediatric Infectious Disease Journal, 2014, Vol. 2(3): e15439.

122. *Determination of extended spectrum beta-lactamases, metallo-beta-lactamases and AmpC-beta-lactamases among carbapenem resistant Pseudomonas aeruginosa isolated from burn patients.* **Davood, K., Neyestanaki A., Mirsalehian, F., Rezagholizadeh, F., Jabalameli, M., Taherikalani, M., E.,.** 8, 1556-1561, s.l. : Burns, 2014, Vols. 40,.

123. *Structural basis of metallo-β-lactamase, serine-β-lactamase and penicillin-binding protein inhibition by cyclic boronates.* **Brem, J., Cain, R., Cahill, S., McDonough, MA., Clifton, IJ., Jiménez-**

References

Castellanos, JC., Avison, MB., Fishwick. JS., Schofield, CJ. s.l. : Nature Communications, 2016, Vol. 12406.

124. *Metallo-β-Lactamases: Structure, Function, Epidemiology, Treatment Options, and the Development Pipeline.* **Boyd, SE., Livermore, DM., Hooper, DC., Hope, WW.** 10, s.l. : Antimicrobial Agents and Chemotherapy, 2020, Vol. 64.

125. *Emergence of Various NDM-Type-Metallo-β-Lactamase-Producing Escherichia coli Clinical Isolates in Nepal.* **Shrestha, B., Tada, T., Shimada, K., Shrestha, S., Ohara, H., Pokhrel, BM., Sherchand, JB., Kirikae, T.** 12, s.l. : Antimicrobial Agents and Chemotherapy, 2017, Vol. 61.

126. *Diversity of New Delhi metallo-beta-lactamase-producing bacteria in China.* **Xiaofeng Hu, Xuebing Xu, Xu Wang, Wencheng Xue, Haijian Zhou, Ling Zhang, Qiuxia Ma, Rongtao Zhao, Guozheng Li, Peng Li, Chuanfu Zhang, Yun Shi, Jian Wang, Leili Jia, Rongzhang Hao, Ligui Wang, Dayang Zou, Xuelin Li.** s.l. : International Journal of Infectious Diseases, 2017, Vol. 55.

127. *Unusual metallo-β-lactamases may constitute a new subgroup in this family of enzymes.* **Hou, Chun-Feng D., Phelan, Emer K., Miraula, Manfredi, Ollis, David., Schenk, Gerhard., Mitic, Natasa.** s.l. : American Journal of Molecular Biology, 2014, Vols. 4, 11-15.

128. *Prevalence and molecular characterisation of New Delhi metallo-β-lactamases NDM-1, NDM-5, NDM-6 and NDM-7 in multidrug-resistant Enterobacteriaceae from India.* **Rahmanab, M., Kumar, S., Kashi, S., Prasada, N., Ovejeroc, CN., Kumar, B., Aparna, P., Avinash, T., Ashwini, SK., Bruno, S., Gonzalez-Zornc.** 1, 30-37, s.l. : International Journal of Antimicrobial Agents, 2014, Vols. 44,.

129. *Resistance Determinants and Mobile Genetic Elements of an NDM-1-Encoding Klebsiella pneumoniae Strain.* **Hudson CM, Bent ZW, Meagher RJ, Williams KP (2014) Resistance Determinants and Mobile Genetic Elements of an NDM-1-Encoding Klebsiella pneumoniae Strain. PLOS ONE June 9(6): e99209.** s.l. : PloS One, 2014 , Vol. 9(6): e99209.

130. *Clinical Variants of New Delhi Metallo-β-Lactamase Are Evolving To Overcome Zinc Scarcity.* **Stewart, AC., Bethel, C R., VanPelt, J., Bergstrom, A., Cheng, Z., Miller, C G., Williams, C., Poth, R., Morris, M., Lahey, O., Nix, J C., Tierney, D L., Page, R C., Crowder, M W., Bonomo, R A., Fast, W.** s.l. : ACS Infectious Diseases, 2017, Vols. 3, 12, 927–940.

131. *The latest advances in β-lactam/β-lactamase inhibitor combinations for the treatment of Gram-negative bacterial infections.* **Papp-Wallace, KM.** 17, 2169–2184., s.l. : Expert Opinion on Pharmacotherapy, 2019, Vol. 20.

132. *Cefiderocol: A Novel Agent for the Management of Multidrug-Resistant Gram-Negative Organisms.* **Wu, JY., Srinivas, P., Pogue, JM.** s.l. : Infectious Diseases and Therapy , 2020, Vol. 9.

133. *Recent research and development of NDM-1 inhibitors.* **Wang, T., Xu, K., Zhao, L., Tong, R., Xiong, L., Shi, J.** 113667, s.l. : European Journal of Medicinal Chemistry, 2021, Vol. 223.

134. *Efforts towards the inhibitor design for New Delhi metallo-beta-lactamase (NDM-1).* **Kalyan, C., Venkata, N., Ellebrecht, M., Tripathi, SK.** 113747, s.l. : European Journal of Medicinal Chemistry, 2021, Vol. 225.

135. *Discovery of an Effective Small-Molecule Allosteric Inhibitor of New Delhi Metallo-β-lactamase (NDM).* **Thomas, PW., Cho, EJ., Bethel, CR., Smisek, T., Ahn, YC., Schroeder, JM., Thomas, CA., Dalby, KN., Beckham, JT., Crowder, MW., Bonomo, RA., Fast, W.** 4 , s.l. : ACS Infectious Diseases, 2022, Vol. 8.

136. *Imitation of β-lactam binding enables broad-spectrum metallo-β-lactamase inhibitors.* **Brem, J., Panduwawala, T., Hansen, J.U. et al.** 15-24, s.l. : Nature Chemistry, 2022, Vol. 14.

137. *The antimicrobial peptide thanatin disrupts the bacterial outer membrane and inactivates the NDM-1 metallo-β-lactamase.* **Ma, B., Fang, C., Lu, L. et al.** 3517, s.l. : Nature Communications, 2019, Vol. 10.

138. *Enzyme Inhibitors: The Best Strategy to Tackle Superbug NDM-1 and Its Variants.* **Li, X., et al.** 1:197, s.l. : International Journal of Molecular Sciences, 2022, Vol. 23.

139. *The urgent need for metallo-β-lactamase inhibitors: an unattended global threat.* **Mojica, MF., Rossi, MA., Vila, AJ., Bonomo, RA.** 1, s.l. : The Lancet Infectious Diseases, 2022, Vol. 22.

140. *New metallo β-lactamase NDM-1.* **Raghunath, D.** s.l. : The Indian Journal of Medical Research., 2010, Vols. 132(5):478-481.

141. *Structure of New Delhi metallo-β-lactamase 1 (NDM-1).* **Green, V. L., Verma, A., Owens, R.J., Phillips, S.E.V., Carr, S.B.** s.l. : Acta Crystallographica Section F: Structural Biology Communications, 2011, Vols. Oct 1; 67(Pt 10): 1160–1164.

142. *Immobilized-metal affinity chromatography (IMAC): a review.* **Block, H., Maertens, B., Spriestersbach, A., Brinker, N., Kubicek, J., Fabis, R., Labahn, J., Schafer, F.** s.l. : Methods in Enzymology, 2009, Vols. 463, Pages 439-473.

143. *Immobilized metal ion affinity chromatography.* **Porath, J.** s.l. : Protein Expression and Purification, 1992, Vols. 3, Issue 4, 263-281.

144. *Structural basis of ubiquitin recognition by the deubiquitinating protease USP2.* **Parrado, S., D'Arcy, A., Eidhoff, U., Gerhartz, B., Hassiepen, U., Pierrat, B., Riedl, R., Vinzenz, D., Worpenberg, S., Kroemer, M.** s.l. : Structure, 2006, Vols. 14, 1293–1302.

145. *Transformation of Plasmid DNA into E. coli Using the Heat Shock Method.* **Froger, A., Hall, JE.** s.l. : Journal of Visualised Experiments, 2007, Vol. 6.

146. *Protein expression in E. coli minicells by recombinant plasmids.* **Richard B. Meagher, Robert C. Tait, Mary Betlach, Herbert W. Boyer.** 3, s.l. : CellPress, 1977, Vol. 10.

147. *Overexpression, purification, and characterization of the cloned metallo-β-lactamase L1 from Stenotrophomonas maltophilia.* **Crowder, M. W., Walsh, T. R., Banovic, L., Pettit, M., & Spencer, J.** 4, s.l. : Antimicrobial Agents and Chemotherapy, 1998, Vol. 42.

148. *Fast Protein Liquid Chromatography. Methods in molecular biology .* **Madadlou, Ashkan & O'Sullivan, Siobhan & Sheehan, David.** s.l. : Methods in Molecular Biology, 2011, Vol. 681.

149. *Purification of proteins using polyhistidine affinity tags.* **Bornhorst A, J., Falke, J.** s.l. : Methods in Enzymology, 2000, Vols. 326, Pages 245-254.

150. *9.19 - Bacterial Protein Overexpression Systems and Strategies.* **Kinsland, C.** 695-721, s.l. : Comprehensive Natural Products II, 2010, Vol. 9.

151. *Peptide mapping by limited proteolysis in sodium dodecyl sulfate and analysis by gel electrophoresis.* **Cleveland, D W., Fischer, S G., Kirschner, M W., and Laemmli, U K.** s.l. : The Journal of Biological Chemistry, 1977, Vols. 252, No. 3; 1102 -1106. .

152. *An efficient system for high-level expression and easy purification of authentic recombinant proteins.* **Catanzariti, A-M., Soboleva, A T., Jans, A D., Board, G P., Baker, T R.** s.l. : Protein Science, 2004, Vols. 13(5) 1331-1339.

153. *Principles of enzyme assay and kinetic studies. Enzyme assays, a practical approach.* **Tipton, K. F. (1992). Principles of enzyme assay and kinetic studies. Enzyme assays, a practical approach. IRL, Oxford, 1-58.** s.l. : Tipton, K. F. (1992). Principles of enzyme assay and kinetic studies. Enzyme assays, a practical approach., 1992, Vols. Oxford, 1-58.

154. *Promiscuous metallo-β-lactamases: MIM-1 and MIM-2 may play an essential role in quorum sensing networks.* **Miraula, M., Schenk, G., Mitic, N.** s.l. : Journal of Inorganic Biochemistry, 2014, Vols. 162, Pages 366 - 375.

155. *The carbon dioxide hydration activity of carbonic anhydrase: I. Stop-flow kinetic studies on the native human isoenzymes B and C.* **Khalifah., R.G.** s.l. : Journal of Biological Chemistry, 1971, Vols. 246 2561–2573.

156. *Catalytic properties of murine carbonic anhydrase IV.* **Hurt, JD., Tu, C., Laipis, PJ., Silverman, DN.** s.l. : Journal of Biological Chemistry, 1997, Vols. 272 13512–13518.

157. *Haloalkane dehalogenases: steady-state kinetics and halide inhibition.* **Schindler, JF., Naranjo, PA., Honaberger, DA., Chang, CH., Brainard, JR., Vanderberg, LA., Unkefer, JC.** s.l. : Biochemistry, 1999, Vols. 38 5772–5778.

158. *Heterologous overexpression, purification, and in vitro characterization of AHL lactonases.* **Thomas, PW., Fast, W.** s.l. : Methods Molecular Biology, 2011, Vols. 692 275–290.

159. *Structure and Specificity of a Quorum-Quenching Lactonase (AiiB) from Agrobacterium tumefaciens,.* **Liu, D., Thomas, PW., Momb, J., Hoang, QQ., Petsko, GA., Ringe, D., Fast, W.** s.l. : Biochemistry, 2007, Vols. 46 11789–11799.

160. *Structural and functional characterization of Salmonella enterica serovar Typhimurium YcbL: An unusual Type II glyoxalase.* **Stamp, AL., Owen, P., El Omari, K., Nichols, CE., Lockyer, M., Lamb, HK., Charles, IG., Hawkins, AR., Stammers, DK.** s.l. : Protein Science, 2010, Vols. 19, 1897-1905.

161. *NDM-4 metallo-β-lactamase with increased carbapenemase activity from Escherichia coli.* **Nordmann, P., Boulanger, E. A., and Poirel, L.** s.l. : Antimicrobial. Agents Chemotherapy , 2012, Vols. 56:4 2184 - 2186. .

162. *NDM-8 metallo-β-lactamase in a multidrug-resistant Escherichia coli strain isolated in Nepal.* **Tada, T., Miyoshi-Akiyama, T., Dahal, K R., Sah, K M., Ohara, H., Kirikae, T., Pokhrel, M B.** s.l. : Antimicrobial Agents Chemotherapy, 2013, Vols. 57(5): 2394-2396.

163. *NDM-12, a Novel New Delhi Metallo-β-Lactamase Variant from a Carbapenem-Resistant Escherichia coli Clinical Isolate in Nepal.* **Tada, T., Shrestha, B., Miyoshi-Akiyama, T., Shimada, K., Ohara, H., Kirikae, T., Pokhrel, BM.** 10, s.l. : Antimicrobial Agents and Chemotherapy, 2014, Vol. 58.

164. *Current techniques for single-cell lysis.* **Brown, RB., Audet, J.** s.l. : J. R. Soc. Interface, 2008, Vols. 5 S131–S138.

165. *Effect of Imidazole on the Solubility of a His-Tagged Antibody Fragment.* **Hamilton, S., Odili, J., Pacifico, MD., Wilson, GD., and Kupsch, JM.** 6, s.l. : Hybridoma and Hybridomics, 2004, Vol. 22.

166. *Reliable method for high quality His-tagged and untagged E. coli phosphoribosyl phosphate synthase (Prs) purification.* **Walter, BM., Szulc, A., Glinkowska, MK.** s.l. : Protein Expression and Purification, 2020, Vol. 169.

167. **Bioscience.** USP2, His-tag (E. coli-derived) Recombinant. *Bioscience.* [Online]

168. *Bestimmung der Absorption des rothen Lichts in farbigen Flüssigkeiten.* **Beer, A.** 78-88, s.l. : Annalen der Physik, 1852, Vol. 62.

169. *The origins of Beer's law.* **Pfeiffer, HG., and Liebhafsky, HA.** 3, s.l. : Journal of Chemical Education, 1951, Vol. 28.

170. *Protein ubiquitination: a regulatory post-translational modification.* **Wilkinson, KD.** 2: 211-229, s.l. : Anti cancer drug design, 1987, Vol. 2.

171. *Using deubiquitylating enzymes as research tools.* **Baker, T R., Catanzariti, A-M., Karunasekara, Y., Soboleva, A T., Sharwood, R., Whitney, S., Board, G P.** s.l. : Methods in Enzymology, 2005, Vols. Vol. 398 0076-6879/05. .

172. *Structural Basis of Ubiquitin Recognition by the Deubiquitinating Protease USP2.* **Renatus, M., Parrado, SG., et al.** 1293–1302, s.l. : Structure, 2006, Vol. 14.

173. *Enzyme assays.* **Bisswanger, H.** 1-6, s.l. : Perspectives in Science, 2014, Vol. 1.

174. *Die Kinetik der Invertinwirkung.* **Michaelis, L., Menten, ML.** s.l. : Biochem, 1913, Vols. 49: 333–369.

175. *The Kinetics of Invertase Action.* **Goody, RS., Johnson, AK.** s.l. : Biochemistry, 2011, Vols. 50, 39, 8264–8269.

176. *Quantitative Analysis of the Effect of Salt Concentration on Enzymatic Catalysis.* **Park, C., Raines, RT.** 46, s.l. : Journal of the American Chemical Society, 2001, Vol. 123.

177. *A novel New Delhi metallo-β-lactamase variant, NDM-14, isolated in a Chinese Hospital possesses increased enzymatic activity against carbapenems.* **Zou, D., Huang, Y., Zhao, X., Liu, W.,**

References

Dong, D., Li, H., Wang, X., Huang, S., Wei, X., Yan, X., Yang, Z., Tong, Y., Huang, L., Yuan, J. s.l. : Antimicrobial Agents and Chemotherapy, 2015, Vols. 59, No. 4.